# Development of Assay Systems for the Identification and Functional Characterization of Inhibitors Targeting the Transcriptional Regulator PqsR of *Pseudomonas aeruginosa*

## Dissertation

Zur Erlangung des Grades des Doktors der Naturwissenschaften der Naturwissenschaftlich- Technischen Fakultät der Universität des Saarlandes

Von


**Apotheker**

**Benjamin Kirsch**


Saarbrücken

2016

| | |
|---|---|
| Tag der Prüfung: | 10.02.17 |
| Dekan: | Prof. Dr. Guido Kickelbick |
| Vorsitzender: | Prof. Dr. Claus M. Lehr |
| Berichterstatter : | Prof. Dr. Rolf W. Hartmann |
| | Prof. Dr. Dr. h.c. Hans H. Maurer |
| Akad. Beisitzer: | Dr. Matthias Engel |

Die vorliegende Arbeit wurde von Januar 2012 bis März 2016 unter Leitung von Univ.-Prof. Dr. Rolf W. Hartmann in der damaligen Fachrichtung 8.2 Pharmazie am Lehrstuhl für Pharmazeutische und Medizinische Chemie der Universität des Saarlandes und am Helmholtz Institut für Pharmazeutische Forschung Saarland (HIPS) angefertigt.

“I´m gonna have to science the shit out of this“

Mark Watney, The Martian

# Papers Included In This Thesis:

**A** **"Optimization of anti-virulence PqsR antagonists regarding aqueous solubility and biological properties resulting in new insights in structure-activity relationships"**

Cenbin Lu*, Benjamin Kirsch*, Christine K. Maurer, Johannes C. de Jong, Andrea Braunshausen, Anke Steinbach, and Rolf W. Hartmann

*Eur J Med Chem* **2014**, 79:173-183

* Authors contributed equally.



**B** **"Overcoming the unexpected functional inversion of a PqsR antagonist in Pseudomonas aeruginosa: an in vivo potent antivirulence agent targeting pqs quorum sensing"**

Cenbin Lu, Christine K. Maurer, Benjamin Kirsch, Anke Steinbach, and Rolf W. Hartmann

*Angew Chem Int Ed Engl* **2014**, 53:1109-1112

# Contribution Report:

The following contributions to the papers A and B included in this thesis are declared by the author:

**A** The author established, planned, and supervised the reporter gene experiments, and contributed to the composition of the manuscript.

**B** The author performed the reporter gene assays in *E. coli* and *P. aeruginosa*, developed and conducted the metabolization experiments, and contributed to the composition of the manuscript.

# Further Publications that are not Part of the Thesis

**C** **"From in vitro to in cellulo: Structure-activity relationship of (2-nitrophenyl)methanol derivatives as inhibitors of PqsD in Pseudomonas aeruginosa"**

Michael P. Storz, Giuseppe Allegretta, Benjamin Kirsch, Martin Empting and Rolf W. Hartmann

*Org Biomol Chem* **2014**, 12: 6094–6104.

**D** **"Identification of Small-Molecule Antagonists of the Pseudomonas aeruginosa Transcriptional Regulator PqsR: Biophysically Guided Hit Discovery and Optimization"**

Tobias Klein, Claudia Henn, Johannes C. de Jong, Christina Zimmer, Benjamin Kirsch, Christine K. Maurer, Dominik Pistorius, Rolf Müller, Anke Steinbach and Rolf W. Hartmann

*ACS Chem Biol* **2012**, 7: 1496–1501.

**E** **"Discovery of Antagonists of PqsR, a Key Player in 2-Alkyl-4-quinolone-Dependent Quorum Sensing in Pseudomonas aeruginosa"**

Cenbin Lu, Benjamin Kirsch, Christina Zimmer, Johannes C. de Jong, Claudia Henn, Christine K. Maurer, Mathias Müsken, Susanne Häussler, Anke Steinbach and Rolf W. Hartmann

*Chem Biol* **2012**, 19: 381–390.

**F** **"Discovery and Biophysical Characterization of 2-Amino-Oxadiazoles as Novel Antagonists of PqsR, an Important Regulator of Pseudomonas aeruginosa Virulence"**

Michael Zender, Tobias Klein, Claudia Henn, Benjamin Kirsch, Christine K. Maurer, Dagmar Kail, Christiane Ritter, Olan Dolezal, Anke Steinbach and Rolf W. Hartmann

*J Med Chem* **2013**, 56: 6761–6774.

# Table of Contents

# Introduction

## Antibiotic resistance

During the last decades, public health service has been facing an increasing number of antibiotic resistant pathogens impairing the successful treatment of infectious diseases (Neu, 1992). Today, multi-resistant bugs represent a considerable threat to society. Since the "golden antibiotic age" in the 1950s, we observe the alarming trend that the number of new antibiotics decreases, while bacteria simultaneously grow resistant to more and more drugs (Hart, 1998). Besides several factors like the careless use of antibiotics, the ability of bacteria to protect themselves in a variety of ways has made resistant pathogens arise. As in general, available antibiotic drugs act bactericidally or at least bacteriostatically, the bugs are forced to develop mechanisms to survive. This so called “selective pressure” promotes the onset of resistance against an antibiotic treatment. Especially in case of β-lactam antibiotics like ampicillin, carbenicillin, or amoxicillin, a more than 900-fold increase in the formation of different β-lactamases has been observed since the 1970s. In addition to these drug-degrading enzymes, the bacterial resistance machinery comprises efflux systems, target alterations, and the establishment of alternative metabolic pathways (reviewed by Davies and Davies, 2010). The basis for those phenotypes is formed by resistance factors, the so-called "r genes", which can be acquired by bacteria through, for example, spontaneous mutation or horizontal gene transfer (reviewed by Bennett, 2008). The latter is critical for spreading different resistance factors amongst various bacterial species creating the feared "superbugs" like the pan-resistant microorganism *Vibrio cholerae* (Lipp et al., 2002; Davies and Davies, 2010). These facts demand novel concepts in antimicrobial drug therapy. In recent years, compounds that impair bacterial pathogenicity rather than their viability have attracted more and more attention. The desired benefit of this approach is reduction of selective pressure making the occurrence of resistance less probable.

## Pseudomonas aeruginosa

The Gram-negative opportunistic pathogen *Pseudomonas aeruginosa* (PA) is a rod-shaped microorganism prevalent in nosocomial infections and burn wounds. PA is ubiquitarily present in the environment and its arsenal of adaptive mechanisms allows the colonization of various surfaces under manifold conditions. Especially, plants and soil are considered an endless reservoir of *Pseudomonades* (Green et al., 1974). Additionally, PA is one of the most frequently found germs regarding hospital-acquired infections (Jarvis and Martone, 1992). Studies have shown the presence of the bacterium in sinks, on metal surfaces, floors, and the hands of nurses (Chitkara and Feierabend, 1981). Severe infections with this opportunistic pathogen are favored in individuals with a hampered immune defense like HIV patients (Franzetti et al., 1992) or people undergoing chemotherapeutical treatments (Bendig et al., 1987; Lyczak et al., 2000). Furthermore, burn wound victims have a high prevalence for the occurrence of PA- associated infections due to a damaged, no longer protecting skin layer (reviewed by Bodey et al., 1983) that facilitates bacterial invasion of the host. A set of various secreted virulence factors causing host immune modulation and tissue damage makes this pathogen a major threat especially for patients suffering from cystic fibrosis (CF). (Lyczak et al., 2000; Davies, 2002) Lacking the proper mucociliary clearance, these patients have a high prevalence for chronic, persistent PA infections affecting bronchia and the deep lung. Besides the Gram-negative cell envelope, which depicts the first barrier for antibiotic agents, this pathogen uses a variety of multidrug efflux pumps (reviewed by Li and Nikaido, 2009) and β-lactamases (Wolter and Lister, 2013) to withstand an effective treatment. Its ability to encapsulate itself within a biofilm protects the bacterial community in an additional gel-like barrier during a chronic infection state (Høiby et al., 2010). These facts render PA an unneglectable threat that urgently requires new and effective ways of treatment.

## Quorum sensing (QS)

The possibility to survive under difficult conditions is favored by cooperation. In fact, this is true for most organisms including animals, humans, and also bacteria. While the most common form of communication is based on the creation of sounds and noises, microorganisms have developed their own language. Both, Gram-positive and Gram-negative pathogenic species such as *Burkholderia*, *Vibrio,* and *Pseudomonas* - only to name a few - are capable of organizing their group behavior with the help of a complex, small molecule-based system called “quorum sensing” or QS. This system acts as a communication network between the single microbes and allows a directed cell-to-cell crosstalk. Small molecules, the so-called autoinducers (AIs) or signal molecules, are synthesized and secreted by each cell. With increased cell numbers in a population, these AIs reach a certain threshold concentration. In neighboring bacteria as well as in an intrinsic autoregulatory way, the signal molecules bind to intracellular target receptors activating the transcription of different genes associated e.g. with virulence factors. In case of PA, the QS network comprises three major regulatory subsystems, namely, the *las*, the *rhl*, and the Pseudomonas Quinolone System (PQS system). Recently, a fourth regulatory system named the integrated quorum sensing system (IQS) that is able to mimic some functions of the *las* system (Lee et al., 2013) has been reported (Figure 1). Basically, the regulatory systems consist of a signal synthase, and an intracellular response unit. It was shown that, especially in acute infection states, the QS system is highly active creating a huge amount of virulence factors. Remarkably, QS is down-regulated after PA has established a chronic infection state (van Delden and Iglewski, 1998) accompanied by biofilm formation and the presence of persister cells. Recently, an overview on the complexity and the hierarchy of the different PA QS systems was given (Lee and Zhang, 2015). The present thesis hereby focuses especially on the PQS QS system.

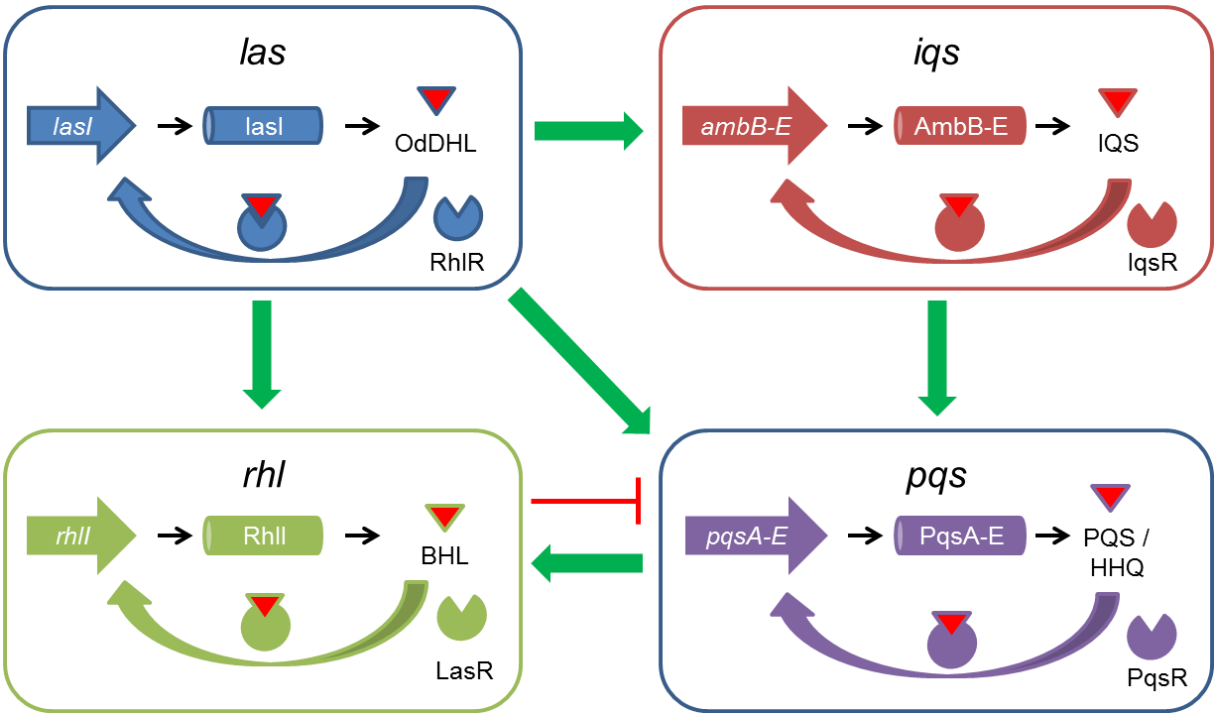


**Figure 1:** Organization and hierarchy of the four QS systems. Each system is composed of a signal molecule synthesis machinery (lasI, AmbB-E,RhlI, and PqsA-E), autoinducer (OdDHL, IQS, BHL, and PQS/HHQ), and receptor (RhlR, IqsR, LasR and PqsR). Stimulating effects are indicated as thick green arrows. Inhibitory effects are marked as red line. Figure was modified, based on (Lee and Zhang, 2015).

## Virulence factors and biofilm formation

PA evokes its pathogenic effects via a set of different virulence factors. Besides cell-associated factors like pili and flagella, which are needed for adhesion and motility of the bacterium, it makes use of a variety of secreted factors like proteases, siderophores, pyocyanin, and hydrogen cyanide as summarized in a recent review (Strateva and Mitov, 2011). These enable the microorganism to disturb the human immune system, circumvent antibiotic treatment, and compete with other bacteria for nutrition sources. This finally favors its persistent survival in a variety of environmental niches (Lyczak et al., 2000).

## Pyocyanin

The virulence factor pyocyanin is one of the most conserved virulence factors among the *Pseudomonas* species, produced by more than 90% of the isolated strains (Smirnov and Kiprianova, 1990). Its synthesis involves a complex pathway comprising the *phzA-G* operons as well as the *phzH*, *phzM,* and *phzS* genes. These genes transform the initial substrate chorismate into the phenazine pyocyanin (Mavrodi et al., 2001; Ortiz-Castro et al., 2014). This redox-active exotoxin is considered as key virulence factor. It exerts pleiotropic effects like, for instance, impairment of the cilia in the airway epithelium, immunological cell growth, and interference with components of the host's immune system. In addition to the effects targeting the host, it allows *Pseudomonas* to dominate rivaling microorganisms by exhibiting fungicidal and antimicrobial effects as mentioned in a review by Ran et al. (Ran et al., 2003). Taken together, pyocyanin is an important part in the virulence machinery of this pathogen that facilitates persistence and severe infections.

## Proteolytic Virulence Factors

The multiple roles of elastase as virulence factor during the PA-associated infection processes have been reviewed in detail by several groups (Wretlind and Pavlovskis, 1983; Galloway, 1991). The elastases A (LasA) and B (LasB) of PA are secreted proteases that are especially relevant during the acute infection state (van Delden and Iglewski, 1998). Among other effects these elastases take part in the degradation process of human elastin, an important component of the lung tissue, in a cooperative manner (Galloway, 1991). The loss of elastin is directly connected with a hindrance in lung tissue and blood vessel elasticity leading to tissue damage in the human host. Additionally, elastase has been shown to destroy surfactant proteins, namely SP-A and SP-D, both important players in host's immune reaction processes (Wright, 2005). *In vivo* studies conducted by Giannoni et al. further demonstrated that SP-A and AP-D strongly enhance pulmonary clearance of PA in a mouse model (Giannoni et al., 2006). Studies performed by Woods and coworkers (Woods et al., 1982) revealed a reduced virulence of PA isolates lacking proper elastase activity.

Furthermore, such mutants were shown to become more easily cleared from the host's airways than the native, elastase-possessing strain (Blackwood et al., 1983).

In summary, elastase fulfills a major role in PA pathogenicity rendering it a powerful bacterial tool to combat the host's immune system and allow persistence of the bacterial community.

## Motility Factors

The initial colonization and later spreading of a pathogen requires the ability to be mobile. In bacteria such as PA, this task is not only fulfilled by flagella and pili but also by excreted fatty films allowing them to "slide" along the tissue they colonize (reviewed in Strateva and Mitov, 2011). The pili of PA are of particular importance in the first step of the colonization process. As cell-associated virulence factors they recognize the solid cell surface of the host aiding in initial attachment of the pathogen. These pili also give PA the ability of twitching motility (Bradley, 1980). Furthermore, these cell-associated factors do not only favor a host- bacteria but also interbacterial contacts. This renders the pili an important feature in the process of biofilm formation (O'Toole and Kolter, 1998). In addition to their role in the bacterial attachment, recently, Persat and coworkers demonstrated that the type IV pili are also involved in the regulation of the virulence factor machinery (Persat et al., 2015). However, the movement of PA does not only depend on these cell- associated structures. As mentioned above, the organism surrounds itself with a slimy layer to slide along the cell surfaces. Of the various components that are forming this layer, the rhamnolipids (RLs) are of particular interest in the anti-virulence therapy. As summarized in diverse representative reviews (Soberón-Chávez et al., 2005; Abdel-Mawgoud et al., 2010), RLs are present as a mixture of different RL congeners, the composition of which varies among distinct *Pseudomonas* strains. In PA, the RLs synthesis is controlled by two operons carrying the *rhlAB* and *rhlC* genes, respectively. The regulation of these genes directly depends on the *rhl* QS system, but has also been shown to be under indirect control of the PQS system (Diggle et al., 2003). The excreted RLs fulfil several distinct functions in the bacterial environment. In addition to their contribution to pathogenicity, they also render the

bacteria able to survive under difficult circumstances. Due to their amphiphilic character, these compounds allow the uptake of nutrition factors and substrates that possess poor solubility such as n-alkanes. Like elastase and pyocyanin (Wilson et al., 1988; Jaffar-Bandjee et al., 1995), high amounts of rhamnolipis can also be found in the sputum of patients that have fallen ill with CF. Kownatzki et al. were the first that drew a connection between the amount of rhamnolipids produced by PA and the declined health status of infected patients (Kownatzki et al., 1987). Reviews report several effects affecting the host ranging from hemolytic activity to cytotoxic effects on different immune cells (Abdel-Mawgoud et al., 2010). Last but not least, rhamnolipids are also involved in the biofilm formation as they favor primary cell-adhesion due to an increase in surface hydrophobicity. Taken together, these observations render the RLs an important part in pathogenicity and bacterial survival.

## Hydrogen Cyanide

Various bacteria, including *Burkholderia*, *Chromobacterium*, and *Pseudomonas* species form hydrogen cyanide (HCN) during the “bacterial cyanogenesis”. This toxic virulence factor evokes strong inhibition of the cellular respiratory chain and, as an effect, causes cell growth inhibition or –killing. Studies revealed that sputum samples of patients suffering from cystic fibrosis contained up to 130 µM of HCN excreted by PA (Ryall et al., 2008). Due to its various effects on cells, HCN is believed to be the primary toxic virulence factor secreted by PA. It caused e.g. increased mortality rates in a nematode based infection model (Gallagher and Manoil, 2001). Furthermore, mutational studies conducted by Gallagher and coworkers indicate that an interference with PA’s PQS system not only reduces the virulence factor pyocyanin, but also decreases HCN production (Gallagher et al., 2002). This fact furthermore renders PQS QS an attractive target for novel therapeutics.

## Biofilm

One of the major barriers for agents targeting PA is represented by the biofilm matrix. This barrier consists of various proteins, extracellular nucleic acids, RLs, and polysaccharides, mainly the alginate (Flemming and Wingender, 2010; Høiby et al., 2010). This enables the bacteria not only to protect themselves against antibiotic treatment but in addition against the host's immune defensive mechanisms. Besides the protecting aspects, the bacteria use proteins, embedded in the extracellular matrix, to ensure access to vital nutrition factors by degrading biopolymers that can be used as carbon sources. Amongst other factors, this set of distinct enzymatic and non-enzymatic proteins also contributes to virulence and structural integrity of the biofilm (Flemming and Wingender, 2010). Besides the virulence factor producing cells, this protective film harbors cells that remain in a "sleeping mode". These dormant cells possess a low rate of metabolism and cell division, turning them less sensitive against an antibiotic treatment (Lewis, 2008). *In vitro* studies have shown that the process of biofilm development occurs in a stepwise manner starting with the bacteria's adhesion followed by different maturation stages. In the final state, the grown bacterial mass is released again allowing further spreading of the infection (Sauer et al., 2002; Davies, 2003; Wagner et al., 2016) (Figure 2).

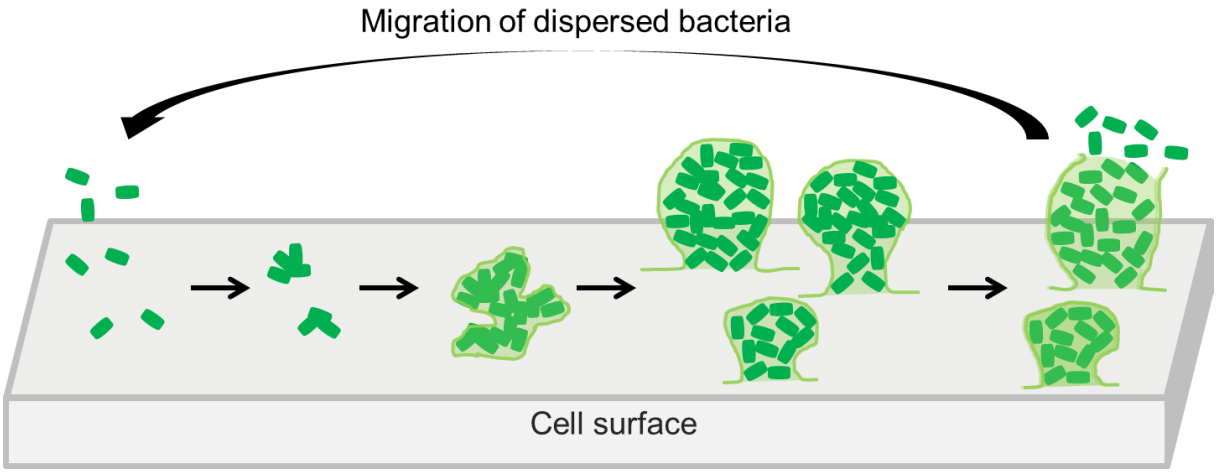


**Figure 2:** The process of *in vitro* biofilm formation. Figure was modified, based on (Seong-Cheol et al., 2011).

From left to right: reversible adhesion → irreversible adhesion → microcolony formation → biofilm maturation → dispersion of the bacteria

## The transcriptional regulator PqsR

Each QS system has its specific signal molecules and its respective regulators responsible for gene transcription. In case of the PQS system, this role is played by the central transcriptional regulator MvfR (multiple virulence factor regulator), also called PqsR (*Pseudomonas* quinolone signal receptor), a 37.2 kDa membrane-associated protein. PqsR belongs to the LysR type transcriptional regulator family (LTTR), which represents the largest group of bacterial transcription factors (Cao et al., 2001; Zaim, 2003). Like many additional members of this protein family, PqsR is composed of a C-terminal coinducer-binding domain and an N-terminally located DNA-binding domain formed by a helix-turn-helix (HTH) motif (Schell, 1993; Xu et al., 2012; Kefala et al., 2012). Under addition of its coinducers PQS (Pseudomonas Quinolone Signal) or HHQ (2-heptyl-4(1H)-quinolone), PqsR promotes the transcriptional activation of the *pqsABCDE* operon that is responsible for the synthesis of HHQ and PQS. In this way PqsR activity is controlled in an autoinductive manner. (Figure 3) Further regulated genes involve the *phnAB* operon, that takes part in the phenazine biosynthesis (Cao et al., 2001). Furthermore, it indirectly regulates numerous genes promoting bacterial pathogenicity as shown by a transcriptome analysis of a PqsR- deficient knockout strain (Déziel et al., 2005). A blockade of PqsR by antagonistic compounds has been shown to reduce PA pathogenicity and persister cell formation leading to an enhanced survival rate in different animal infection models (Lu et al., 2014b; Starkey et al., 2014).

The present thesis was focused on the characterization of small molecules modulating the PQS receptor PqsR. Studies carried out by Déziel et al. and Cao et al. (Cao et al., 2001; Déziel et al., 2005) showed that, amongst others, PqsR regulates pyocyanin and elastase B production. Mutational studies revealed a complete deficiency in pyocyanin production for strain lacking PqsR activity, leading to a reduced pathogenicity (Déziel et al., 2004; Xiao et al., 2006a). In addition to pyocyanin, elastase and rhamnolipids are also decreased in a PqsR mutant genotype (Diggle et al., 2003). Taken together, these findings render PqsR an attractive target for the anti-virulence therapy.

Besides the PqsR antagonists, several so called “quorum sensing inhibitors” (QSIs) are currently being developed by several groups.

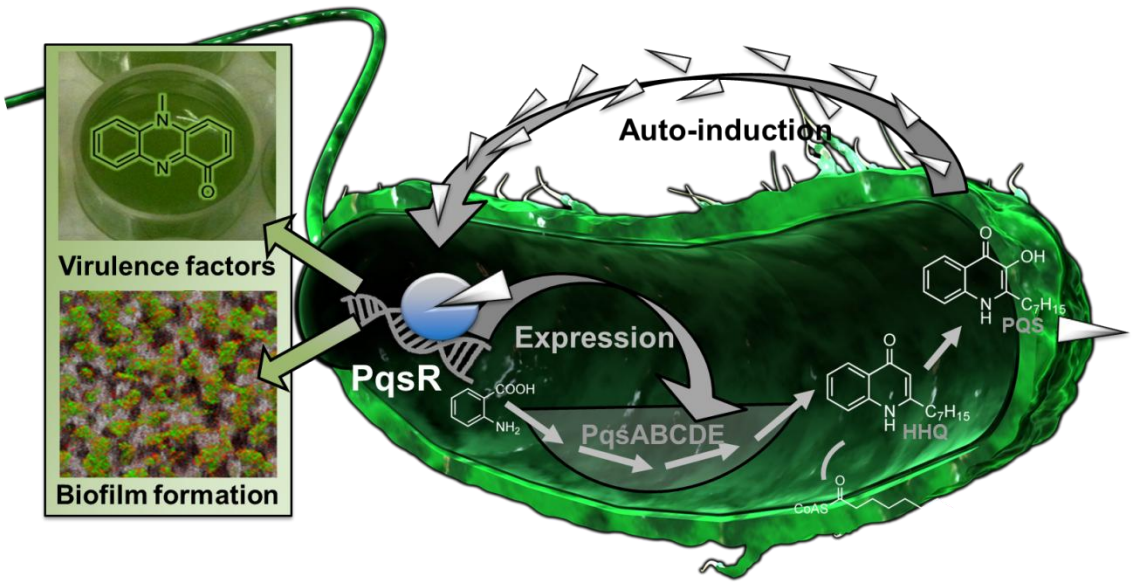


**Figure 3:** The role of PqsR within the quorum sensing network The transcriptional regulator PqsR activates the gene transcription of the *pqsA-E* operon upon induction by its autoinducer PQS. The figure was designed by my colleague Dr. Martin Empting.

## QS inhibitors targeting PQS QS

The so-called QSIs are derived from distinct compound classes. The molecular diversity reaches from small molecule inhibitors to large molecular weight natural compounds. To date, numerous QSIs are published that have been developed by several groups. Basically, these inhibitors can act via a) an interference with the signal molecule synthesis b) by targeting the signal molecules themselves c) a blockade of the signal receptors or involving multiple of the just mentioned mechanisms (Maurer et al., 2015; Wagner et al., 2016; Thomann et al., 2016). For the PQS system, case a) is represented by compounds that inhibit the formation of the two main PqsR ligands, namely HHQ and PQS. HHQ is formed in a complex synthesis pathway involving the enzymes PqsA – PqsE (Coleman et al., 2008; Dulcey et al., 2013; Drees and Fetzner, 2015). The final step involves the hydroxylation of HHQ to form its potent derivative PQS, which is conducted by the FAD- dependent monooxygenase PqsH (Gallagher et al., 2002; Déziel et al., 2004). Compounds addressing the first step in the HHQ synthesis, namely the PqsA-mediated conversion from anthranilate to anthraniloyl-coenzyme A (Coleman et al., 2008), can act either as “false substrates” that are converted into “false products” or

inhibitors of PqsA. This approach efficiently reduced PQS levels in PA (Calfee et al., 2001; Lesic et al., 2007). Several inhibitor classes targeting the PqsD enzyme, which catalyzes the second step in the HHQ synthesis, showed signal molecule reduction and anti-biofilm activities (Storz et al., 2012; Storz et al., 2014; Allegretta et al., 2015).

To target the autoinducer molecules themselves, different groups reported approaches including enzymatic degradation and antibody- mediated absorption. For the PQS system, Pustelny et al. (Pustelny et al., 2009) were able to show that the dioxygenase Hod was able to degrade the signal molecule PQS, leading to decreased virulence in a plant model. In addition to PQS system-targeting agents, numerous groups have undertaken efforts in developing a variety of compounds addressing the *las* and *rhl* QS systems to fight PA. An overview of different QSIs and treatment strategies targeting the pathogen's different regulatory systems was recently given in detail by Wagner and Sommer et al. (Wagner et al., 2016).

To disturb the signal transduction, another option is antagonizing PqsR, which serves as the response unit within the PQS QS system. Both, ligand (HHQ)-based derivatives and structurally unrelated compounds have shown promising activities in *in cellulo* and *in vivo* models. The blockade of PqsR successfully provided a proof-of-concept for an anti-virulence therapy against PA infections (Hodgkinson et al., 2010; Klein et al., 2012; Lu et al., 2012; Zender et al., 2013; Ilangovan et al., 2013; Lu et al., 2014b; Starkey et al., 2014). The application of dual inhibitor targeting PqsD and PqsR has recently been shown to be effective in protecting *Galleria mellonella* larvae from a lethal infection further highlighting the benefit of a PQS system blockade to reduce the bacteria's pathogenicity (Thomann et al., 2016). Furthermore, such a dual approach or the directed blockade of PqsR, have turned out to be more beneficial than just inhibiting the autoinducer synthesis machinery. Storz et al discovered potent inhibitors of PqsD, that were able to slightly reduce the virulence factor pyocyanin, but only at very high concentrations (Storz et al., 2012; Thomann et al., 2016). Starkey and coworkers recently reported the, to date, most potent antivirulence compound for PA that is a PqsR antagonist (Starkey et al., 2014).

## Assay systems

For the investigation of the cellular potency and the functional characterization of the presented compounds, mainly two assay variants were used. In case of the cellular effects, we used a ß-galactosidase-based reporter gene system in both, *E. coli* DH5α and *P. aeruginosa* PA14 Δ*pqsA* strains. For the mechanistic studies described in chapter 1, a cell-free system using the principle of fluorescence polarization (FP) was applied.

## β- Galactosidase reporter gene assay

Reporter gene assay systems are used throughout the drug development process and are available in many different configurations that are suitable for eukaryotic and prokaryotic cell setups that have been addressed in several reviews (Bronstein et al., 1994; Naylor, 1999; New et al., 2003). Reporter gene readouts might be bacterial survival, formation of colored products, or the expression of fluorescing molecules. This technique is commonly used to monitor gene transcription-or translation-regulated effects in the cellular environment. Basically, these systems can be divided into invasive and non-invasive assays. The non-invasive methods, like Green Fluorescent Protein (GFP) or Luciferase expression systems allow readout without the lysis of the cells. The reporter gene system used in the present thesis is based on the expression of the enzyme β-galactosidase and belongs to the invasive reporter gene methods. It is a popular reporter gene as it allows an easy colorimetric readout. In contrast to GFP-based transcription products, the β-galactosidase requires the addition of a cleavable substrate to monitor the activity. The underlying mechanism behind the ß-galactosidase reporter system is shown in Figure 4. Expression of the *lacZ* gene is triggered by the transcriptional regulator. After expression of the enzyme, the cells have to be lysed to allow interaction between the substrate ortho-nitrophenol β-*D*-galactopyranoside (ONPG), which is then cleaved into β-galactose and the yellow ortho-nitrophenol (ONP). The absorption of the formed ONP can be measured at 420 nm.

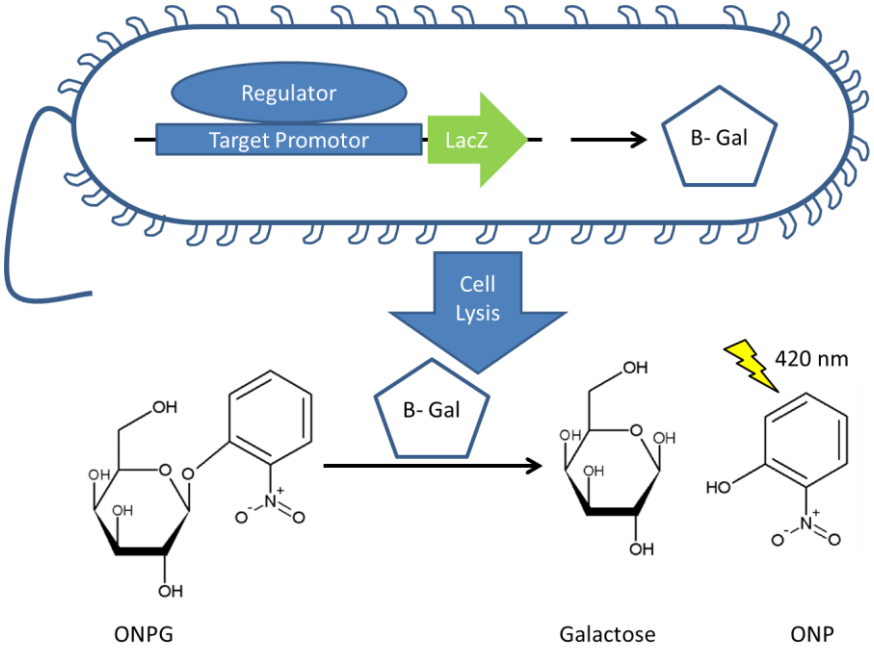


**Figure 4:** Principle of the ß-galactosidase reporter gene assay.

## Fluorescence polarization assay

The usage of FP in screening processes has been thoroughly investigated in the recent years. The range of application is broad as this method allows investigation of diverse biomolecular processes such as protein - DNA, protein- ligand, and protein-protein interactions (Jameson and Sawyer, 1995; Checovich et al., 1995; Hill and Royer, 1997; Huang, 2003). The assay is carried out in a cell- free environment using purified protein and fluorescent-labeled probes of either ligand or protein. Here, a variety of different labeling probes can be applied to ensure best signal strength and minimized interference. In this thesis, FP competition experiments were used to investigate PqsR- DNA interactions under simultaneous addition of different PqsR ligands. Such an approach requires purified receptor, a labeled DNA probe, and diverse unlabeled competitor DNAs. Figure 5 explains the underlying mechanism of FP.

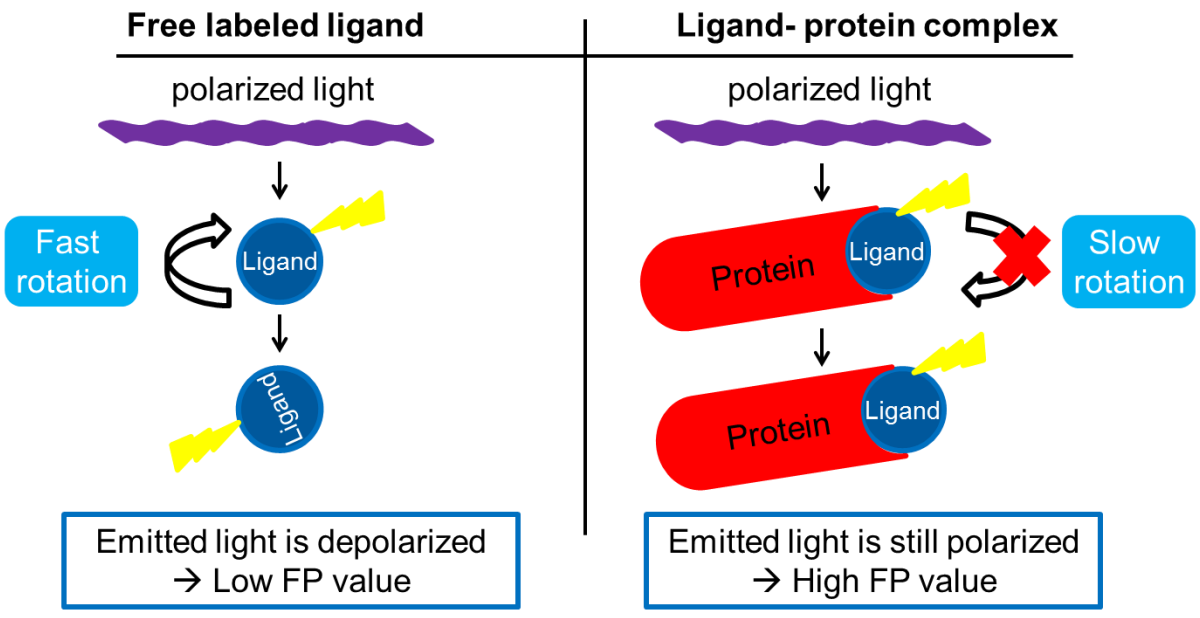


**Figure 5:** Mechanism of fluorescence polarization to monitor protein- ligand interactions.

# Aim of the Thesis

Every novel compound determined for the treatment of a disease needs a reliable characterization in the first instance. In case of the antagonistic compounds targeting the PqsR receptor, information about their functionality and potency form the basis in the drug discovery process. A central part of the present thesis is dedicated to achieve this goal: the development of cell-based reporter gene systems in both, *E. coli* and *P. aeruginosa*. To avoid effects caused by the complex QS regulatory cascade that is present in PA, the *E. coli* assay will be chosen as initial test system. Additionally it lacks *Pseudomonas*-specific pharmacokinetic (PK) issues like e.g. PA enzymes. This provides a sensitive way to monitor direct effects on the target itself. In a second step, selected antagonists will be further evaluated in the more complex *P. aeruginosa*- based reporter gene system. The possibility of a metabolization by PA enzymes shall be investigated as a reason for an altered potency and functionality observed for compounds exhibiting decreased activity in PA. This goal can be achieved by using different PA mutant strains in combination with LCMS-MS based methods. In order to understand the molecular mechanisms behind an agonistic or inverse agonistic functionality, an *in vitro* fluorescence polarization based assay shall be developed.

# Results

## Chapter 1: "Molecular mechanism of inverse agonism on the global virulence regulator PqsR for repressive control in *Pseudomonas aeruginosa*"

**The following persons contributed to this chapter:**

**Benjamin Kirsch:**
Constructed, expressed and purified the protein, conducted the fluorescence polarization experiments and the reportergene assays in *E.coli* and *P.aeruginosa*.

**Michael Zender:**
Synthesized compound 2 and performed the ITC titration experiment.

**Simone Amann:**
Assisted in conducting the reportergene assays.

### Introduction

The human pathogen *P. aeruginosa* causes severe acute and chronic infections of wounds and of the lung especially in immunocompromised individuals (e.g. HIV). Furthermore, it is most prevalent in patients suffering from cystic fibrosis causing increased mortality (Davies, 2002; Sordé et al., 2011). Emerging high-level antibiotic-resistance of this pathogen towards common treatment (Bonomo and Szabo, 2006), results in an urgent demand for novel anti-infectives. A promising strategy is to target non-vital functions associated with the pathogenicity of a bacterium, thus, exerting a reduced selective pressure and resistance development. PqsR, also known as MvfR (multiple virulence factor regulator), is a global transcriptional regulator within the cell-to-cell signaling network of *P. aeruginosa*. In association with two other *N*-acyl L-homoserine lactone (AHL)–dependent quorum sensing (QS) systems (*las* and *rhl*), the *Pseudomonas* quinolone signal (PQS) QS is involved in the regulation of numerous genes that function in controlling virulence and pathogenesis, biofilm formation and antibiotic resistance via the expression of efflux pumps (Déziel et al., 2005) (Figure 1).

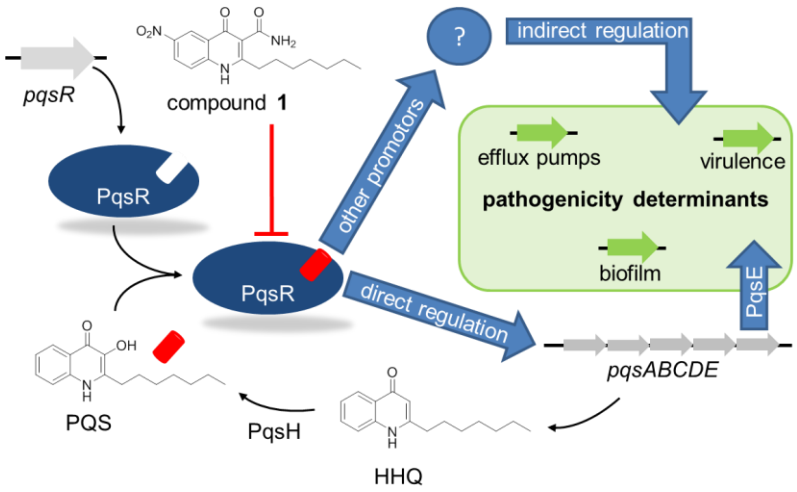


**Figure 1:** The global regulator PqsR has key functions in P. aeruginosa pathogenesis. Upon binding of its co-inducer PQS, PqsR directly binds to the promotor of the pqsABCDE operon thus driving the biosynthesis of HHQ, the PQS precursor. PqsR´s direct or indirect regulon involves genes for the production of virulence factors, biofilm and antibiotic efflux. Compound **1** is a potent PqsR antagonist that represses the expression of the virulence factor pyocyanin and strongly reduces the mortality rate caused by P. aeruginosa in animal models (Lu et al., 2014b).

PqsR is a member of the largest group of prokaryotic *lysR*-type transcriptional regulators (LTTR) and, as such, composed of a *C*-terminal co-inducer recognition domain and a highly conserved *N*-terminal DNA binding domain containing a helix-turn-helix motif (Kefala et al., 2012; Xu et al., 2012). LTTRs exist and function as dimers or tetramers or even higher oligomerization states (Hryniewicz and Kredich, 1994; Maddocks and Oyston, 2008; Zhou et al., 2010; Gong and Maser, 2012; Vadlamani et al., 2015) that interact with several mostly inverted repeat (pseudo-palindromic) sequences on target DNA (Goethals et al., 1992). The presence of a co-inducer triggers a 6- to 200- fold enhancement of gene transcription by increasing affinity to target sequences near the -35 bp region within the promotor (Dubbs et al., 2004; Schell, 1993). In case of PqsR, transcriptional activation requires the binding of the co-inducer PQS (*Pseudomonas* quinolone signal; 2-heptyl-3-hydroxy-4(1H)-quinolone) or its biological precursor HHQ (2-heptyl-4(1H)-quinolone) which both possess multifunctional roles in the QS regulation (Wade et al., 2005, Xiao et al., 2006; Diggle et al., 2007). PqsR directly binds to the *pqsA* promotor region and activates the transcription of the HHQ biosynthetic operon *pqsABCDE* in an autoregulatory manner (Wade et al., 2005, Xiao et al., 2006; Xiao et al., 2006a; Diggle et al., 2007). HHQ is converted into the more potent ligand PQS by PqsH

which is independent of PqsR (Gallagher et al., 2002; Déziel et al., 2004). Known to control a large set of virulence-associated genes, blockers of this regulator have been developed by us and other groups (Lu et al, 2012; Ilangovan et al., 2013; Zender et al., 2013; Lu et al., 2014a; Lu et al. 2014b; Starkey et al., 2014). Their effectiveness as anti-virulence agents has been proven in animal models (Lu et al., 2014c; Starkey et al., 2014). Interestingly, it has been shown that a potent PqsR antagonist can reduce the formation of antibiotic-tolerant persister cells (Starkey et al., 2014). The biochemical characterization of these PqsR antagonists implicated the investigation of PqsR-ligand interactions by state-of-the-art methods like Isothermal Titration Calorimetry (ITC) (Klein et al., 2012; Zender et al., 2013), Surface Plasmon Resonance (SPR) (Klein et al., 2012; Zender et al., 2013), and X-ray crystallography (Ilangovan et al., 2013). The functional response to compounds has been monitored in reporter gene assays and by the determination of extracellular 4-alkyl quinolone levels in *P. aeruginosa*. However, the mechanism of the modulation of PqsR activity by a ligand (agonist or antagonist) on a molecular basis has not been investigated, yet. The present study is directed to explore the process associated with co-inducer triggered transcriptional activation and antagonist-mediated repression of this important virulence regulator. This objective led us to determine the, *to date* uncertain oligomerization state of full-length PqsR in solution and investigate the binding pattern to promotor DNA using fluorescence polarization in combination with mutated nucleotides. Furthermore, we sought to shed light on the impact of different ligands on protein-DNA interaction and demonstrate the relevance of our *in vitro* results in life bacteria. Our studies revealed a tetrameric form in solution for the full-length MBP-tagged PqsR that occupied two distinct binding sites on the promotor DNA when bound by its co-inducer PQS. In contrast, the unliganded and antagonist- liganded form showed a different binding pattern. Notably, the antagonist enhanced DNA-binding affinity of PqsR one of the identified interaction sites on the target DNA in our *in vitro* setup. This new binding region (site I) turned out to be mandatory for PqsR activity in *P. aeruginosa* using a mutated reporter gene construct.

## Results

### Characterization of PqsR

Soluble and active full-length PqsR was overexpressed and purified with a maltose-binding protein (MBP) tag at its *C*-terminus. ITC was performed to ensure an intact ligand binding domain for the obtained fusion protein (Figure 2).

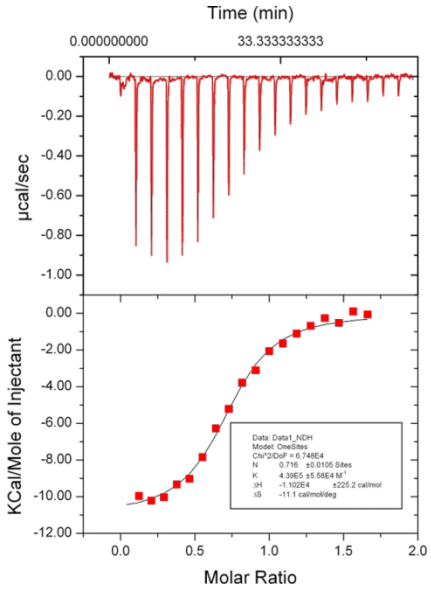


**Figure 2:** ITC titration curve of PqsR and 4-tert-butyl benzamide

To gain insight into the oligomerization state of PqsR in solution, a protein cross-linking study using the reagent bis(sulfosuccinimidyl)suberate (BS3) was conducted.

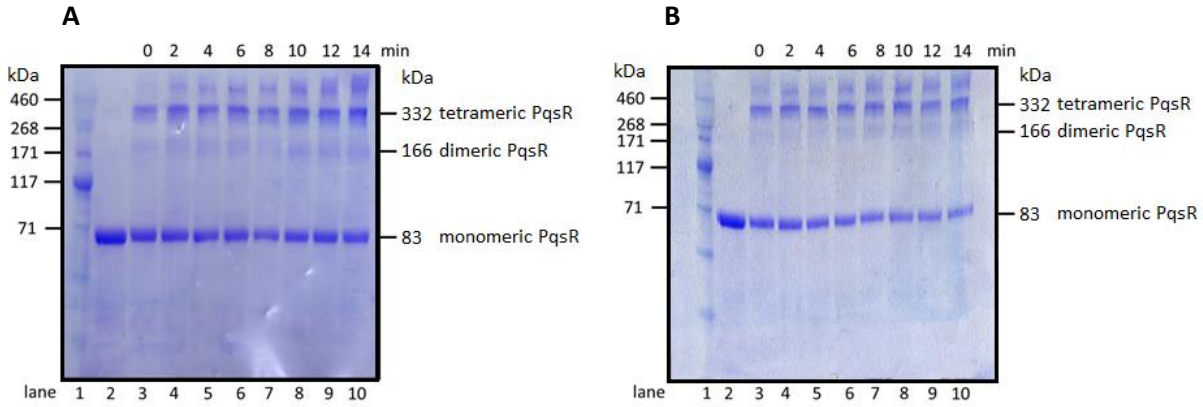


**Figure 3:** Determination of the oligomerization state of PqsR by protein cross-linking using BS3. Reactions (consisting of 12 µg of purified PqsR) were separated on a 12% SDS-PAGE. Lane 1: HiMark prestained protein standard (ThermoFisher Scientific, Germany), lane 2: free PqsR, lane 3-10: quenching of the cross-linking reaction after 2 min time intervals.

The cross-linking reaction consisting of purified PqsR and a five-fold excess of BS3 was stopped after several time points (0-14 min). The electrophoretic separation of the reaction mixture on a SDS-polyacrylamide gel revealed that the tetrameric state of PqsR (332 kDa, Figure 3A) is likely the predominant form in solution. On the contrary, the dimeric species (166 kDa) is barely visible.

This finding corresponds to many other members of the LTTR family possessing a tetrameric quaternary structure (Miller and Kredich, 1987; Schell, 1990; Hryniewicz and Kredich, 1994; Muraoka et al., 2003; Vadlamani et al., 2015). Additionally, we investigated the influence of compound **1** (Figure 1), a potent PqsR antagonist, in this cross-linking experiment. Interestingly, we did not observe a change in the oligomeriziation state of PqsR due to the presence of an equimolar amount of **1** (5 µM; Figure 3B).

**Binding pattern of PqsR on *pqsA* promotor and impact of the co-inducer**

In order to explore PqsR binding sites at the *pqsA* promotor, protein-DNA interactions were quantified by fluorescence polarization (FP) experiments. Through biochemical mutational studies, Xiao and coworkers previously verified the importance of the typical LTTR recognition element (TTCCGACTCGGAA, from -51 to -35 bp relative to the transcriptional start site (TSS) of the *pqsA* gene) for the activation mechanism (Xiao et al., 2006a). Thus, initial fluorescence polarization measurements were conducted with a fluorescein-labeled, 51 bp DNA fragment that included this important region. As depicted in Figure 4, PqsR binds this fragment irrespective of the co-inducer PQS with moderate binding affinity. Noteworthy, PQS strongly promotes the transcriptional activation of *pqsAp-lacZ* fusion in reporter gene assay (Figure 5A).

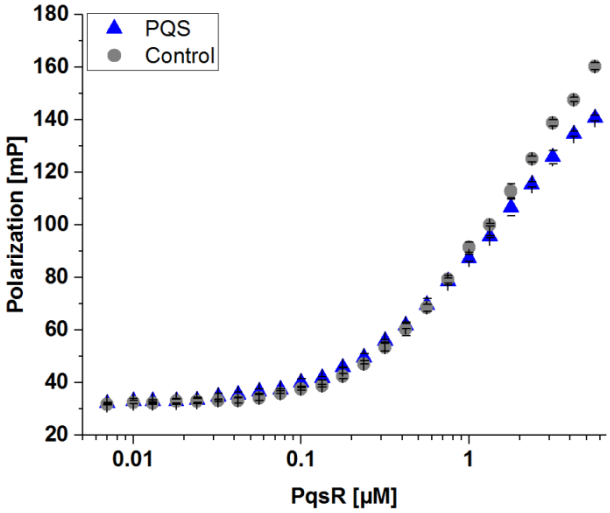


**Figure 4:** Fluorescence polarization titration curves. Each probe contained 10 nM of fluorescein-labeled 51 bp DNA fragment from -64 to –12 bp relative to *pqsA* TSS supplemented with DMSO as a control (Control) or 2 µM PQS (PQS). Protein was added at increasing concentrations (0.007 – 5.6 µM). Data represent the mean values and standard deviations of one experiment with n=2.

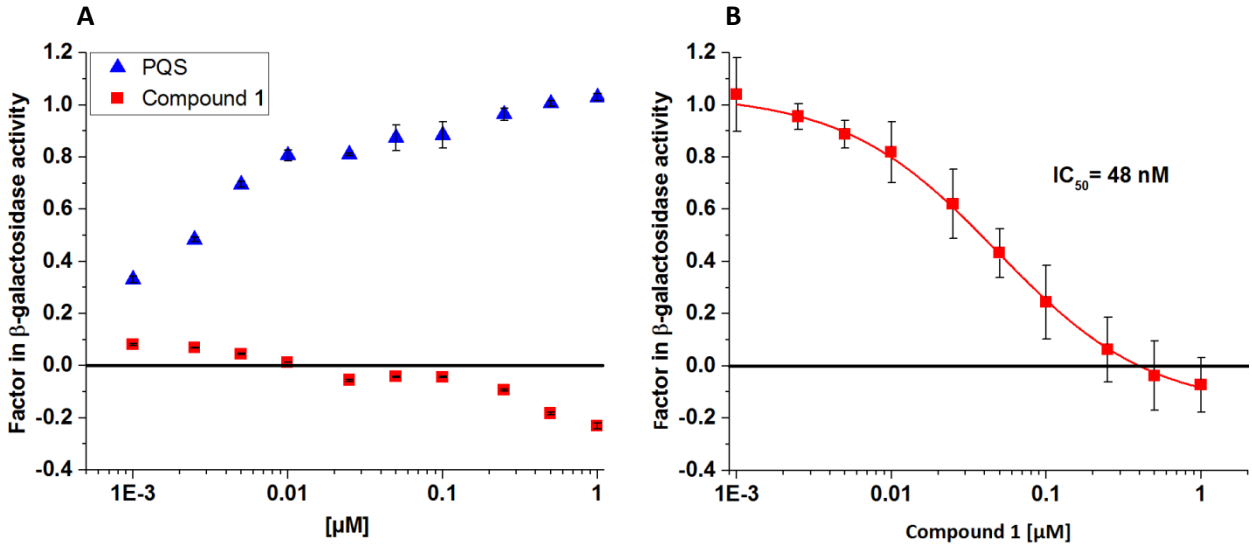


**Figure 5: A** Dose-dependent agonistic activity of PQS and inverse agonistic activity of compound **1**. Reporter gene assay was carried out in *E. coli* DH5α x pEAL08-2 (Cugini et al., 2007) harboring plasmid-borne PqsR and *pqsA*p-*lacZ* fusion. Compound **1** acts as inverse agonist as it decreases the basal activity. Data represent the mean values and standard deviations of one experiment with n=4. **B** Compound **1** decreases the PQS-induced activity. In the latter case, compound **1** was tested in competition to 50 nM PQS. β-galactosidase activity is expressed as factor in relation to the stimulation caused by 50 nM PQS (= 1.0). Basal expression level is defined as 0. Data represent the mean values and standard deviations of five independent experiments with n=4.

In order to localize more precisely potential PqsR interaction hotspots on DNA, we tested a set of serial site-directed mutants of the native *pqsA* promotor DNA fragment in FP competition experiments in the absence and presence of PQS or an antagonist. We altered base pair topology of cassettes of six adjacent residues by replacing adenine by guanine and cytosine by thymine. By this means, we generated 9 variants of the native 51 bp oligo and evaluated their affinity. From the data summarized in Table 1 and Figure 6, two adjacent PqsR binding sites I and II are evident. PqsR binding site I is formed by a 13 bp pseudo-palindromic sequence positioned -64 to -52 nucleotides upstream of the *pqsA* TSS and a second palindromic 13 bp binding site II corresponding to the LTTR recognition element is located in direct vicinity downstream to site I extending from -51 bp to -39 bp. The novel identified site I and additionally the upstream half of site II are bound in the absence or presence of any ligand (fragments 1-3) whereas the downstream positioned half of site II is only addressed upon binding of PQS (fragment 4). These findings render site I acting as a central anchor site, being generally important for PqsR-DNA interactions. Site I and II differ in their DNA sequence, but share the length and the inverted repeat character of the recognition motif separated by a 3 bp spacer. To determine if interaction with site II depends on site I, 5 bp and 10 bp spacers were introduced. Both modifications reduced the affinity in the presence of PQS by factor 3 to 5 indicating that the vicinity of site I and site II is of importance for efficient binding, which might be due to cooperativity. The results for apo PqsR and co-inducer-liganded PqsR further support the notion of a two-site transcriptional activation model proposed for some members of the LTTR family. According to this model, one tetramer is supposed to bind two sites where each site is occupied by one dimer of the tetramer (Maddocks and Oyston, 2008).

**Table 1** Determination of $EC_{50}$ values derived from FP competition experiments. The native labeled DNA fragment was competed with nine mutated *pqsA* promotor DNA fragments in the absence (Apo) and presence of PQS (2 µM) or compound **2** (10 µM). Site I is marked in bold and site II is underlined. Replaced residues (A→G, C →T) are marked in blue. $EC_{50}$ represents the effectiveness of unlabeled DNA to compete with the labeled DNA fragment. Data represent mean values and standard deviations of at least two independent experiments with n=2.

| name | sequences of native and artificial promotor DNA fragments from -64 to -12 bp relative to TSS (5´→ 3´) | $EC_{50}$ Apo [nM] | $EC_{50}$ + PQS [nM] | $EC_{50}$ + cpd.**2** [nM] |
|---|---|---|---|---|
| native | **CGAAACTTTTTCG**TTCGGACTCCGAATATCGCGCTTCGCCCAGCGCCGCTA | 183 +/- 33 | 152 +/- 9 | 236 +/- 66 |
| 1 | **CGAAGTCCCCTCG**TTCGGACTCCGAATATCGCGCTTCGCCCAGCGCCGCTA | 568 +/- 19 | 1758 +/- 464 | 472 +/- 14 |
| 2 | **CGAAACTCCCCTA**TTCGGACTCCGAATATCGCGCTTCGCCCAGCGCCGCTA | 439 +/- 38 | 512 +/- 18 | 390 +/- 16 |
| 3 | **CGAAACTTTTTCG**CCTAAGCTCCGAATATCGCGCTTCGCCCAGCGCCGCTA | 490 +/- 46 | 572 +/- 24 | 502 +/- 103 |
| 4 | **CGAAACTTTTTCG**TTCGGACCTTAGGTATCGCGCTTCGCCCAGCGCCGCTA | 216 +/- 1 | 1372 +/- 259 | 281 +/- 82 |
| 5 | **CGAAACTTTTTCG**TTCGGACTCCGAATACTATATTTCGCCCAGCGCCGCTA | 67 +/- 5 | 63 +/- 2 | 66 +/- 1 |
| 6 | **CGAAACTTTTTCG**TTCGGACTCCGAATATCGCGCTTTATTTGGCGCCGCTA | 118 +/- 27 | 135 +/- 12 | 157 +/- 34 |
| 7 | **CGAAACTTTTTCG**TTCGGACTCCGAATATCGCGCTTCGCCCAGCATTATCA | 164 +/- 12 | 143 +/- 2 | 181 +/- 37 |
| 8 | **CGAAACTTTTTCG**AGCGCTTCGGACTCCGAATATCGCGCTTCGCCCGTGAC | 445 +/- 75 | 495 +/- 58 | N.d. |
| 9 | **CGAAACTTTTTCG**CGCCGCTAGTTTCGGACTCCGAATATCGCGCTTCGCCC | 508 +/- 36 | 687 +/- 76 | N.d. |

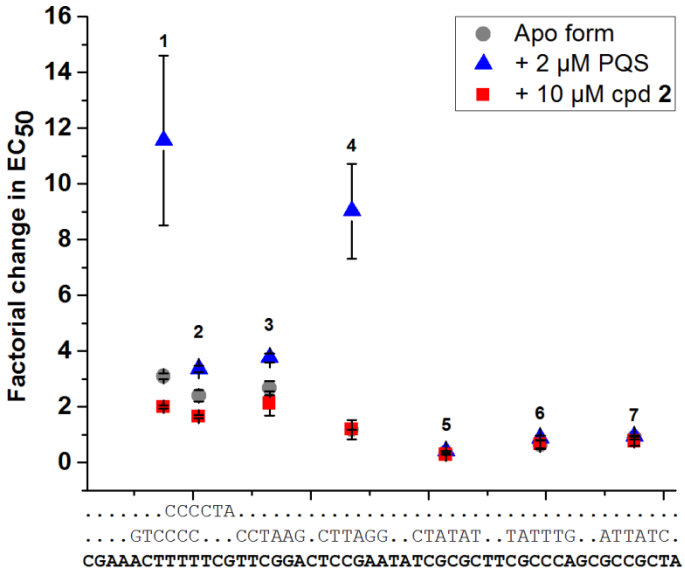


**Figure 6:** Graphical view of the results presented in Table 1 showing the factorial impact of the six residue mutations on $EC_{50}$. Factors are calculated in relation to the native DNA fragment (see Table 1). $EC_{50}$ values were determined in the absence (Apo form) or presence of PQS or compound **2** (cpd **2**). Native DNA sequence is marked in bold. The mutated six residue nucleotide sequences are shown above. Each data point marks the middle of the respective six nucleotide mutation. Data represent the mean values and standard deviations of at least two independent experiments with n=2. Numbers above each data point refer to the respective DNA fragment number.

## PqsR blocker enhances protein-DNA interaction

The differential functional outcome of PqsR-responsive transcription (activation or repression) depends on the type of ligand that interacts with the co-inducer binding domain. Recently, our own laboratory reported compound **1** as highly active PqsR antagonist with *in vivo* activity. Analyzing its dose-response curve in our heterologous reporter gene assay, we observed characteristics of inverse agonism as evidenced by the repression of basal and PQS-induced activity (Figure 5) as well as competitive binding to the ligand-binding domain (Lu et al., 2014b). In the presence of compound **1**, we most interestingly observed a strong increase in affinity ($K_d$ > 2 µM vs $K_{d\ (+cpd\ \mathbf{2})}$ = 0.45 µM) for *pqsA* promotor DNA fragment extending from –85 to –35 bp (Figure 7).

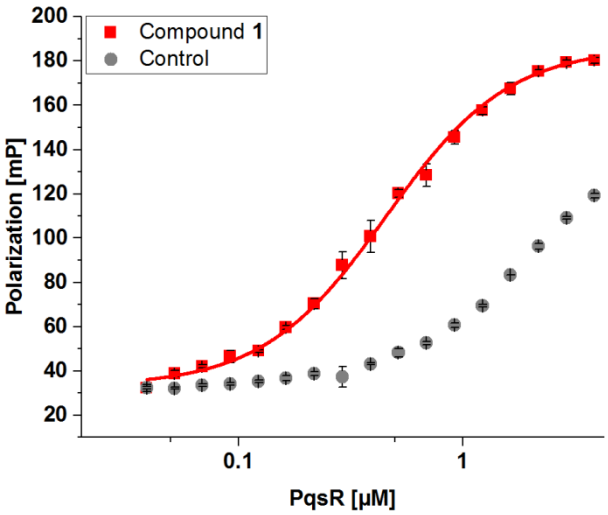


**Figure 7:** Fluorescence polarization titration curves. Each probe contained 10 nM of fluorescein-labeled 51 bp DNA fragment from -85 to –35 bp relative to *pqsA* TSS supplemented with DMSO as a control (Control) or 5 µM compound **1** (compound **1**). Protein was added at increasing concentrations (0.007- 5.6 µM). Data represent the mean values and standard deviations of one experiment with n=2.

To investigate whether this phenomenon is restricted to quinolone-derived compounds, we tested this fragment in the presence of a structurally distinct compound class (compound **2**; structure undisclosed). This newly discovered PqsR inverse agonist possesses improved physicochemical properties and potent inhibitory activity towards PqsR, which was determined by the repression of PqsR-mediated transcriptional activation in *E. coli* reporter gene assay and reduction of HHQ formation in *P. aeruginosa* (Table 2). As presented in Figure 8, compound **2** also increases the affinity of PqsR to the *pqsA* promotor fragment in a dose-dependent manner. These data encouraged us to further explore the occupancy of PqsR on DNA upon binding of an inverse agonist in more detail.

**Table 2** Activity of PqsR inverse agonists on transcriptional activation in *E. coli* reporter gene assay and extracellular HHQ level of *P. aeruginosa* PA14. Data represent mean values and standard deviations of at least two independent experiments with n=4 for reportergene experiments and n=3 for HHQ assay.

| Cpd. | *E. coli* reporter gene $IC_{50}$ [nM] | HHQ in PA14 inhibition [%] |
|---|---|---|
| **1** | 35 ± 4 | 54% at 15 µM |
| **2** | 423 ± 103 | 33 % at 50 µM |

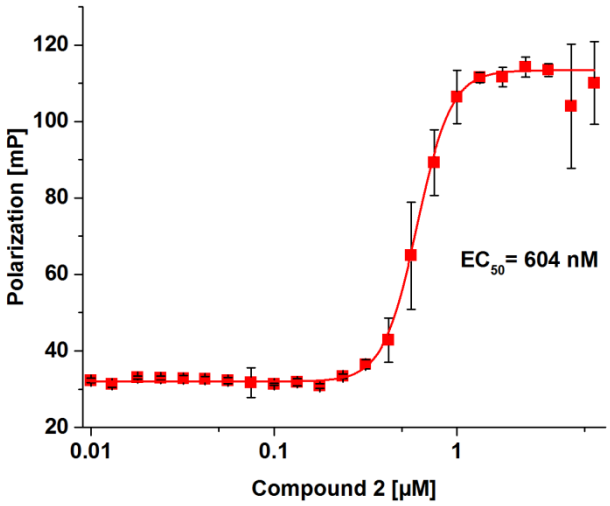


**Figure 8:** Fluorescence polarization titration curves for compound **2**. Each probe contained 10 nM of fluorescein-labeled 51 bp DNA fragment from -85 to –35 bp relative to *pqsA* TSS supplemented with 1 µM protein. Compound **2** was added at increasing concentrations (0 – 100 µM). Data represent the mean values and standard deviations of one experiment with n=2.

## Determination of inverse agonist-liganded PqsR binding sites by mutational analysis

Serial mutants of the native *pqsA* promotor fragment (DNA sequences **10**-**23,** Figure 9/Table 3) were analyzed for their binding capability ($K_d$) in fluorescence polarization competition experiments in the presence of compound **2**. Again, we conducted exchanges of a set of six residues of the native 51 bp *pqsA* promotor. Among these 14 variants (**10**-**23**), fragments **10**-1**5** did not considerably alter the affinity ($K_d$ values ranging from 28 to 59 nM). In contrast, fragments **16**-**19** showed a strongly reduced binding affinity in the presence of compound **2**. These variants harbor mutations within the above identified anchor site I with a major impact on protein-DNA interaction in case of fragment **17** (Figure 9). Notably, mutations within the downstream half of site II did not greatly influence affinity (fragments **22** and **23**). Mutations within the upstream located side of site II (fragment **19**) led to a moderate impairment of binding affinities indicating a partial occupancy of this region. Further work investigated the minimal DNA sequence length essential for PqsR binding. For that purpose, a focused set of truncated DNA fragments was constructed and tested

within this *in vitro* setup in the presence of compound **2**. The results confirmed the former observations of a partial occupancy of site II (Table 4).

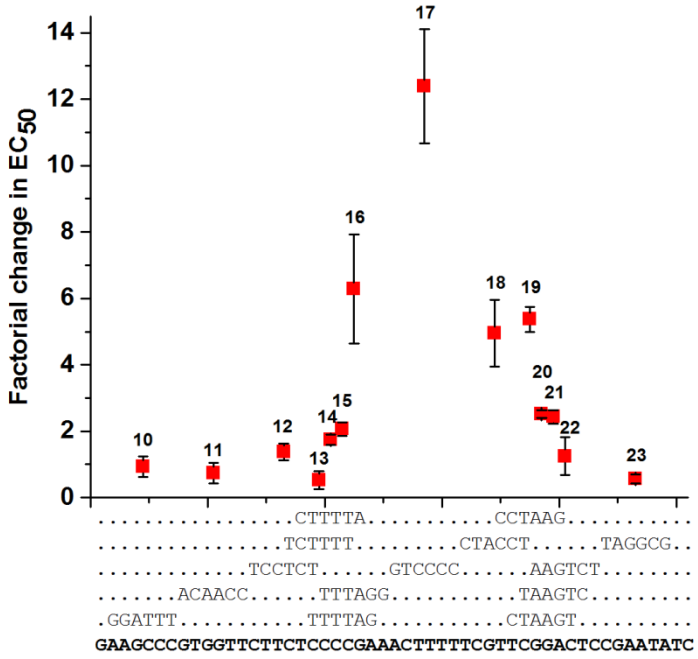


**Figure 9**: Graphical view of the results shown in Table 3 highlighting the factorial impact of the six residue mutations on $EC_{50}$. Factors are calculated in relation to the native DNA fragment (see Table 3). Native DNA sequence is marked in bold. The mutated six residue nucleotide sequences are indicated above. Each data point marks the middle of the respective six nucleotide mutation. Data represent the mean values and standard deviations of at least two independent experiments with n=2. Numbers above each data point refer to the respective DNA fragment number.

**Table 3** Determination of equilibrium constants (Kd) calculated from EC50 values for PqsR and the native or artificial pqsA promotor DNA fragments in the presence of compound 2 (10 µM) by fluorescence polarization competition experiments. Replaced residues (A→G, C →T) are marked in blue. Site I is marked in bold, site II is underlined. Data represent mean values and standard deviations of at least two independent experiments with n=2.

| name | mutated promotor fragments -85 to -35 bp relative to *pqsA* TSS (5´→3´) | $EC_{50}$ [nM] | $K_d$ [nM] |
|---|---|---|---|
| native | GAAGCCCGTGGTTCTTCTCCC**CGAAACTTTTTCG**TTCGGACTCCGAATATC | 64 +/- 12 | 28 +/- 6 |
| 10 | GGGATTTGTGGTTCTTCTCCC**CGAAACTTTTTCG**TTCGGACTCCGAATATC | 60 +/- 20 | 27 +/- 9 |
| 10 | GGGATTTGTGGTTCTTCTCCC**CGAAACTTTTTCG**TTCGGACTCCGAATATC | 60 +/- 20 | 27 +/- 9 |
| 11 | GAAGCCCACAACCCTTCTCCC**CGAAACTTTTTCG**TTCGGACTCCGAATATC | 47 +/- 20 | 21 +/- 9 |
| 12 | GAAGCCCGTGGTTTCCTCTCC**CGAAACTTTTTCG**TTCGGACTCCGAATATC | 88 +/- 16 | 39 +/- 7 |
| 13 | GAAGCCCGTGGTTCTTTCTTTT**GAAACTTTTTCG**TTCGGACTCCGAATATC | 34 +/- 17 | 15 +/- 8 |
| 14 | GAAGCCCGTGGTTCTTCCTTT**TA**AAACTTTTTCGTTCGGACTCCGAATATC | 112 +/- 10 | 50 +/- 4 |
| 15 | GAAGCCCGTGGTTCTTCTTTT**TAG**AACTTTTTCGTTCGGACTCCGAATATC | 132 +/- 13 | 59 +/- 6 |
| 16 | GAAGCCCGTGGTTCTTCTCTT**TAGG**ACTTTTTCGTTCGGACTCCGAATATC | 402 +/- 105 | 179 +/- 46 |
| 17 | GAAGCCCGTGGTTCTTCTCCC**CGAAGTCCCC**TCGTTCGGACTCCGAATATC | 793 +/- 110 | 352 +/- 49 |
| 18 | GAAGCCCGTGGTTCTTCTCCC**CGAAACTTTTCTA**CCTGGACTCCGAATATC | 317 +/- 64 | 141 +/- 29 |
| 19 | GAAGCCCGTGGTTCTTCTCCC**CGAAACTTTTTCG**CCTAAGCTCCGAATATC | 344 +/- 24 | 153 +/- 11 |
| 20 | GAAGCCCGTGGTTCTTCTCCC**CGAAACTTTTTCG**TCTAAGTTCCGAATATC | 161 +/- 7 | 71 +/- 3 |
| 21 | GAAGCCCGTGGTTCTTCTCCC**CGAAACTTTTTCG**TTTAAGTCCCGAATATC | 156 +/- 13 | 69 +/- 6 |
| 22 | GAAGCCCGTGGTTCTTCTCCC**CGAAACTTTTTCG**TTCAAGTCTCGAATATC | 80 +/- 36 | 36 +/- 16 |
| 23 | GAAGCCCGTGGTTCTTCTCCC**CGAAACTTTTTCG**TTCGGACTCTAGGCGTC | 36 +/- 9 | 16 +/- 4 |

**Table 4** Equilibrium constants ($K_d$) and $EC_{50}$ values of truncated pqsA promotor DNA fragments determined in the presence of compound 2 (10 µM) by fluorescence polarization competition experiments with site I in bold and site II underlined. Data represent mean values and standard deviations of at least two independent experiments with n=2.

| name | truncated *pqsA* promotor fragments (5´→ 3´) | $EC_{50}$ [nM] | $K_d$ [nM] |
|---|---|---|---|
| native | GAAGCCCGTGGTTCTTCTCCC**CGAAACTTTTTCG**TTCGGACTCCGAATATC | 64 +/- 12 | 28 +/- 7 |
| 24 | GTGGTTCTTCTCCC**CGAAACTTTTTCG**TTCGGACTCCGAATATC | 103 +/- 14 | 46 +/- 6 |
| 25 | CTTCTCCC**CGAAACTTTTTCG**TTCGGACTCCGAATATC | 107 +/- 14 | 48 +/- 6 |
| 26 | C**CGAAACTTTTTCG**TTCGGACTCCGAATATC | 225 +/- 2 | 100 +/- 1 |
| 27 | GAAGCCCGTGGTTCTTCTCCC**CGAAACTTTTTCG**TTCGGACTC | 79 +/- 5 | 35 +/- 2 |
| 28 | GAAGCCCGTGGTTCTTCTCCC**CGAAACTTTTTCG**TTCGGA | 230 +/- 16 | 102 +/- 7 |
| 29 | GAAGCCCGTGGTTCTTCTCCC**CGAAACTTTTTCG**TTC | > 3000 | > 1332 |
| 30 | GTGGTTCTTCTCCC**CGAAACTTTTTCG**TTCGGACTC | 132 +/- 21 | 59 +/- 9 |
| 31 | CTTCTCCC**CGAAACTTTTTCG**TTCGGACTC | 159 +/- 1 | 71 +/- 1 |

### *In vivo* regulatory role of the identified binding site I

In addition to the *in vitro* FP experiments, gene expression experiments were conducted to explore the relevance of the novel identified site I in the control of the *pqsABCDE* operon in the whole-cell environment. For this purpose, we introduced six site-directed mutations within nucleotides most critical for DNA binding (Table 3, fragment **17**) and measured the PqsR-mediated expression of β-galactosidase activity of *pqsA*p-*lacZ* transcriptional fusions in the absence and presence of the natural agonist PQS. Initially, the heterologous host *E. coli* was chosen to decouple transcription of the *pqsA* promotor from the complexity of the native regulation in *P. aeruginosa*. In the absence of any ligand, *E. coli* strain containing plasmid pEAL08-2 with mutated binding site I showed a reduced basal expression level of β-galactosidase compared to wild-type (Figure 10).

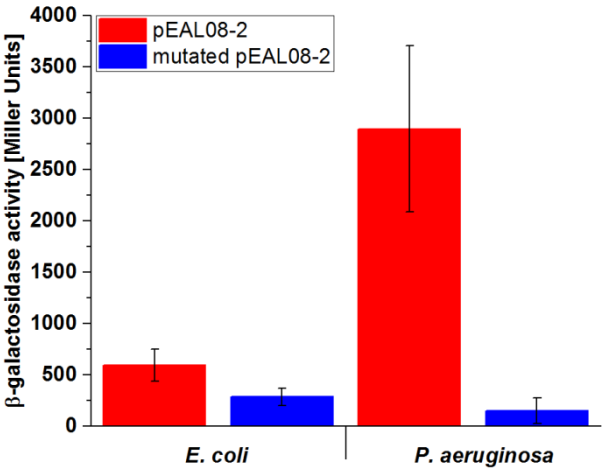


**Figure 10:** Basal reporter gene expression levels of pEAL08-2 wildtype and –mutant plasmid in *E.coli* and PA. Data represent the mean values and standard deviations of at least two experiments with n=4.

Interestingly, the 6 bp alteration in site I caused a strong decrease of PQS-induced transcriptional activation (Figure 11 A & C) which is in accordance with impaired DNA binding ability in *in vitro* FP assay (Figure 9, Table 1, fragment 1). In a similar fashion, the basal β-galactosidase level of *E. coli* cells harboring wild-type plasmid pEAL08-2 is reduced in response to increasing concentrations of compound **2**. Furthermore, switching to the plasmid with the 6 bp mutation within the promotor site leads to a heterologous system which is not responsive to compound **2** anymore (Figure 11 B & D). Finally, we obtained comparable results with mutated and wild-type plasmids (pEAL08-2/ mutated pEAL08-2) introduced in PQS-deficient *P. aeruginosa* PA14 Δ*pqsA* strain. While the transcriptional activity of PqsR could be induced (addition of PQS) or suppressed (addition of compound **2**) using the wild-type plasmid, compound **2** did not have a repressive effect on β-galactosidase expression when the addressed 6 bp were mutated. The transcriptional activation was only slightly enhanced under addition of PQS. Furthermore, a strong decrease in basal activity was observed (Figure 10). To conclude, the observed impacts of mutations on the transcriptional activity of the promotor suggest that site I is mandatory for productive binding of PqsR in the whole cell environment.

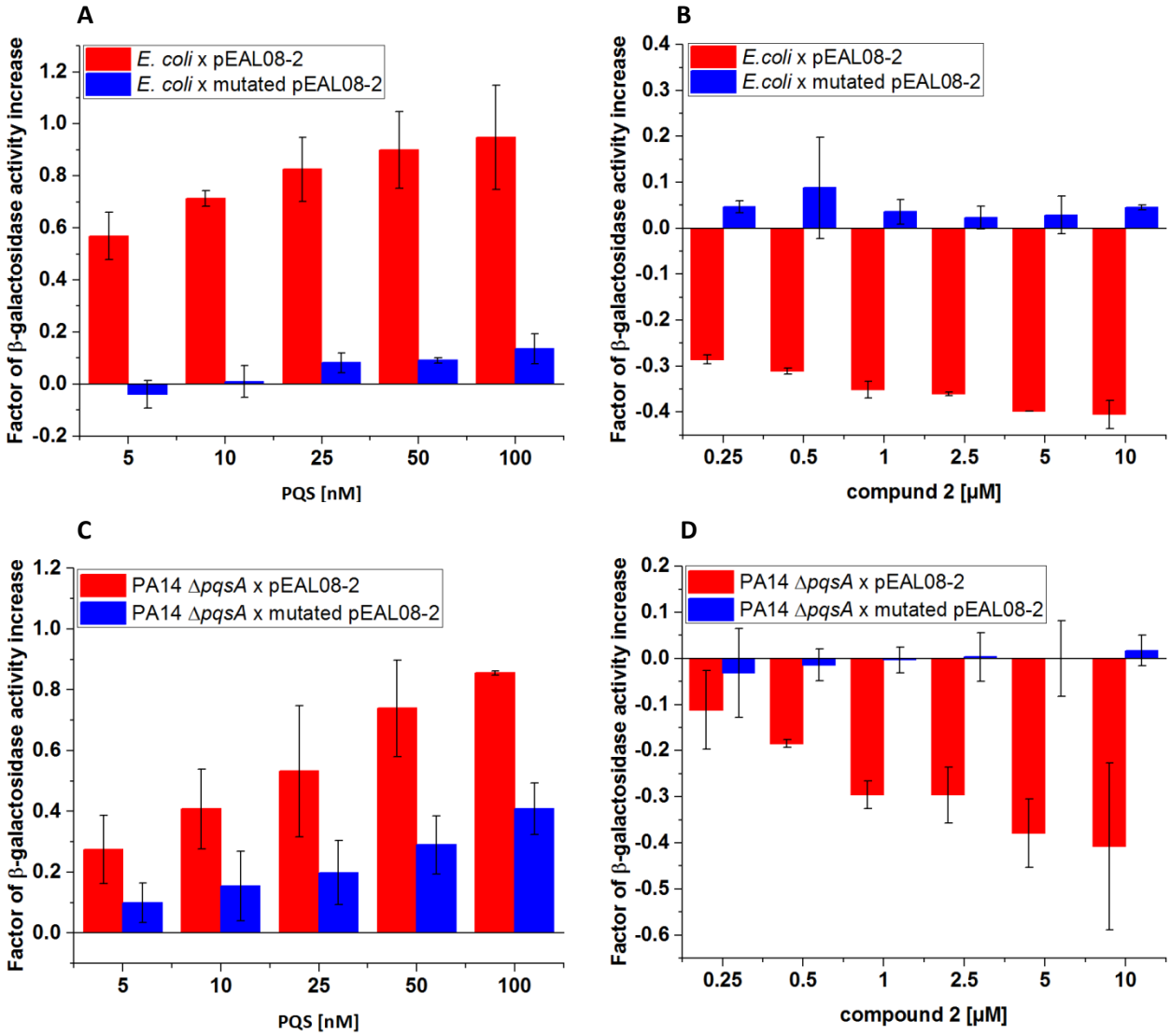


**Figure 11**: Reporter activity of *E. coli* DH5α (**A** & **B**) and *P. aeruginosa* PA14 Δ*pqsA* cells (**C** & **D**) harboring plasmid pEAL08-2 with native or mutated binding site I within the *pqsA* promotor. β-galactosidase activity was quantified in the absence or presence of either PQS (**A** & **C**) or compound **2** (**B** & **D**) and is represented as factor of galactosidase activity increase in relation to basal level (=0). Data represent the mean values and standard deviations of at least two independent experiments with n=4.

## Discussion

Fluorescence polarization (FP) assays can be used to investigate interactions of macromolecules with a variety of ligands (for a review see Lea and Simeonov, 2011). The smaller interaction partner is labelled with a fluorescence probe which is excited with linear polarized light. Due to the free rotation of the unbound labelled ligand depolarization of the emitted light occurs. If the dye-conjugated molecule binds to a macromolecular partner, its rotational speed is decreased due to the higher mass of the resulting ligand-receptor complex. This leads to an increase of anisotropy of the emitted light and, thus, higher fluorescence polarization. This change in polarization of emitted light upon binding can be detected using fluorescence spectrometers equipped with polarization filters and used to determine binding affinities. If the mass difference between the interaction partners is big enough, even macromolecule-macromolecule interactions (e.g. between DNA and protein) can be investigated (Anderson et al.; Sevenich et al., 1998);. Hence, FP was the method of choice to gain more insight into the molecular recognition events between transcriptional regulator PqsR and the respective promotor DNA. In the present study, the application of fluorescence polarization for quantitative protein-DNA analysis in combination with mutated nucleotides led to the identification of two distinct adjacent PqsR binding sites. We have found that site I seems to be a hotspot for PqsR-DNA interaction regardless of the presence of agonist, inverse agonist, or simply no ligand. The co-inducer PQS, however, induces binding to an additional site II, which has been reported to be important for transcription activation as evidenced by *in vivo* gene expression experiments (Xiao et al., 2006a). Although fluorescence-polarization-based quantitative protein-DNA analysis does not consider supercoiled DNA as in the *in vivo* situation, it represents a rapid and facile method to gain insight into interaction propensities between these biomacromolecules. Through highlighting novel regions of affinity within the promotor sequence, our results further support the perception of a transcriptional activation mechanism proposed for some other functionally characterized LTTR proteins (Muraoka et al., 2003; Lochowska et al., 2001). The presence of the applied inverse agonists of differing structural scaffolds led to an interaction profile of PqsR on DNA similar to unliganded PqsR. As a major difference to apo PqsR, however, the receptor-DNA interaction was strongly enhanced using a specific 51 bp oligomer when the inverse agonist was present. The data suggest that inverse agonists arrest PqsR in an unproductive state. Presumably, this prevents

favorable contacts between the regulator and RNA polymerase at site II of the *pqsA* promotor region essential for transcriptional activation (Tropel and van der Meer, 2004). The interaction with an enlarged DNA region upon PQS binding might be the result of conformational switches which render the regulator capable of binding to the divergent recognition element. Another possibility could involve a second binding site that is addressed under addition of the inverse agonist, located upstream or downstream of the promotor region. However, the exact mechanism of transcriptional activation and repression remains to be elucidated. It has to be noted, that a possible influence of the MBP-tag within the used full-length PqsR construct on the protein-DNA interaction cannot be ruled out completely. However, results presented in this work strongly support that the general interaction characteristics of PqsR are not impaired: The homotetrameric quaternary structure observed in our chemical crosslinking experiments is typical for most LTTRs and the affinity of the natural ligand PQS to this full-length MBP-tagged construct is similar to the one determined for the soluble (crystallizable) ligand binding domain. Hence, the general fold of the protein should not be affected by the tag. Importantly, we determined a substantial affinity to the LTTR box binding motif indicating that the expected binding capabilities have been conserved qualifying this construct as a suitable tool to facilitate interaction studies. To understand ligand-dependent structural changes responsible for differential DNA interaction, X-ray structures of full-length PqsR in complex with target DNA and PqsR ligands would be of great interest. Nevertheless, the results provide an exciting example of mechanism of action of an inverse agonist acting on this important anti-virulence target on a molecular basis and close a knowledge gap between ligand-protein interaction and functional response. These novel insights offer new perspectives for future anti-virulence drug development to fight the clinically highly relevant pathogen *Pseudomonas aeruginosa*.

## Materials and methods

### Construction of PqsR expression vector

A 1040 bp DNA fragment containing the *pqsR* gene of *P .aeruginosa* PAO1 was amplified using primers P1 and P2 (Sigma Aldrich, Germany) (Table 5). After digestion with *Mfe*I and *EcoR*I, the yielded fragment was cloned into the *Mfe*I restriction site of pMALC5e vector (New England Biolabs, Germany) using T4 DNA ligase (Invitrogen, Germany). Restriction enzymes were purchased from New England Biolabs, Germany.

**Table 5** Primers used in this study. Restriction sites are underlined.

| name | sequence 5´ → 3´ | function |
|---|---|---|
| P1 | TAACAATTGCACACAGGAAACAGAATT | *pqsR* forw (*Mfe*I) |
| P2 | TGGAGAATTCTCTACTCTGGTGCGGCGCG | *pqsR* rev (*EcoR*I) |
| P3 | GAGACCCGGGCTGCAGCAATTGGGAAGCCTGCAAATGGCAGGCGAGGC | overlap fragment 1 (f) |
| P4 | GATATTCGGAGTCCGAACGAGGGGACTTCGGGGAGAAGAACCACGGGCTTC | overlap fragment 1 (r) |
| P5 | GAAGCCCGTGGTTCTTCTCCCCGAAGTCCCCTCGTTCGGACTCCGAATATC | overlap fragment 2 (f) |
| P6 | GAGAGTCGACGACAGAACGTTCCCTCTTCAGCGATATGC | overlap fragment 2 (r) |

### Heterologous expression and purification of PqsR

100 ml of LB medium containing 100 µg/ml of Ampicillin were inoculated with *E. coli* BL21 (λDE3) harboring PqsR-MBP expression plasmid. Cultures were incubated over night at 37°C and 150 rpm. 1 liter of TB medium containing 100 µg/ml Ampicillin was inoculated with 10 ml of overnight culture and cells were grown until an $OD_{600}$ ~ 0.5 at 37°C and 150 rpm. To start the protein expression, IPTG was added at a final concentration of 0.3 mM and cells were incubated for 14 h at 22°C and 150 rpm. Cells were harvested through centrifugation for 20 min at 4000 xg, 8°C. The pellet was resuspended in 100 ml of lysis buffer (25 mM Tris-HCl pH 8.0, 150 mM NaCl, 5 mM β-mercaptoethanol and 0.5 mM PMSF). Resuspended cells were lysed using a french press. The yielded lysate was centrifuged at 25000 xg for 20 minutes at 4°C and filtered through a 0.45 µM syringe filter prior to FPLC purification. Purification of C-terminal MBP-tagged PqsR was performed in a two-step purification using FPLC (Äkta pure, GE Healthcare Lifesciences, Germany). Initially, an affinity chromatography using MBPTrap HP column (GE Healthcare Lifesciences) was

performed with 20 mM Tris, pH 8.0, 200 mM NaCl, 1 mM EDTA, 0-10 mM maltose. This was followed by a second purification step via FPLC size exclusion chromatography using HiLoad 16/600 Superdex 200 column (GE Healthcare Lifesciences, Germany) in 20 mM Tris, pH 8.0, 1 mM EDTA. Protein aliquots were frozen in liquid nitrogen and stored at -80 °C in 20 mM Tris, pH 8.0, 1 mM EDTA, 10 % glycerol. Purity of the protein was verified using SDS PAGE.

Construction of pEAL08-2 mutant reporter gene plasmid

DNA fragments of the *pqsA* promotor were PCR amplified using primer pairs P3/P4 and P5/P6 (Sigma Aldrich, Germany) as sown in table 5. The two amplified fragments were fused by overlap PCR. Finally, the overlap PCR product was cloned into the *Xho*I and *Sal*I restriction sites of plasmid pEAL08-2 (Cugini et al., 2007) to yield pEAL08-2 mutant plasmid. Restriction enzymes were purchased from New England Biolabs, Germany.

Reporter gene assays in *E.coli* and *P. aeruginosa*

pEAL08-2 plasmid harboring *pqsR* and β-galactosidase *lacZ* gene under control of the *pqsA* promotor or the pEAL08-2 mutant plasmid were transformed in *E.coli* DH5α and in a *P. aeruginosa* PA14 Δ*pqsA* transposon mutant strain. Assays were performed as previously described (Lu et al., 2014b). $IC_{50}$ values were calculated using Origin 9G software.

Determination of extracellular levels of HHQ in *P. aeruginosa*

For the quantification of extracellular HHQ levels, a previously reported method was used (Lu et al., 2014b) following an altered procedure (Lépine et al., 2003; Lépine et al., 2004) A *P. aeruginosa* PA14 Δ*pqsH* culture was grown for 17 h at 37°C in the presence of a DMSO control or compound respectively. 4-alkyl quinolones were extracted with ethyl acetate and quantified using 5,6,7,8-tetradeutero-2-heptyl-4(1*H*)-quinolone (HHQ-$d_4$) as internal standard. Analysis was performed as described before (Storz et al., 2012) using UHPLC-MS/MS. The following ions were monitored (mother ion [m/z], product ion [m/z], scan time [s], scan width [m/z], collision energy [V], tube lens offset [V]): HHQ: 244, 159, 0.5, 0.01, 30, 106; HQNO: 260, 159, 0.1, 0.01, 25, 88; HHQ-*d4* (IS): 248, 163, 0.1, 0.01, 32, 113. Data analysis was conducted

using Xcalibur software. Given data represent the mean of at least two independent experiments with measured triplicate values.

Fluorescence polarization assay

Fluorescein-labeled and unlabeled single-stranded DNA was purchased from Sigma Aldrich, Germany. Double-stranded oligonucleotides were prepared by annealing equimolar amounts of sense and antisense strands in 10 mM Tris, pH 7.9 followed by heating to 95°C for 6 minutes. Mixtures were allowed to cool down to room temperature for two hours. PqsR was diluted to 2 µM in 20 mM Tris, pH 8.0, 1 mM EDTA. The final mixture contained 10 nM fluorescein-labeled DNA, 1 µM PqsR and either compound **1** (5 µM) or **2** (10 µM) or DMSO as solvent control. Reactions were incubated for 2 hours at 25°C and fluorescence polarization was measured using BMG Labtech ClarioStar (BMG Labtech, Germany). $K_d$ values of PqsR and fluorescein-labeled DNA fragments were determined using 10 nM labeled DNA under addition of PqsR (0 – 5.6 µM), incubated with either DMSO or agonist respectively. For competition experiments, mixtures of 0.4 µM or 1 µM purified protein, 10 nM fluorescein-labeled DNA, unlabeled competitor DNA (0 – 25 µM) and DMSO or 2 µM PQS or 10 µM compound **2** were prepared. All reactions were incubated for 2h at 25°C. Fluorescence polarization was measured using a BMG ClarioStar platereader adjusted to $\lambda_{ex}$ = 485 nm and $\lambda_{em}$=520 nm. $K_d$ values for the unlabeled DNA fragments were calculated using equations (1) and (2).

Equation (1):

$$B = \frac{Kd,l + LT + RT - \overline{[(Kd,l + LT + RT)\text{^}2 - 4 * RT * LT]}}{2}$$

Equation (2):

$$Kd = \frac{0{,}5 * B * IC50 * Kd,l}{LT * RT \ + 0{,}5 * B * (-RT - LT + 0{,}5 * B - Kd,l)}$$

Using equation (1) (Invitrogen Corporation, 2006), the amount of labeled DNA bound to PqsR ($B$) can be calculated. The $EC_{50}$ values derived from the competition experiments for the unlabeled DNA fragments can be transformed in $K_d$ values using equation (2) (Nikolovska-Coleska et al., 2004). In direct titration experiments using

the labeled DNA fragment and PqsR under addition of compound **2** (100 µM), the $K_d$ of the labeled DNA was determined to be 201 nM. Variables: $Kd,l$= $K_d$ determined for the labeled DNA fragment; $LT$ = concentration of labeled DNA; $RT$= concentration of the receptor; $IC50$= $IC_{50}$ from the competition experiment; $Kd$= affinity of the unlabeled DNA fragment. Curve fitting was done using OrigonPro2015 and MARS data analysis software (BMG Labtech).

Cross-linking study

Crosslinking was conducted by the addition of 25 µM of bis[sulfosuccinimidyl]suberate to 5 µM PqsR-MBP. Reaction was carried out in phosphate-buffer (34 mM NaCl, 100 mM $K_2HPO_4$, pH 7.4, 2.7 mM KCl, 18 mM $KH_2PO_4$) that additionally contained either 1% DMSO or 5 µM of compound **1**. Prior to addition of BS3, the mixtures were preincubated for 90 min at 25 °C. The reaction was quenched in 2 min time intervals by addition of 60 mM Tris and analyzed on a 12% SDS-PAGE.

Isothermal Titration Calorimetry

ITC using purified PqsR-MBP (60 µM in 20 mM Tris, pH 8.0, 1 mM EDTA) and 4-*tert*-butyl benzamide was carried out as described before for truncated PqsR (Klein et al., 2012).

# Chapter 2: Publication A:
# “Optimization of anti-virulence PqsR antagonists regarding aqueous solubility and biological properties resulting in new insights in structure-activity relationships”
# (DOI: 10.1016/j.ejmech.2014.04.016)

European Journal of Medicinal Chemistry 79 (2014) 173–183

Contents lists available at ScienceDirect

European Journal of Medicinal Chemistry

journal homepage: http://www.elsevier.com/locate/ejmech

Short communication

## Optimization of anti-virulence PqsR antagonists regarding aqueous solubility and biological properties resulting in new insights in structure–activity relationships

Cenbin Lu [a,1], Benjamin Kirsch [a,1], Christine K. Maurer [a], Johannes C. de Jong [a], Andrea Braunshausen [a], Anke Steinbach [a], Rolf W. Hartmann [a,b,*]

[a] Helmholtz-Institute for Pharmaceutical Research Saarland, Campus C2.3, 66123 Saarbrücken, Germany
[b] Pharmaceutical and Medicinal Chemistry, Saarland University, Campus C2.3, 66123 Saarbrücken, Germany

ARTICLE INFO

*Article history:*
Received 29 October 2013
Received in revised form
3 April 2014
Accepted 4 April 2014
Available online 5 April 2014

*Keywords:*
*Pseudomonas aeruginosa* infection
Bacterial communication
*Quorum sensing* inhibitor
PqsR antagonist
Structure–activity relationship
Structure–property relationship

ABSTRACT

Increasing antibiotic resistance urgently requires novel therapeutic options to combat bacterial infections. The anti-virulence therapy selectively intervening with pathogenicity without affecting bacterial viability is such a strategy to overcome resistance. We consider the virulence regulator PqsR as an attractive target in the human pathogen *Pseudomonas aeruginosa*, and recently discovered the first PqsR antagonists, which, however, suffered from poor aqueous solubility. In this work, the antagonists were structurally modified to become more soluble, and their structure–activity as well as structure–property relationships were studied. A novel promising compound with improved solubility and enhanced anti-virulence activity was discovered ($IC_{50}$: 3.8 μM, pyocyanin). Our findings emphasize the crucial role of substituents at the 3-position and the carbonyl group at the 4-position for ligand–receptor interactions, and illuminate the way for further optimization of PqsR antagonists as anti-virulence agents.



### 1. Introduction

The opportunistic human pathogen *Pseudomonas aeruginosa* is one of the most common causes of nosocomial infections and a major problem in cystic fibrosis (CF) patients leading to inflammation, chronic persistent lung infections and high mortality [1,2]. Like many other pathogenic bacteria, *P. aeruginosa* expresses a battery of tissue-damaging virulence factors to facilitate infection via a cell density dependent cell-to-cell communication system known as *quorum sensing* [3] by secreting and sensing of signal molecules termed autoinducers (AIs). *P. aeruginosa* utilizes a unique species-specific *pqs* QS system [4], which is composed of two AIs, PQS (*P*seudomonas Quinolone Signal, Chart 1) and HHQ (2-heptyl-4-hydroxyquinoline), as well as PqsR which functions as a receptor and a virulence regulator [5,6]. The *pqs* QS system regulates expression of multiple virulence genes, such as *phzA1-G1*, which are involved in the biosynthesis of pyocyanin, *hcnAB*, responsible for the production of hydrogen cyanide, and *lasB*, which encodes elastase B [5,7]. Besides, PqsR drives the biosynthesis of its AI HHQ through activation of the *pqs* operon *pqsABCD*. HHQ is further converted to the more potent PQS by PqsH [8–10]. Thus, a positive autoinducing loop is triggered via stimulation of PqsR by PQS and HHQ [11].

The anti-virulence therapy using QS inhibitors (QSIs) selectively intervening with pathogenicity, e.g. by repressing the production of virulence factors, without impairing bacterial viability is discussed as an alternative approach to conventional anti-bacterial therapy. It is supposed that in anti-virulence therapy the selection pressure is reduced. This treatment option is therefore regarded as a promising strategy to overcome the rising and challenging resistance problem [12–14].

The critical virulence regulator PqsR has attracted rising attention by researchers as a favorable target for QSIs [15,16]. Based on the scaffold of the natural agonist HHQ, we recently developed the first PqsR antagonists. The compounds showed $IC_{50}$ values in the low nanomolar range (Chart 1) and reduced the production of the virulence factor pyocyanin in *P. aeruginosa* [17]. However, a major

* Corresponding author. Helmholtz-Institute for Pharmaceutical Research Saarland, Pharmaceutical and Medicinal Chemistry, Saarland University, Campus C2.3, 66123 Saarbrücken, Germany.
*E-mail addresses:* rolf.hartmann@helmholtz-hzi.de, rwh@mx.uni-saarland.de (R.W. Hartmann).
[1] These authors contributed equally to this work.

http://dx.doi.org/10.1016/j.ejmech.2014.04.016
0223-5234/

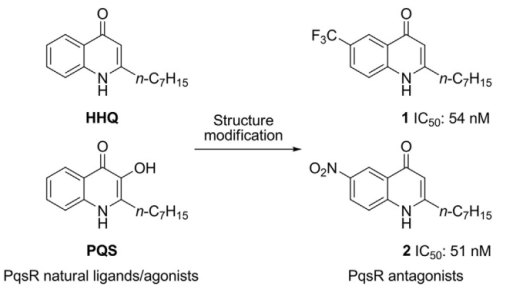


**Chart 1.** Discovery of the first PqsR antagonists by ligand-based approach.

drawback of these compounds is their poor aqueous solubility (<5 μM in 2% DMSO). This physicochemical property is essential for a compound to be considered as a drug candidate since a good solubility is important for pharmacokinetic properties [18]. Insufficient solubility is often the cause for failures in drug development [19]. Aiming at the improvement of the aqueous solubility we herein describe structure modifications of our PqsR antagonists and their impact on the biological properties of the new compounds, and discuss the obtained structure–activity (SAR) as well as structure–property relationships (SPR).

## 2. Results and discussion

### 2.1. Design

First, we suspected that the intermolecular stacking [20] or H-bond between the NH group at 1-position and the carbonyl group at 4-position may contribute to the poor solubility. Thus, a methyl group was introduced to block such interactions (compound class 1, Chart 2). Second, to increase the hydrophilicity, polar or ionisable groups were introduced into the molecule: oxygen was inserted into the alkyl side chain (compound class 2); the 3-position was substituted with e.g. amide, amino, carboxylic or hydroxamic acid groups (compound class 3); the benzene moiety substituted with electron withdrawing groups was replaced by pyridine (compound class 4). The structure modifications were performed based on antagonist **2** due to the good synthetic accessibility of the nitro compounds.

### 2.2. Chemistry

HHQ, **1**, **2**, **14**, **16**, **18**, **22**, **26** and **36** were synthesized as previously described [17]. Stirring of HHQ, **1** or **36** with methyl iodide under basic conditions yielded the class 1 compounds **3**–**5** (Scheme 1). Compounds **6**, **7**, **9** and **10** of class 2 were obtained by Conrad–Limpach cyclization: condensation of the β-ketoesters **33** and **34** with aniline or substituted anilines followed by cyclization of the resulting enamine in refluxing diphenyl ether yielded the desired products. Compound **11** was obtained via decarboxylation of **24** (Scheme 2). **6** was further converted to **8** by nitration. For preparation of class 3 and 4 compounds, the intermediates of the quinolone-3-carboxylic esters **17**–**20** and **29** were prepared by condensation of the isatoic anhydride derivatives with the β-ketoesters **32**–**34** under sodium hydride catalysis (Scheme 2). After hydrolysis of the quinolone-3-carboxylic esters the resulting acids **21**–**24** and **30** were further derivatized: **21** and **22** were condensed with ammonia or hydroxylamine to give the carboxamide **25** and the hydroxamic acids **27** and **28**, respectively. Decarboxylation of **30** at high temperature afforded **31**. Nitration of HHQ gave **12** (Scheme 1), which was further reduced to **13**. Reduction of the ester **17** with lithium aluminium hydride gave the hydroxymethyl compound **15** (Scheme 2).

### 2.3. Biological and physicochemical properties

The PqsR-mediated transcriptional effect of the compounds was evaluated as previously described in a β-galactosidase reporter gene assay in *Escherichia coli* containing the plasmid pEAL08-2. The latter encodes PqsR which is under control of the tac promoter and the β-galactosidase reporter gene *lacZ* controlled by the *pqsA* promoter. The solubility was initially determined based on observation of the solution clarity [17]. The eight best compounds were chosen for determination of PqsR antagonistic properties and calculation of logP values. Their aqueous solubility was determined using a standard HPLC protocol [21].

**Compound class 1**. The *O*-methylation of HHQ decreased the solubility of the molecule and led to neither agonistic nor antagonistic activity (**3**, Table 1), suggesting a critical role of the carbonyl group (but not NH group, see below) for the ligand–receptor interaction. As this modification led to a total loss of activity, we refrained from performing *O*-methylation with PqsR antagonists. The two *N*-methylated derivatives **4** and **5** revealed a moderate antagonistic activity with improved solubility compared with **1** (Tables 1 and 2). This result indicates the importance of the NH hydrogen for antagonistic activity. The better solubility might be due to the disruption of intermolecular interactions.

**Compound class 2**. Introduction of oxygen into the alkyl side chain of the antagonists **1** and **2** close to the quinolone core (**7** and **8,** Tables 1 and 2) resulted in a moderate antagonistic activity and an enhanced solubility (6–15 times). Interestingly, in case the oxygen was located far from the quinolone core (**10** and **11**), the potency was dramatically decreased (32–69 fold), whereas the solubility was strongly increased (15–66 fold). Similar as observed for the antagonists, the oxygen far from the core also made the agonists less potent (comparing **6** and **9**, Table 1). Overall, this data suggests that on one hand, the alkyl side chain-binding pocket of PqsR does not tolerate a deeply intruding oxygen (far from the core). On the other hand, such an oxygen imparts significant improvement of solubility possibly due to a better solvation without being shielded by the core.

**Compound class 3**. Most of the derivatives (**12**, **13**, **15**, **21**, **25** and **27**, Table 1) lacking the nitro group in 6-position displayed a moderate to strong agonistic activity regardless of the groups in 3-position. Particularly, removal of the nitro group in the antagonist **2** from the 6- into the 3-position resulted in agonist **12**, indicating that not only the electron-withdrawing property but also the position of the nitro group plays a crucial role for the antagonistic effect. Interestingly, the unique exception is the carboxylic acid ester **17**. Its weak antagonistic activity may be contributed to steric rather than electronic effects in contrast to **12**. However, a further introduction of a nitro group into the 6-positon of the ester (**18**, for **19** and **20**, combined with ether side chains) did not enhance the antagonistic activity. Substitution of the 3-position of antagonists **2**, **8** and **11** with a hydroxy (**14**), hydroxamic acid (**28**) or negatively ionizable group (carboxylic acids **22**–**24**) totally or partially reverses the functionality from antagonism to agonism, implying that the electron-donating property may favor PqsR stimulation. Most interestingly, a highly active antagonist **16** was regained from the pure agonist **14** through exchange of the hydroxy by a hydroxymethyl at the 3-position (Tables 1 and 2). Compound **26** with 3-carboxamide, as described in a previous work [22], is a potent antagonist. Overall, the result implies that substituents at the 3-

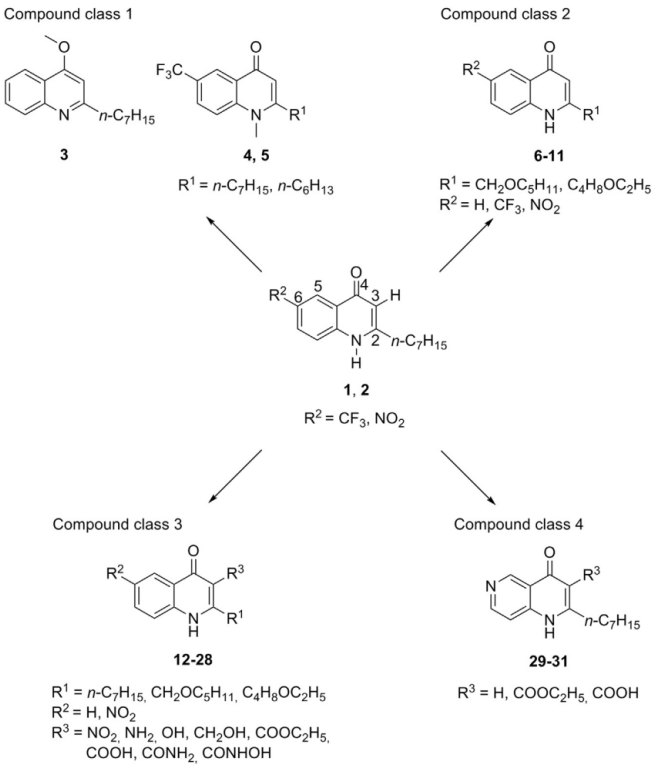


**Chart 2.** Structure modifications of PqsR antagonists **1** and **2** leading to compound classes 1–4.

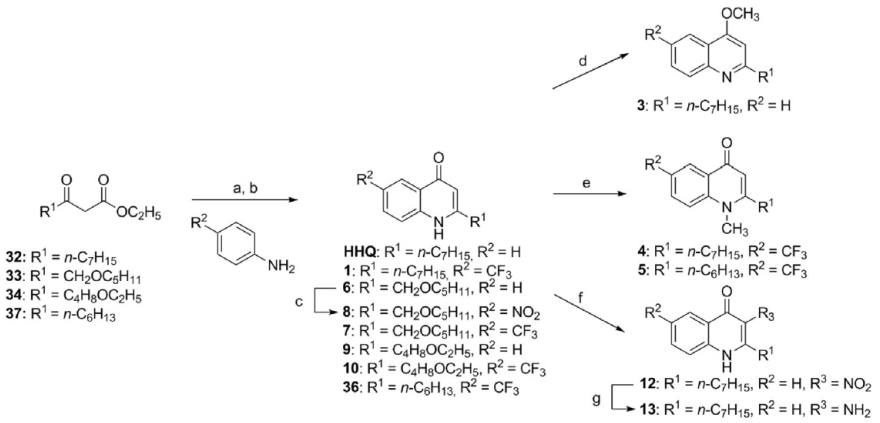


**Scheme 1.** Reagents and conditions: (a) *p*-TsOH·$H_2O$, *n*-hexane, reflux; (b) $Ph_2O$, reflux; (c) conc. $HNO_3$, conc. $H_2SO_4$, 0 °C – r.t.; (d) MeI, $Cs_2CO_3$, DMF, r.t.; (e) MeI, KOH, MeOH, r.t.; (f) conc. $HNO_3$, propionic acid, 110 °C; (g) $Fe^0$, $NH_4Cl$, EtOH, reflux.

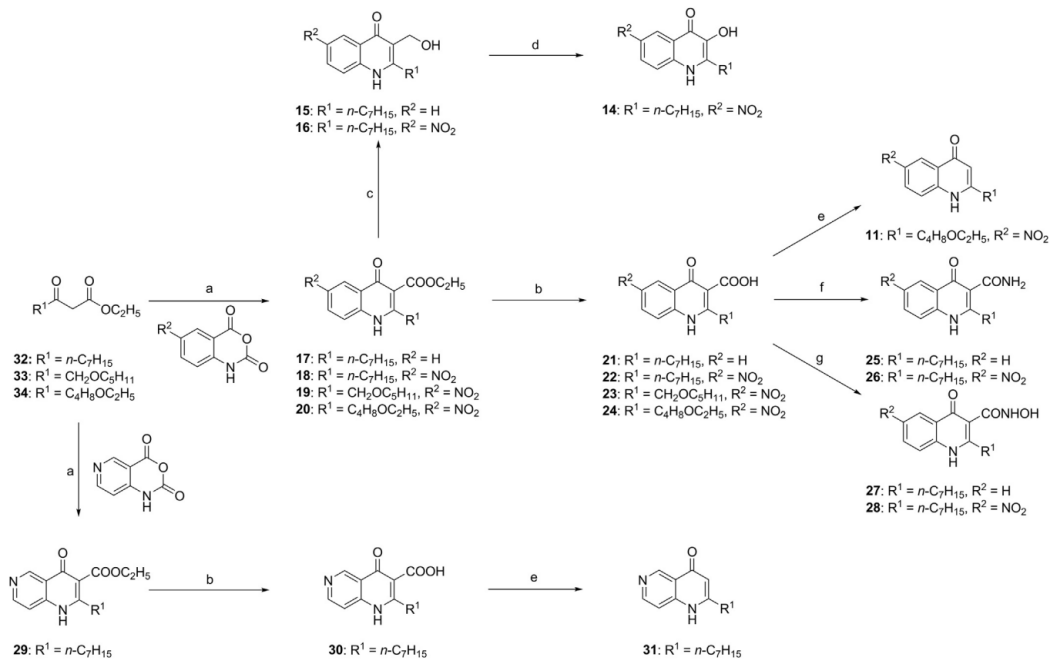


**Scheme 2.** Reagents and conditions: (a) NaH, dry DMF, r.t. then HCl; (b) NaOH, $H_2O$, reflux then HCl; (c) $LiAlH_4$, dry THF, 0 °C – r.t.; (d) $MnO_2$, dry THF, r.t. then $B(OH)_3$, conc. $H_2SO_4$, $H_2O_2$, THF, r.t.; (e) 310 °C; (f) *N,N′*-carbonyldiimidazole, $NH_3 \bullet H_2O$, dry DMF, 0 °C – r.t.; (g) *N,N′*-carbonyldiimidazole, *N*-methylmorpholine, $NH_2OH \cdot HCl$, dry DMF, 0 °C – r.t.

position are of decisive importance for the ligand functionality. Substitution in 3-position with amino or ionizable groups (**13**, **21**–**24**, **27** and **28**) resulted in a good solubility with the hydroxamic acids as the best compounds (>200 μM), while hydroxymethyl, ester and carboxamide groups led to either moderate enhancement (**15**, **16**, **18**, **19**, **25** and **26**) or slight reduction (**17** and **20**) of solubility compared with the corresponding unsubstituted compounds. The introduction of a nitro (**12**) or hydroxy group (**14**) did not make the compounds more soluble.

**Compound class 4**. Compound **31** shows agonistic properties (Table 1). Similar to the observation for the corresponding compounds from class 3 (**17** and **21**), the 3-ester **29** is an antagonist, whereas the 3-carboxylic acid **30** revealed agonistic activity. This result shows that the nitro group cannot be replaced by an aromatic ring nitrogen at same position without losing antagonism. As expected, all pyridine derivatives showed a good solubility.

According to the *in silico* prediction, the clogP values of the eight selected compounds are reduced except for compound **16** (Table 2, calculation with ACD Percepta Classic method). The decreased logP values are generally correlated to the enhanced water solubility.

In the next step the selected antagonists were evaluated for their effects on the production of the autoinducer PQS and the virulence factor pyocyanin in *P. aeruginosa*. Similar to the potent anti-virulence compound **26**, **16** with a hydroxymethyl group at the 3-position was able to efficiently repress the biosynthesis of PQS and pyocyanin, whereas all compounds unsubstituted in 3-position (**4**, **7**, **8**, **10** and **11**) were less active (Table 2). Beside this low antagonistic activity toward PqsR, the metabolic susceptibility in 3-position shall play a critical role for the low effectiveness of the unsubstituted compounds in *P. aeruginosa* as previously described for antagonist **2** [22].

Metal-chelating properties lead to growth inhibition of the bacteria via destabilization of the outer membrane [23,24] or reduction of iron availability [25], which is therefore unwanted for an anti-virulence strategy. The CAS iron chelation assay [26] showed that the most potent antagonists **16** and **26** do not have such undesirable properties (data not shown). As expected, no growth inhibition was observed for all tested antagonists in the PQS and pyocyanin assays (data not shown), indicating that their QS or virulence factor inhibitory effects are not caused via impairing bacterial viability.

## 3. Conclusion

Aiming at the development of more soluble and potent PqsR-targeting QSIs for an anti-virulence therapy, four classes of new quinolone compounds were designed and synthesized based on the scaffold of the first PqsR antagonists, and their SAR as well as SPR were systematically investigated. Particularly, a very promising compound **16** arose from this research with improvement on both aqueous solubility and virulence factor inhibition. Our findings give new insights into the ligand–receptor interactions for PqsR: the substituents at 3-position play a critical role for the ligand functionality, and the carbonyl group at 4-position is essential for the interactions between ligand and protein. These results provide a promising starting point for further optimization of PqsR antagonists to combat *P. aeruginosa* infections.

**Table 1**
Determination of solubility and evaluation of agonistic and antagonistic activities of compounds in reporter gene assay.

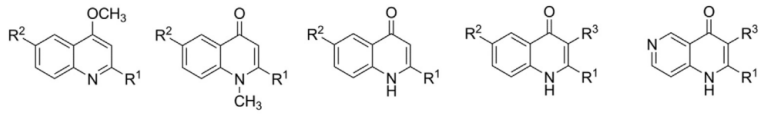


**3** **4,5** **HHQ, 1, 2, 6-11** **12-28** **29-31**

| Compd. | $R^1$ | $R^2$ | $R^3$ | Solubility in 2% DMSO[a], [μM] | PqsR stimulation induced by 5 μM test compd. compared to 50 nM PQS (=1.00)[b] | Inhibition of PqsR stimulation induced by 50 nM PQS in the presence of test compd. (full inhibition = 1.00)[b] | |
|---|---|---|---|---|---|---|---|
| | | | | | | 50 nM | 5 μM |
| *Reference compounds* | | | | | | | |
| **HHQ** | $n$-$C_7H_{15}$ | H | – | 15–50 | 0.75*[c] | – | – |
| **1** | $n$-$C_7H_{15}$ | $CF_3$ | – | <5 | 0.00 | 0.54* | 1.00* |
| **2** | $n$-$C_7H_{15}$ | $NO_2$ | – | <5 | 0.00[d] | 0.73* | 1.00* |
| *Compound class 1: N or O-methylation in 1- or 4-position* | | | | | | | |
| **3** | $n$-$C_7H_{15}$ | H | – | 5–15 | 0.03 | −0.23* | −0.06 |
| **4** | $n$-$C_7H_{15}$ | $CF_3$ | – | 5–15 | 0.00 | 0.31* | 1.00* |
| **5** | $n$-$C_6H_{13}$ | $CF_3$ | – | 15–50 | 0.00 | 0.45* | 1.00* |
| *Compound class 2: introduction of oxygen into 2-alkyl side chain* | | | | | | | |
| **6** | $CH_2OC_5H_{11}$ | H | – | >200 | 0.89* | 0.11 | 0.06 |
| **7** | $CH_2OC_5H_{11}$ | $CF_3$ | – | 15–50 | 0.00 | 0.29* | 1.00* |
| **8** | $CH_2OC_5H_{11}$ | $NO_2$ | – | 15–50 | 0.00 | 0.49* | 1.00* |
| **9** | $C_4H_8OC_2H_5$ | H | – | >200 | 0.31* | 0.54* | 0.42* |
| **10** | $C_4H_8OC_2H_5$ | $CF_3$ | – | >200 | 0.02 | 0.08 | 0.69* |
| **11** | $C_4H_8OC_2H_5$ | $NO_2$ | – | 50–100 | 0.13 | 0.06 | 0.72* |
| *Compound class 3: substitution in 3-position* | | | | | | | |
| **12** | $n$-$C_7H_{15}$ | H | $NO_2$ | <5 | 0.84* | 0.14 | 0.17 |
| **13** | $n$-$C_7H_{15}$ | H | $NH_2$ | 50–100 | 1.22* | −0.04 | −0.07 |
| **14** | $n$-$C_7H_{15}$ | $NO_2$ | OH | <5 | 1.25* | −0.31* | −0.29* |
| **15** | $n$-$C_7H_{15}$ | H | $CH_2OH$ | 50–100 | 0.49* | 0.05 | 0.28* |
| **16** | $n$-$C_7H_{15}$ | $NO_2$ | $CH_2OH$ | 5–15 | 0.00 | 0.45* | 1.00* |
| **17** | $n$-$C_7H_{15}$ | H | $COOC_2H_5$ | 5–15 | 0.00 | 0.18 | 0.32* |
| **18** | $n$-$C_7H_{15}$ | $NO_2$ | $COOC_2H_5$ | 5–15 | 0.00 | −0.08 | 0.20* |
| **19** | $CH_2OC_5H_{11}$ | $NO_2$ | $COOC_2H_5$ | 15–50 | 0.00 | 0.02 | 0.13 |
| **20** | $C_4H_8OC_2H_5$ | $NO_2$ | $COOC_2H_5$ | 5–15 | 0.09 | 0.02 | 0.27* |
| **21** | $n$-$C_7H_{15}$ | H | COOH | 15–50 | 0.73* | 0.12 | 0.41* |
| **22** | $n$-$C_7H_{15}$ | $NO_2$ | COOH | 15–50 | 0.78* | 0.11 | 0.34* |
| **23** | $CH_2OC_5H_{11}$ | $NO_2$ | COOH | 50–100 | 0.48* | 0.07 | 0.06 |
| **24** | $C_4H_8OC_2H_5$ | $NO_2$ | COOH | 50–100 | 0.42* | 0.01 | 0.33* |
| **25** | $n$-$C_7H_{15}$ | H | $CONH_2$ | 5–15 | 0.65* | 0.08 | 0.27* |
| **26** | $n$-$C_7H_{15}$ | $NO_2$ | $CONH_2$ | 15–50 | 0.00 | 0.60* | 1.00* |
| **27** | $n$-$C_7H_{15}$ | H | CONHOH | >200 | 0.83* | 0.15 | 0.29 |
| **28** | $n$-$C_7H_{15}$ | $NO_2$ | CONHOH | >200 | 0.30* | 0.30* | 0.78* |
| *Compound class 4: replacement of the benzene moiety by pyridine* | | | | | | | |
| **29** | $n$-$C_7H_{15}$ | – | $COOC_2H_5$ | 50–100 | 0.02 | 0.24* | 0.76* |
| **30** | $n$-$C_7H_{15}$ | – | COOH | 50–100 | 0.66* | 0.06 | 0.20 |
| **31** | $n$-$C_7H_{15}$ | – | H | 50–100 | 0.82* | 0.08 | 0.02 |

[a] Aqueous solutions containing 2% DMSO of the test compounds were prepared with final concentrations of 5, 15, 50, 100 and 200 μM. The solution clarity was examined.
[b] β-Galactosidase reporter gene assay was performed in *E. coli* transformed with plasmid pEAL08-2 encoding PqsR and reporter gene *lacZ* controlled by *pqsA* promoter. Mean value of at least two independent experiments with $n = 4$, standard deviation less than 25%. Significance: For the agonist test, induction compared to the basal value; for the antagonist test, reduction of the PQS-induced stimulation. *$p < 0.05$.
[c] Determined at 1 μM.
[d] Determined at 10 μM.

## 4. Experimental

### 4.1. Chemistry

Chemical and Analytical Methods.$^1$H and $^{13}$C NMR spectra were recorded on a Bruker DRX-500 instrument. Chemical shifts are given in parts per million (ppm) with the solvent resonance as internal standard for spectra obtained in $CDCl_3$, MeOH-$d_4$ and DMSO-$d_6$. All coupling constants ($J$) are given in hertz. Mass spectrometry (LC/MS) was performed on a MSQ® electro spray mass spectrometer (Thermo Fisher). The system was operated by the standard software Xcalibur®. A RP C18 NUCLEODUR® 100-5 (125 × 3 mm) column (Macherey–Nagel GmbH) was used as stationary phase with water/acetonitrile mixtures as eluent. All solvents were HPLC grade. Reagents were used as obtained from commercial suppliers without further purification. Flash chromatography was performed on silica gel 60, 70–230 mesh (Fluka) and the reaction progress was determined by thin-layer chromatography (TLC) analyses on silica gel 60, $F_{254}$ (Merck). Visualization was accomplished with UV light and staining with basic potassium permanganate ($KMnO_4$). The melting points were measured using melting point apparatus SMP3 (Stuart Scientific). The apparatus is uncorrected.

The following compounds were prepared according to previously described procedures: 1*H*-pyrido[4,3-*d*][1,3]oxazine-2,4-dione [27], HHQ, PQS, **1**, **2**, **14**, **16**, **18**, **22**, **26**, **32**, **36** and **37** [17].

**Table 2**
Physicochemical properties, PqsR antagonistic effects as well as reduction of PQS and pyocyanin levels in *P. aeruginosa* for selected antagonists.

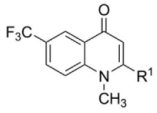

**4**: $R^1 = n\text{-}C_7H_{13}$
**5**: $R^1 = n\text{-}C_6H_{15}$

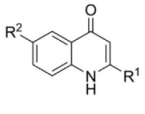

**1**: $R^1 = n\text{-}C_7H_{15}$, $R^2 = CF_3$
**2**: $R^1 = n\text{-}C_7H_{15}$, $R^2 = NO_2$
**7**: $R^1 = CH_2OC_5H_{11}$, $R^2 = CF_3$
**8**: $R^1 = CH_2OC_5H_{11}$, $R^2 = NO_2$
**10**: $R^1 = C_4H_8OC_2H_5$, $R^2 = CF_3$
**11**: $R^1 = C_4H_8OC_2H_5$, $R^2 = NO_2$

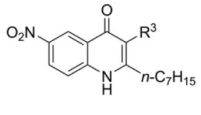

**16**: $R^3 = CH_2OH$
**26**: $R^3 = CONH_2$

| Compd. | clogP[a] | Solubility in 2% DMSO[b], [μM] | PqsR antagonistic activity $IC_{50}$, [nM] | Reduction with compd. at 15 μM, [%] | |
|---|---|---|---|---|---|
| | | | | PQS[c] | Pyocyanin[c] |
| *Reference compounds/starting point* | | | | | |
| **1** | 7.29/6.83 | 1.2 | 54 | −2.4[e] | 27*[e] |
| **2** | 6.73/5.31 | 5.6 | 51 | 14* | 44* |
| *Selected antagonists* | | | | | |
| **4** | 5.60/6.59 | 9.3 | 270 | 8.9 | 58* |
| **5** | 5.07/5.32 | n.d.[d] | 229 | n.d.[d] | n.d.[d] |
| **7** | 5.90/4.90 | 18 | 172 | 21 | 29* |
| **8** | 5.35/3.59 | 34 | 253 | 23* | 27* |
| **10** | 4.93/3.91 | 80 | 1712 | 8.6[e] | 39*[e] |
| **11** | 4.37/3.12 | 85 | 3511 | 13[e] | 23*[e] |
| **16** | 6.94/4.67 | 9.4 | 72 | 33* | 83* ($IC_{50}$: 3.8 μM) |
| **26** | 5.45/3.67 | 7.8 | 35 | 37* | 81* ($IC_{50}$: 2.0 μM) |

[a] The clogP values were calculated with ACD Percepta logP Classic/GALAS.
[b] Solubility was measured with HPLC method.
[c] PQS and pyocyanin assays were performed in *P. aeruginosa* PA14. All compounds were dissolved in LB medium. Mean value of at least two independent experiments with $n = 3$, standard deviation less than 25%. Significance: decrease of PQS levels or pyocyanin production compared to basal value, $^*p < 0.05$.
[d] Not determined.
[e] Determined at 10 μM, 250 μM and 100 μM, respectively.

**Procedure A**. A solution of β-ketoester (9.24 mmol, 1.0 equiv), aniline (9.24 mmol, 1.0 equiv) and *p*-TsOH·$H_2O$ (50 mg, 0.29 mmol, 3 mol %) in *n*-hexane (20 mL) was heated at reflux using a Dean–Stark separator for 5 h. After cooling the solution was concentrated under reduced pressure and the residue was added dropwise to refluxing (260 °C) diphenyl ether (5 mL). Refluxing was continued for 30 min. After cooling to room temperature, diethyl ether (15 mL) was added and the mixture was left standing overnight at 5 °C. The crystalline solid was isolated by filtration and washed with diethyl ether. The product was further purified by recrystallization from ethyl acetate or column chromatography on silica gel [17].

**Procedure B**. Under nitrogen atmosphere β-ketoester (15 mmol, 1.0 equiv) was added to a suspension of sodium hydride (50–65% w/w, 0.72 g, 15 mmol, 1.0 equiv) in dry DMF (50 mL), causing the liberation of hydrogen gas. A solution of isatoic anhydride derivative (15 mmol, 1.0 equiv) in dry DMF (30 mL) was added dropwise and stirred overnight. Most of the solvent was removed under reduced pressure and the remaining solvent treated with 1 M HCl, yielding the crude product as a yellow solid [28]. The 4-oxo-1,4-dihydroquinoline-3-ester derivative was purified by recrystallization from ethyl acetate/methanol or column chromatography on silica gel. The ester was suspended in 10% NaOH solution and heated at reflux for 4 h. After cooling to 0 °C on an ice water bath and extraction with ethyl acetate, the water phase was acidified with conc. HCl to reach a pH of 4.0–6.0. The 4-oxo-1,4-dihydroquinoline-3-carboxylic acid was isolated by filtration, washed with water and dried under vacuum.

*4.1.1. 2-Heptyl-4-methoxyquinoline (**3**)*

A mixture of HHQ (200 mg, 0.82 mmol, 1.0 equiv), $Cs_2CO_3$ (410 mg, 1.26 mmol, 1.5 equiv) and dry DMF (5 mL) was stirred at room temperature for 1 h. Methyl iodide (0.61 g, 4.32 mmol, 5.0 equiv) was added dropwise and the mixture was stirred for further 48 h. The reaction was poured onto water (16 mL) and diluted with chloroform (25 mL). The organic layer was washed with water (16 mL), dried over sodium sulfate and concentrated under reduced pressure [29]. After column chromatography on silica gel (twice, dichloromethane/methanol, 130/1 and n-hexane/ethyl acetate, 15/1) the product was isolated as a white solid (40 mg, 0.16 mmol, 20%), mp 40.5–41.3 °C. $^1$H NMR (500 MHz, $CDCl_3$): $\delta = 0.86$ (t, $J = 7.0$ Hz, 3H), 1.24–1.42 (m, 8H), 1.79 (quint, $J = 7.5$ Hz, 2H), 2.89 (t, $J = 7.5$ Hz, 2H), 4.01 (s, 3H), 6.61 (s, 1H), 7.41 (td, $J = 1.5$, 7.5 Hz, 1H), 7.63 (td, $J = 1.5$, 7.5 Hz, 1H), 7.45 (d, $J = 7.5$ Hz, 1H), 8.11 (dd, $J = 1.0$, 8.0 Hz, 1H). $^{13}$C NMR (125 MHz, $CDCl_3$): $\delta = 14.1$, 22.6, 29.2, 29.6, 30.2, 31.8, 40.0, 55.5, 99.8, 120.0, 121.5, 124.7, 128.3, 129.6, 148.8, 162.3, 164.3. LC/MS: *m/z* 257.91 $[M+H]^+$, 95.8%.

*4.1.2. 2-Heptyl-1-methyl-6-(trifluoromethyl)quinolin-4(1H)-one (**4**)*

Methyl iodide (0.46 g, 3.24 mmol, 10.1 equiv) was added to a solution of **1** (100 mg, 0.32 mmol, 1.0 equiv), KOH (56 mg, 1.00 mmol, 3.1 equiv) in methanol (1 mL) and the mixture was stirred overnight at room temperature. After the precipitate was removed by filtration, the solvent was evaporated under reduced pressure [30]. After column chromatography on silica gel (dichloromethane/methanol, 100/1) the product was isolated as a white solid (25 mg, 0.08 mmol, 25%), mp 125.1–126.3 °C. $^1$H NMR (500 MHz, MeOH-$d_4$): $\delta = 0.92$ (t, $J = 7.0$ Hz, 3H), 1.31–1.53 (m, 8H), 1.74 (quint, $J = 7.5$ Hz, 2H), 2.90 (t, $J = 7.5$ Hz, 2H), 3.92 (s, 3H), 6.35 (s, 1H), 7.99–8.04 (m, 2H), 8.59–8.60 (m, 1H). $^{13}$C NMR (125 MHz, MeOH-$d_4$): $\delta$ = 14.4, 23.7, 29.6, 30.1, 30.3, 32.9, 35.6, 35.7, 112.1, 119.4, 124.4 (q, $J_{CF} = 4$ Hz), 125.5 (q, $J_{CF} = 270$ Hz), 126.6, 126.7 (q,

$J_{CF}$ = 33 Hz), 129.5 (q, $J_{CF}$ = 3 Hz), 145.3, 160.0, 178.9. LC/MS: *m/z* 325.79 $[M+H]^+$, 99.9%.

*4.1.3. 2-Hexyl-1-methyl-6-(trifluoromethyl)quinolin-4(1H)-one (**5**)*

The title compound was prepared using the same method as for the synthesis of **4** from **36** (100 mg, 0.34 mmol). After column chromatography on silica gel (dichloromethane/methanol, 100/1) the product was isolated as a white solid (30 mg, 0.10 mmol, 28%), mp 101.2–103.9 °C. $^1$H NMR (500 MHz, MeOH-$d_4$): $\delta$ = 0.94 (t, $J$ = 7.0 Hz, 3H), 1.35–1.52 (m, 6H), 1.74 (quint, $J$ = 7.5 Hz, 2H), 2.90 (t, $J$ = 8.0 Hz, 2H), 3.92 (s, 3H), 6.36 (s, 1H), 8.00–8.04 (m, 2H), 8.59–8.60 (m, 1H). $^{13}$C NMR (125 MHz, MeOH-$d_4$): $\delta$ = 14.4, 23.6, 29.6, 30.0, 32.6, 35.6, 35.7, 112.1, 119.4, 124.4 (q, $J_{CF}$ = 4 Hz), 129.5 (q, $J_{CF}$ = 3 Hz), 126.6, 126.8 (q, $J_{CF}$ = 33 Hz), 125.5 (q, $J_{CF}$ = 270 Hz), 145.3, 160.0, 178.9. LC/MS: *m/z* 311.94 $[M+H]^+$, 95.0%.

*4.1.4. 2-(Pentyloxymethyl)quinolin-4(1H)-one (**6**)*

The title compound was prepared according to procedure A from **33** (2.16 g, 10 mmol) and aniline (0.93 g, 10 mmol). After removal of solvent under reduced pressure and column chromatography on silica gel (dichloromethane/methanol, 60/1) the product was isolated as a brown solid (200 mg, 0.82 mmol, 8%), mp 107.9–110.2 °C. $^1$H NMR (500 MHz, DMSO-$d_6$): $\delta$ = 0.86 (t, $J$ = 7.0 Hz, 3H), 1.28–1.32 (m, 4H), 1.57 (quint, $J$ = 7.5 Hz, 2H), 3.48 (t, $J$ = 6.5 Hz, 2H), 4.45 (s, 2H), 6.05 (s, 1H), 7.27–7.30 (m, 1H), 7.60–7.65 (m, 2H), 8.05 (dt, $J$ = 1.0, 7.5 Hz, 1H), 11.58 (br, 1H). $^{13}$C NMR (125 MHz, DMSO-$d_6$): $\delta$ = 13.9, 21.9, 27.7, 28.7, 68.7, 70.2, 107.1, 118.2, 122.9, 124.8, 125.0, 131.7, 140.1, 149.5, 176.9. LC/MS: *m/z* 245.94 $[M+H]^+$, 99.9%.

*4.1.5. 2-(Pentyloxymethyl)-6-(trifluoromethyl)quinolin-4(1H)-one (**7**)*

The title compound was prepared according to procedure A from **33** (2.16 g, 10 mmol) and 4-(trifluoromethyl)aniline (1.61 g, 10 mmol). After recrystallization from ethanol the product was isolated as a white solid (1.51 g, 4.82 mmol, 48%), mp 215.8–216.5 °C. $^1$H NMR (500 MHz, DMSO-$d_6$): $\delta$ = 0.85 (t, $J$ = 7.1 Hz, 3H), 1.24–1.33 (m, 4H), 1.57 (quint, $J$ = 6.9 Hz, 2H), 3.49 (t, $J$ = 6.6 Hz, 2H), 4.48 (s, 2H), 6.18 (s, 1H), 7.82 (d, $J$ = 8.8 Hz, 1H), 7.93 (dd, $J$ = 8.8, 2.2 Hz, 1H), 8.32 (d, $J$ = 1.6 Hz, 1H), 11.93 (br, 1H). $^{13}$C NMR (125 MHz, DMSO-$d_6$): $\delta$ = 13.8, 21.9, 27.7, 28.7, 68.5, 70.3, 108.0, 119.9, 122.4 (q, $J_{CF}$ = 4 Hz), 123.2 (q, $J_{CF}$ = 32 Hz), 124.1, 124.2 (q, $J_{CF}$ = 272 Hz), 127.6 (q, $J_{CF}$ = 3 Hz), 142.3, 150.8, 176.3. LC/MS: *m/z* 313.97 $[M+H]^+$, 96.1%.

*4.1.6. 6-Nitro-2-(pentyloxymethyl)quinolin-4(1H)-one (**8**)*

A solution of **6** (80 mg, 0.33 mmol) in conc. $H_2SO_4$ (1 mL) was cooled to 0 °C, and a mixture of conc. $H_2SO_4$ (32 μL) and conc. $HNO_3$ (32 μL) was added slowly, maintaining the temperature at 0 °C. After the addition was complete, the mixture was allowed to reach room temperature with stirring for additional 2 h. The solution was poured onto ice, and the resulting precipitate was filtered and washed with water to give crude product [31]. After preparative thin layer chromatography on silica gel (dichloromethane/methanol, 20/1) the product was isolated as a yellow solid (25 mg, 0.09 mmol, 27%). mp 187.3–189.6 °C. $^1$H NMR (500 MHz, MeOH-$d_4$): $\delta$ = 0.93 (t, $J$ = 7.0 Hz, 3H), 1.33–1.43 (m, 4H), 1.69 (quint, $J$ = 7.5 Hz, 2H), 3.60 (t, $J$ = 6.5 Hz, 2H), 4.56 (s, 2H), 6.38 (s, 1H), 7.76 (d, $J$ = 9.5 Hz, 1H), 8.44 (dd, $J$ = 2.5, 9.0 Hz, 1H), 9.01 (d, $J$ = 2.5 Hz, 1H). $^{13}$C NMR (125 MHz, MeOH-$d_4$): $\delta$ = 14.4, 23.6, 29.4, 30.3, 69.9, 72.6, 109.2, 121.0, 122.9, 125.3, 127.3, 145.0, 154.2, 180.1. LC/MS: *m/z* 290.98 $[M+H]^+$, 99.0%.

*4.1.7. 2-(4-Ethoxybutyl)quinolin-4(1H)-one (**9**)*

The title compound was prepared according to procedure A from **34** (0.65 g, 3.0 mmol) and aniline (280 mg, 3.0 mmol). After removal of solvent under reduced pressure, column chromatography on silica gel (dichloromethane/methanol, 60/1–40/1) and preparative thin layer chromatography on silica gel (dichloromethane/methanol, 20/1) the product was isolated as a white solid (60 mg, 0.24 mmol, 8%), mp 98.3–100.5 °C. $^1$H NMR (500 MHz, MeOH-$d_4$): $\delta$ = 1.18 (t, $J$ = 7.0 Hz, 3H), 1.65–1.71 (m, 2H), 1.82–1.88 (m, 2H), 2.76 (t, $J$ = 7.5 Hz, 2H), 3.47–3.51 (m, 4H), 6.25 (s, 1H), 7.40 (td, $J$ = 1.0, 7.5 Hz, 1H), 7.59 (d, $J$ = 9.0 Hz, 1H), 7.70 (td, $J$ = 1.5, 7.5 Hz, 1H), 8.22 (d, $J$ = 8.0 Hz, 1H). $^{13}$C NMR (125 MHz, MeOH-$d_4$): $\delta$ = 15.5, 27.0, 30.2, 34.7, 67.2, 71.1, 108.9, 119.1, 125.1, 125.5, 126.0, 133.4, 141.6, 156.9, 180.7. LC/MS: *m/z* 245.85 $[M+H]^+$, 95.4%.

*4.1.8. 2-(4-Ethoxybutyl)-6-(trifluoromethyl)quinolin-4(1H)-one (**10**)*

The title compound was prepared according to procedure A from **34** (1.08 g, 5.00 mmol) and 4-(trifluoromethyl)aniline (0.81 g, 5.00 mmol). After recrystallization from ethanol the product was isolated as a white solid (280 mg, 0.89 mmol, 18%), mp 149.6–151.1 °C. $^1$H NMR (500 MHz, DMSO-$d_6$): $\delta$ = 1.17 (t, $J$ = 7.1 Hz, 3H), 1.62 (quint, $J$ = 6.6 Hz, 2H), 1.86 (quint, $J$ = 7.3 Hz, 2H), 2.78 (t, $J$ = 7.4 Hz, 2H), 3.44 (t, $J$ = 6.0 Hz, 2H), 3.45 (q, $J$ = 6.9 Hz, 2H), 6.25 (d, $J$ = 1.3 Hz, 1H), 7.72 (d, $J$ = 8.8 Hz, 1H), 7.76 (dd, $J$ = 8.8, 1.9 Hz, 1H), 8.64 (s, 1H), 12.26 (bs, 1H). $^{13}$C NMR (125 MHz, DMSO-$d_6$): $\delta$ = 15.2, 26.5, 28.4, 33.6, 66.4, 70.5, 109.4, 119.1, 123.6 (q, $J_{CF}$ = 4 Hz), 124.1 (q, $J_{CF}$ = 272 Hz), 124.3, 125.6, 127.9 (q, $J_{CF}$ = 3 Hz), 142.1, 155.8, 178.4. LC/MS: *m/z* 313.99 $[M+H]^+$, 95.7%.

*4.1.9. 2-(4-Ethoxybutyl)-6-nitroquinolin-4(1H)-one (**11**)*

Compound **24** (150 mg, 0.45 mmol) was carefully purged with nitrogen under stirring, then slowly heated past its melting point to 310 °C under inert atmosphere with continued stirring for 8 min. The reaction was cooled to room temperature after the evident evolution of carbon dioxide ceased. The resulting solid was dissolved in a dichloromethane/methanol (15/1) solution. Insoluble material was removed by filtration and the solvents were removed under reduced pressure [32]. The residue was purified by column chromatography on silica gel (dichloromethane/methanol, 60/1) to give the product as a yellow solid (103 mg, 0.36 mmol, 80%), mp 232.9–233.8 °C. $^1$H NMR (500 MHz, MeOH-$d_4$): $\delta$ = 1.11 (t, $J$ = 7.0 Hz, 3H), 1.61 (quint, $J$ = 7.0 Hz, 2H), 1.78 (quint, $J$ = 7.0 Hz, 2H), 2.69 (d, $J$ = 7.5 Hz, 2H), 3.42 (q, $J$ = 7.0 Hz, 4H), 6.20 (s, 1H), 7.62 (d, $J$ = 9.0 Hz, 1H), 8.37 (dd, $J$ = 2.5, 9.0 Hz, 1H), 8.96 (d, $J$ = 2.5 Hz, 1H). $^{13}$C NMR (125 MHz, MeOH-$d_4$): $\delta$ = 13.9, 25.2, 28.7, 33.2, 65.7, 69.5, 108.8, 119.1, 121.4, 123.4, 125.7, 143.5, 156.7, 178.5. LC/MS: *m/z* 290.70 $[M+H]^+$, 96.8%.

*4.1.10. 2-Heptyl-3-nitroquinolin-4(1H)-one (**12**)*

At 110 °C conc. $HNO_3$ (65% w/w, 15 μL, 0.30 mmol, 2.5 equiv) was added to a stirred suspension of HHQ (30 mg, 0.12 mmol, 1.0 equiv) in propionic acid (3 mL). The reaction mixture was heated for further 2 h with vigorous stirring. The resulting suspension was poured into ice. The solids were isolated by filtration washed with cold water and dried under vacuum to yield the product as a yellow solid (12 mg, 0.04 mmol, 33%) [33], mp 258.0–259.1 °C. $^1$H NMR (500 MHz, DMSO-$d_6$): $\delta$ = 0.85 (t, $J$ = 6.5 Hz, 3H), 1.25–1.34 (m, 8H), 1.70 (quint, $J$ = 7.5 Hz, 2H), 2.73 (t, $J$ = 7.5 Hz, 2H), 7.45 (t, $J$ = 7.5 Hz, 1H), 7.66 (d, $J$ = 7.5 Hz, 1H), 7.78 (t, $J$ = 7.5 Hz, 1H), 8.15 (d, $J$ = 8.0 Hz, 1H), 12.32 (br, 1H). $^{13}$C NMR (125 MHz, DMSO-$d_6$): $\delta$ = 13.9, 22.0, 28.1, 28.4, 28.6, 30.3, 31.0, 118.7, 124.8, 125.2, 125.3, 133.2, 135.6, 138.6, 149.4, 167.5. LC/MS: *m/z* 289.00 $[M+H]^+$, 96.7%.

*4.1.11. 3-Amino-2-heptylquinolin-4(1H)-one (**13**)*

A suspension of **12** (40 mg, 0.14 mmol, 1.0 equiv) in ethanol (2 mL) was heated at reflux. $Fe^0$ (80 mg, 1.40 mmol, 10 equiv) and an aqueous solution of $NH_4Cl$ (74 mg dissolved in 0.56 mL of water)

were added. The reaction was stirred at reflux to completeness. The warm mixture was filtered through a Celite patch and the remaining solids were washed several times with warm EtOH. The filtrates were combined and concentrated [33]. The residue was purified by preparative thin layer chromatography on silica gel (dichloromethane/methanol, 10/1) to give the product as a brown solid (13 mg, 0.05 mmol, 36%), mp 190.3–192.0 °C. $^1$H NMR (500 MHz, MeOH-$d_4$): $\delta$ = 0.89 (t, $J$ = 7.0 Hz, 3H), 1.28–1.48 (m, 8H), 1.76 (quint, $J$ = 7.5 Hz, 2H), 2.83 (t, $J$ = 8.0 Hz, 2H), 7.27–7.30 (m, 1H), 7.54 (d, $J$ = 3.5 Hz, 2H), 8.21 (d, $J$ = 8.5 Hz, 1H). $^{13}$C NMR (125 MHz, MeOH-$d_4$): $\delta$ = 14.4, 23.7, 28.8, 30.2, 30.7, 31.3, 32.9, 118.8, 123.8, 125.6, 128.6, 131.3, 138.6, 139.5, 171.2. LC/MS: $m/z$ 258.99 $[M+H]^+$, 99.9%.

#### 4.1.12. 2-Heptyl-3-(hydroxymethyl)quinolin-4(1H)-one (**15**)

At 0 °C $LiAlH_4$ (120 mg, 3.16 mmol, 2.0 equiv) was added to a stirred solution of **17** (500 mg, 1.59 mmol, 1.0 equiv) in dry THF (30 mL). After stirring at room temperature for 2 h ethyl acetate (10 mL) was added at 0 °C and after filtration the solvent was removed under reduced pressure [34]. The residue was purified by column chromatography (dichloromethane/methanol, 40/1) to give the product as a white solid (128 mg, 0.47 mmol, 30%), mp 297.2–298.6 °C. $^1$H NMR (500 MHz, DMSO-$d_6$): $\delta$ = 0.86 (t, $J$ = 7.0 Hz, 3H), 1.25–1.40 (m, 8H), 1.67 (quint, $J$ = 7.5 Hz, 2H), 2.73 (t, $J$ = 8.0 Hz, 2H), 4.48 (d, $J$ = 5.5 Hz, 2H), 4.58 (t, $J$ = 5.5 Hz, 1H), 7.26 (td, $J$ = 1.0, 7.5 Hz, 1H), 7.52 (d, $J$ = 8.0 Hz, 1H), 7.60 (td, $J$ = 1.0, 8.0 Hz, 1H), 8.07 (dd, $J$ = 1.5, 8.0 Hz, 1H), 11.39 (s, 1H). $^{13}$C NMR (125 MHz, DMSO-$d_6$): $\delta$ = 13.9, 22.0, 28.4, 29.0, 29.3, 31.1, 31.2, 54.1, 117.7, 118.0, 122.6, 123.9, 125.1, 131.3, 139.4, 152.3, 176.1. LC/MS: $m/z$ 315.86 $[M+H]^+$, 98.9%.

#### 4.1.13. Ethyl 2-heptyl-4-oxo-1,4-dihydroquinoline-3-carboxylate (**17**)

The title compound was obtained according to procedure B from **32** (3.40 g, 16 mmol), sodium hydride (50–65% w/w, 0.72 g, 15 mmol) and isatoic anhydride (2.45 g, 15 mmol). After recrystallization from ethyl acetate/methanol the product was isolated as a white solid (2.68 g, 8.51 mmol, 57%), mp 151.1–153.0 °C. $^1$H NMR (500 MHz, DMSO-$d_6$): $\delta$ = 0.85 (t, $J$ = 7.0 Hz, 3H), 1.25–1.34 (m, 11H), 1.66 (quint, $J$ = 7.5 Hz, 2H), 2.63 (t, $J$ = 8.0 Hz, 2H), 4.23 (q, $J$ = 7.0 Hz, 2H), 7.34 (td, $J$ = 1.5, 7.5 Hz, 1H), 7.56 (d, $J$ = 8.0 Hz, 1H), 7.67 (td, $J$ = 1.5, 7.5 Hz, 1H), 8.05 (dd, $J$ = 1.5, 7.5 Hz, 1H), 11.77 (br, 1H). $^{13}$C NMR (125 MHz, DMSO-$d_6$): $\delta$ = 13.9, 14,1, 22.0, 28.3, 28.7, 28.9, 31.0, 31.9, 60.3, 114.8, 118.1, 123.6, 124.4, 124.9, 132.2, 139.3, 152.1, 166.8, 173.6. LC/MS: $m/z$ 315.86 $[M+H]^+$, 98.9%.

#### 4.1.14. Ethyl 6-nitro-4-oxo-2-(pentyloxymethyl)-1,4-dihydroquinoline-3-carboxylate (19)

The title compound was prepared according to procedure B from **33** (234 mg, 1.08 mmol), sodium hydride (50–65% w/w, 58 mg, 1.21 mmol) and 6-nitro-1*H*-benzo[*d*][1,3]oxazine-2,4-dione (200 mg, 0.96 mmol). After column chromatography on silica gel (*n*-hexane/ethyl acetate, 1.2/1) and recrystallization from ethyl acetate the product was isolated as a yellow solid (25 mg, 0.07 mmol, 7.3%), mp 207.6–209.0 °C. $^1$H NMR (500 MHz, DMSO-$d_6$): $\delta$ = 0.85 (t, $J$ = 7.0 Hz, 3H), 1.27–1.29 (m, 7H), 1.55 (quint, $J$ = 7.5 Hz, 2H), 3.47 (t, $J$ = 7.0 Hz, 2H), 4.26 (q, $J$ = 7.0 Hz, 2H), 4.56 (s, 2H), 7.92 (d, $J$ = 9.0 Hz, 1H), 8.47 (dd, $J$ = 2.5, 9.0 Hz, 1H), 8.81 (d, $J$ = 2.5 Hz, 1H), 12.32, (br, 1H). $^{13}$C NMR (125 MHz, DMSO-$d_6$): $\delta$ = 13.8, 14.0, 21.9, 27.5, 28.5, 60.7, 67.1, 70.7, 115.3, 120.6, 121.5, 124.2, 126.5, 142.9, 143.2, 150.1, 165.2, 173.1. LC/MS: $m/z$ 362.76 $[M+H]^+$, 98.8%.

#### 4.1.15. Ethyl 2-(4-ethoxybutyl)-6-nitro-4-oxo-1,4-dihydroquinoline-3-carboxylate (**20**)

The title compound was prepared according to procedure B from **34** (1.7 g, 7.87 mmol), sodium hydride (50–65% w/w, 360 mg, 7.50 mmol) and 6-nitro-1*H*-benzo[*d*][1,3]oxazine-2,4-dione (1.57 g, 7.55 mmol) After column chromatography on silica gel (*n*-hexane/ethyl acetate, 1.2/1) and recrystallization from ethyl acetate the product was isolated as a yellow solid (2.6 g, 7.18 mmol, 95%), mp 210.4–211.7 °C. $^1$H NMR (500 MHz, DMSO-$d_6$): $\delta$ = 1.08 (t, $J$ = 7.0 Hz, 3H), 1.28 (t, $J$ = 7.0 Hz, 3H), 1.56 (quint, $J$ = 7.0 Hz, 2H), 1.73 (quint, $J$ = 7.0 Hz, 2H), 2.67 (t, $J$ = 7.5 Hz, 2H), 3.35–3.40 (m, 4H), 4.27 (q, $J$ = 7.0 Hz, 2H), 7.75 (d, $J$ = 9.5 Hz, 1H), 8.45 (dd, $J$ = 2.5, 9.0 Hz, 1H), 8.79 (d, $J$ = 2.5 Hz, 1H), 12.30 (br, 1H). $^{13}$C NMR (125 MHz, DMSO-$d_6$): $\delta$ = 14.0, 15.1, 25.8, 29.0, 31.9, 60.7, 65.2, 69.2, 116.2, 120.1, 121.5, 123.6, 126.5, 143.0, 143.1, 153.5, 165.9, 173.1. LC/MS: $m/z$ 362.89 $[M+H]^+$, 97.9%.

#### 4.1.16. 2-Heptyl-4-oxo-1,4-dihydroquinoline-3-carboxylic acid (**21**)

The title compound was prepared according to procedure B from **17** (50 mg, 0.16 mmol). The product was isolated as a white solid (32 mg, 0.11 mmol, 69%), mp 219.4–221.7 °C. $^1$H NMR (500 MHz, DMSO-$d_6$): $\delta$ = 0.86 (t, $J$ = 7.0 Hz, 3H), 1.26–1.41 (m, 8H), 1.66 (quint, $J$ = 7.5 Hz, 2H), 3.31 (t, $J$ = 7.5 Hz, 2H, covered by water peak at 3.32), 7.56 (t, $J$ = 7.5 Hz, 1H), 7.77 (d, $J$ = 7.5 Hz, 1H), 7.87 (t, $J$ = 7.5 Hz, 1H), 8.25 (d, $J$ = 7.5 Hz, 1H), 12.96 (br, 1H). $^{13}$C NMR (125 MHz, DMSO-$d_6$): $\delta$ = 13.9, 22.0, 28.3, 29.1, 29.2, 31.1, 33.3, 105.7, 118.8, 122.9, 125.1, 125.8, 133.9, 138.2, 162.4, 166.3, 179.0. LC/MS: $m/z$ 287.92 $[M+H]^+$, 99.9%.

#### 4.1.17. 6-Nitro-4-oxo-2-(pentyloxymethyl)-1,4-dihydroquinoline-3-carboxylic acid (**23**)

The title compound was prepared according to procedure B from **19** (400 mg, 1.10 mmol). The product was isolated as a yellow solid (262 mg, 0.78 mmol, 71%), mp 149.8–150.3 °C. $^1$H NMR (500 MHz, DMSO-$d_6$): $\delta$ = 0.89 (t, $J$ = 7.0 Hz, 3H), 1.29–1.37 (m, 4H), 1.70 (quint, $J$ = 7.0 Hz, 2H), 3.69 (t, $J$ = 7.0 Hz, 2H), 5.16 (s, 2H), 8.42 (d, $J$ = 9.0 Hz, 1H), 8.61 (dd, $J$ = 2.5, 9.0 Hz, 1H), 8.91 (d, $J$ = 2.5 Hz, 1H) 12.59 (br, 1H), 15.55 (br, 1H). $^{13}$C NMR (125 MHz, DMSO-$d_6$): $\delta$ = 13.9, 21.9, 27.5, 28.3, 68.1, 71.4, 106.1, 121.1, 122.1, 123.1, 127.5, 141.5, 144.4, 160.6, 165.5, 178.1. LC/MS: $m/z$ 334.95 $[M+H]^+$, 97.7%.

#### 4.1.18. 2-(4-Ethoxybutyl)-6-nitro-4-oxo-1,4-dihydroquinoline-3-carboxylic acid (**24**)

The title compound was obtained according to procedure B from **20** (0.7 g, 1.93 mmol). The product was isolated as a yellow solid (192 mg, 0.57 mmol, 30%), mp 231.5–232.7 °C. $^1$H NMR (500 MHz, DMSO-$d_6$): $\delta$ = 1.08 (t, $J$ = 7.0 Hz, 3H), 1.62 (quint, $J$ = 7.0 Hz, 2H), 1.73 (quint, $J$ = 7.0 Hz, 2H), 3.29 (t, $J$ = 7.5 Hz, 2H. covered by water peak at 3.33), 3.37–3.41 (m, 4H), 7.92 (d, $J$ = 9.0 Hz, 1H), 8.59 (dd, $J$ = 2.5, 9.0 Hz, 1H), 8.92 (d, $J$ = 2.5 Hz, 1H), 13.24 (br, 1H), 15.67 (br, 1H). $^{13}$C NMR (125 MHz, DMSO-$d_6$): $\delta$ = 15.1, 26.2, 29.3, 33.2, 66.2, 69.3, 107.7, 120.9, 121.5, 122.8, 127.7, 141.7, 144.2, 163.7, 165.5, 178.6. LC/MS: $m/z$ 334.95 $[M+H]^+$, 97.3%.

#### 4.1.19. 2-Heptyl-4-oxo-1,4-dihydroquinoline-3-carboxamide (**25**)

*N,N′*-Carbonyldiimidazole (62 mg, 0.38 mmol, 2.0 equiv) was added to **21** (55 mg, 0.19 mmol, 1.0 equiv) in dry DMF (1 mL). After stirring at 65 °C for 5 h, the mixture was cooled to 0 °C and iced conc. $NH_3 \cdot H_2O$ (5 mL) was added. After stirring overnight at room temperature the solvent was evaporated under reduced pressure. To the residue was added iced water (5 mL) and the precipitate was isolated by filtration [35]. After purification by column chromatography on silica gel (dichloromethane/methanol, 70/1) the product was isolated as a gray solid (38 mg, 0.13 mmol, 68%), mp 215.7–216.9 °C. 1H NMR (500 MHz, DMSO-$d_6$): $\delta$ = 0.85 (t, $J$ = 7.0

Hz, 3H), 1.22–1.38 (m, 8H), 1.67 (quint, $J$ = 7.5 Hz, 2H), 3.13 (t, $J$ = 7.5 Hz, 2H), 7.15 (d, $J$ = 2.5 Hz, 1H), 7.38 (td, $J$ = 1.0, 7.5 Hz, 1H), 7.60 (d, $J$ = 7.5 Hz, 1H), 7.69 (td, $J$ = 1.5, 7.5 Hz, 1H), 8.15 (dd, $J$ = 1.5, 7.5 Hz, 1H), 9.19 (d, $J$ = 2.5 Hz, 1H), 11.94 (br, 1H). $^{13}$C NMR (125 MHz, DMSO-$d_6$): $\delta$ = 13.9, 22.0, 28.4, 29.1, 29.5, 31.2, 33.0, 111.8, 117.9, 124.0, 124.8, 125.4, 132.3, 138.4, 158.2, 167.5, 176.1. LC/MS: *m/z* 287.89 $[M+H]^+$, 99.9%.

#### 4.1.20. 2-Heptyl-N-hydroxy-4-oxo-1,4-dihydroquinoline-3-carboxamide (**27**)

A mixture of **21** (55 mg, 0.19 mmol, 1.0 equiv), *N,N'*-carbonyldiimidazole (62 mg, 0.38 mmol, 2.0 equiv) and dry DMF (2 mL) was stirred for 3 h at 75 °C. The solution was cooled to 0 °C and a mixture of *N*-methylmorpholine (184 mg, 1.80 mmol, 10 equiv), hydroxylammonium chloride (130 mg, 1.90 mmol, 10 equiv) and dry DMF (1 mL) was added and the mixture was stirred overnight at room temperature [36]. The solvent was removed under reduced pressure and the residue was purified by column chromatography on silica gel (dichloromethane/methanol, 40/1) to give the product as a white solid (34 mg, 0.12 mmol, 63%), mp 161.1–161.5 °C. $^1$H NMR (500 MHz, DMSO-$d_6$): $\delta$ = 0.86 (t, $J$ = 7.0 Hz, 3H), 1.25–1.39 (m, 8H), 1.68 (quint, $J$ = 7.0 Hz, 2H), 2.95 (t, $J$ = 8.0 Hz, 2H), 7.37 (td, $J$ = 1.0, 7.5 Hz, 1H), 7.60 (d, $J$ = 8.0 Hz, 1H), 7.69 (td, $J$ = 1.5, 7.5 Hz, 1H), 8.13 (dd, $J$ = 1.0, 8.0 Hz, 1H), 8.90 (br, 1H), 11.44 (s, 1H), 11.95 (br, 1H). $^{13}$C NMR (125 MHz, DMSO-$d_6$): $\delta$ = 13.9, 22.0, 28.4, 29.1, 29.5, 31.2, 32.4, 112.0, 117.0, 123.9, 124.4, 125.3, 132.3, 138.7, 156.3, 164.0, 175.1. LC/MS: no ionization, 98.6%.

#### 4.1.21. 2-Heptyl-N-hydroxy-6-nitro-4-oxo-1,4-dihydroquinoline-3-carboxamide (**28**)

The title compound was prepared using the same method as for the synthesis of **27** from **22** (250 mg, 0.75 mmol). After column chromatography on silica gel (dichloromethane/methanol, 50/1) and recrystallization from ethyl acetate the product was isolated as a yellow solid (38 mg, 0.11 mmol, 15%), mp 200.9–202.8 °C. $^1$H NMR (500 MHz, DMSO-$d_6$): $\delta$ = 0.86 (t, $J$ = 7.0 Hz, 3H), 1.26–1.37 (m, 8H), 1.69 (quint, $J$ = 7.5 Hz, 2H), 2.80 (t, $J$ = 7.5 Hz, 2H), 7.76 (d, $J$ = 9.5 Hz, 1H), 8.45 (dd, $J$ = 3.0, 9.5 Hz, 1H), 8.84 (d, $J$ = 2.5 Hz, 1H), 9.06 (s, 1H), 11.00 (s, 1H), 12.28 (br, 1H). $^{13}$C NMR (125 MHz, DMSO-$d_6$): $\delta$ = 13.9, 22.0, 28.3, 29.0, 29.1, 31.1, 32.2, 115.4, 120.0, 121.7, 123.6, 126.4, 142.8, 143.0, 155.8, 162.4, 174.3. LC/MS: *m/z* 348.00 $[M+H]^+$, 98.5%.

#### 4.1.22. Ethyl 2-heptyl-4-oxo-1,4-dihydro-1,6-naphthyridine-3-carboxylate (**29**)

The title compound was prepared according to procedure B from **32** (1.6 g, 7.48 mmol), sodium hydride (50–65% w/w, 357 mg, 7.44 mmol) and 1*H*-pyrido[4,3-*d*][1,3]oxazine-2,4-dione (1.23 g, 7.50 mmol). The product was isolated as a white solid (1.36 g, 4.28 mmol, 57%), mp 172.3–174.9 °C. $^1$H NMR (500 MHz, MeOH-$d_4$): $\delta$ = 0.80 (t, $J$ = 7.0 Hz, 3H), 1.18–1.35 (m, 11H), 1.65 (quint, $J$ = 7.5 Hz, 2H), 2.66 (t, $J$ = 8.0 Hz, 2H), 4.27 (q, $J$ = 7.0 Hz, 2H), 7.38 (d, $J$ = 6.0 Hz, 1H), 8.49 (d, $J$ = 6.0 Hz, 1H), 9.21 (s, 1H). $^{13}$C NMR (125 MHz, MeOH-$d_4$): $\delta$ = 14.4, 14.5, 23.6, 30.0, 30.5, 32.8, 34.1, 62.6, 113.9, 119.3, 121.2, 146.5, 150.4, 150.8, 157.9, 167.9, 176.6. LC/MS: *m/z* 316.99 $[M+H]^+$, 96.7%.

#### 4.1.23. 2-Heptyl-4-oxo-1,4-dihydro-1,6-naphthyridine-3-carboxylic acid (**30**)

The title compound was prepared according to procedure B from **29** (200 mg, 0.63 mmol). The product was isolated as a white solid (143 mg, 0.50 mmol, 79%), mp 102.3–104.5 °C. $^1$H NMR (500 MHz, DMSO-$d_6$): $\delta$ = 0.86 (t, $J$ = 7.0 Hz, 3H), 1.25–1.34 (m, 6H), 1.39 (quint, $J$ = 7.5 Hz, 2H), 1.66 (quint, $J$ = 7.5 Hz, 2H), 3.26 (t, $J$ = 7.5 Hz, 2H, covered by water peak at 3.33), 7.61 (d, $J$ = 6.0 Hz, 1H), 7.89 (d, $J$ = 6.0 Hz, 1H), 9.38 (s, 1H). $^{13}$C NMR (125 MHz, DMSO-$d_6$): $\delta$ = 13.9, 22.0, 28.3, 29.1, 31.1, 33.6, 108.7, 112.5, 118.3, 143.0, 149.2, 151.5, 164.9, 165.6, 179.0. LC/MS: *m/z* 289.06 $[M+H]^+$, 98.7%.

#### 4.1.24. 2-Heptyl-1,6-naphthyridin-4(1H)-one (**31**)

The title compound was prepared using the same method as for the synthesis of **11** from **30** (292 mg, 1.01 mmol). After recrystallization from diethyl ether/methanol the product was isolated as a gray solid (150 mg, 0.61 mmol, 60%), mp 132.5–133.0 °C. $^1$H NMR (500 MHz, DMSO-$d_6$): $\delta$ = 0.85 (t, $J$ = 7.0 Hz, 3H), 1.25–1.31 (m, 8H), 1.66 (quint, $J$ = 7.5 Hz, 2H), 2.58 (t, $J$ = 7.5 Hz, 2H), 6.04 (s, 1H), 7.40 (d, $J$ = 5.5 Hz, 1H), 8.55 (d, $J$ = 5.5 Hz, 1H), 9.13 (s, 1H), 11.71 (br, 1H). $^{13}$C NMR (125 MHz, DMSO-$d_6$): $\delta$ = 13.9, 22.0, 28.0, 28.3, 28.4, 31.1, 33.2, 110.6, 111.8, 119.4, 144.6, 148.7, 149.7, 155.1, 176.7. LC/MS: *m/z* 245.01 $[M+H]^+$, 98.6%.

#### 4.1.25. Ethyl 3-oxo-4-(pentyloxy)butanoate (**33**)

1-Pentanol (8.82 g, 0.10 mol, 2.0 equiv) was added to a stirred suspension of sodium hydride (8.73 g, 55% in oil, 0.20 mol, 4.0 equiv) in THF (6 mL). After stirring at room temperature for 30 min, ethyl chloroacetoacetate (8.23 g, 50 mmol, 1.0 equiv) was added slowly and stirred overnight at room temperature. Water was added carefully and the organic solvent was evaporated under reduced pressure. The residue was acidified with 1 N HCl and extracted with diethyl ether. The combined organic layers were washed with brine and evaporated under reduced pressure. After bulb-to-bulb distillation (160 °C, 5 mbar) the product was isolated as a slightly orange oil (9.82 g, 45 mmol, 90%) [37]. $^1$H NMR (300 MHz, $CDCl_3$): $\delta$ = 0.84 (t, $J$ = 7.1 Hz, 3H), 1.21 (t, $J$ = 7.1 Hz, 3H), 1.27 (m, 4H), 1.54 (m, 2H), 3.41 (t, $J$ = 6.5 Hz, 2H), 3.45 (s, 2H), 4.02 (s, 2H), 4.13 (q, $J$ = 7.1 Hz, 2H).

#### 4.1.26. Ethyl 7-ethoxy-3-oxoheptanoate (**34**)

Lithium diisopropylamide (24.6 mL, 2 M in THF, 49.1 mmol, 2.4 equiv) was diluted with dry THF (25 mL) and stirred at 0 °C. A solution of ethyl acetoacetate (2.65 g, 20.4 mmol, 1.0 equiv) in THF (7 mL) was added and stirring was continued at 0 °C. After 1.5 h a solution of **35** (3.94 g, 23.7 mmol, 1.2 equiv) in THF (7 mL) was added and the mixture was stirred overnight at room temperature. At 0 °C the mixture was acidified by the addition of sat. $NH_4Cl$ solution (10 mL) and conc. HCl (19 mL). The mixture was extracted with diethyl ether (3 × 50 mL) and the combined organic layers were concentrated under reduced pressure to give the crude product [38]. After column chromatography on silica gel (*n*-hexane/ethyl acetate, 9/1) the product was obtained as a yellow oil (1.93 g, 8.92 mmol, 44%). $^1$H NMR (300 MHz, $CDCl_3$): $\delta$ = 1.12 (t, $J$ = 7.1 Hz, 3H), 1.21 (t, $J$ = 7.1 Hz, 3H), 1.46–1.66 (m, 4H), 2.51 (t, $J$ = 7.0 Hz, 2H), 3.34 (t, $J$ = 6.1 Hz, 2H), 3.36 (s, 2H), 3.39 (q, $J$ = 7.1 Hz, 2H), 4.13 (q, $J$ = 7.1 Hz, 2H).

#### 4.1.27. 1-Bromo-3-ethoxypropane (**35**)

At 0 °C phosphorus tribromide (4.33 g, 16 mmol, 1.0 equiv) was added dropwise to 3-ethoxypropan-1-ol (4.90 g, 47 mmol, 2.9 equiv). The mixture was stirred overnight at room temperature. After diluting with dichloromethane the mixture was washed with sat. $NaHCO_3$ solution, dried over $MgSO_4$. After filtration and evaporation of the solvent the product was obtained as a colorless oil (3.93 g, 23.7 mmol, 50%) [39]. $^1$H NMR (300 MHz, $CDCl_3$): $\delta$ = 1.31 (t, $J$ = 7.2 Hz, 3H), 2.03 (quint, $J$ = 6.2 Hz, 2H), 3.39–3.49 (m, 6H).

### 4.2. Physicochemical properties

#### 4.2.1. Determination of water solubility by HPLC

A calibration curve was made by plotting the area under the curve at 254 nm (UV by HPLC, for compound **7** at 245 nm) against the concentration of each compound injected after performing a

serial dilution (25 μM–0.781 μM in methanol). A saturated solution containing 2% DMSO was then made for each compound in PBS (pH 7.4) by performing dilution using a 10 mM DMSO stock solution of each compound. This solution was sonicated for 30 min and shaken at room temperature for 10 h, filtered and injected into the HPLC to compare the area found at wavelength 254 nm (for compound **7** at 245 nm) with the previously made calibration curve [21].

#### 4.2.2. CAS iron-chelation assay

A 1.5 mL aliquot of PBS (pH 7.2) containing the relevant concentration of test compound was mixed with 1.5 mL of CAS assay solution prepared according to Schwyn and Nylands. A reference was prepared by using PBS (pH 7.2) but without test compound. The samples (s) and reference (r) absorbances at 630 nm were determined after 15 min incubation at room temperature. The percentage of iron-chelating activity was calculated by subtracting the sample $A_{630}$ from that of the reference $A_{630}$ value. Siderophore units are defined as $[Ar - As/Ar]^*100$ = percent of siderophore units [26].

### 4.3. Biology

Yeast extract was purchased from Fluka (Neu-Ulm, Germany), peptone from casein from Merck (Darmstadt, Germany), and Bacto™ Tryptone from BD Biosciences (Heidelberg, Germany). Salts and organic solvents of analytical grade were obtained from VWR (Darmstadt, Germany). *P. aeruginosa* strain PA14 (PA14) was stored in glycerol stocks at −80 °C. The following media were used: Luria Bertani broth (LB), PPGAS medium, and modified M9 minimal medium (20 mM $NH_4Cl$; 12 mM $Na_2HPO_4$; 22 mM $KH_2PO_4$; 8.6 mM NaCl; 1 mM, $MgSO_4$; 1 mM $CaCl_2$; 11 mM glucose).

#### 4.3.1. Reporter gene assay in E. coli

The ability of the compounds to either stimulate or antagonize the PqsR-dependent transcription was analysed as previously described [17] using a β-galactosidase reporter gene assay in *E. coli* expressing PqsR. Briefly, a culture of *E. coli* DH5α cells containing the plasmid pEAL08-2, which encodes PqsR under the control of the *tac* promoter and the β-galactosidase reporter gene *lacZ* controlled by the *pqsA* promoter, were co incubated with test compound. Antagonistic effects of compounds were assayed in the presence of 50 nM PQS. After incubation, β-galactosidase activity was measured spectrophotometrically at $OD_{420\ nm}$ using POLARstar Omega (BMG Labtech, Ortenberg, Germany) and expressed as percent stimulation of controls. For the determination of $IC_{50}$ values, compounds were tested at least at eight different concentrations.

#### 4.3.2. Quantification of extracellular PQS levels

Extracellular levels of PQS produced by PA14 were quantified by UHPLC–MS/MS using the method of Maurer et al. [40] For each sample, cultivation and sample work-up were performed in triplicates. Inhibition values of PQS formation were normalized to $OD_{600}$.

#### 4.3.3. Pyocyanin assay

For analysis of pyocyanin formation, cultivation procedure was the same as for PQS quantification with the exception of using PPGAS medium. Pyocyanin produced by PA14 was quantified using the method of Essar et al. [41] with some modifications, as described in detail by Klein et al. [42]. Briefly, 900 μL of each culture were extracted with 900 μL of chloroform and 800 μL of the organic phase re-extracted with 250 μL of 0.2 M HCl. $OD_{520}$ was measured in the aqueous phase using FLUOstar Omega (BMG Labtech, Ortenberg, Germany). For each sample, cultivation and sample work-up were performed in triplicates. Inhibition values of pyocyanin formation were normalized to $OD_{600}$.

## Acknowledgement

For technical assistance we like to thank Simone Amann and Carina Scheid.

## Appendix A. Supplementary data

Supplementary data related to this article can be found at http://dx.doi.org/10.1016/j.ejmech.2014.04.016.

## References

[1] C. Koch, N. Høiby, Pathogenesis of cystic fibrosis, Lancet 341 (1993) 1065–1069.
[2] J.R. Govan, V. Deretic, Microbial pathogenesis in cystic fibrosis: mucoid *Pseudomonas aeruginosa* and *Burkholderia cepacia*, Microbiological Reviews 60 (1996) 539–574.
[3] S. Swift, J.A. Downie, N.A. Whitehead, A.M.L. Barnard, G.P.C. Salmond, P. Williams, *Quorum sensing* as a population-density-dependent determinant of bacterial physiology, Advances In Microbial Physiology 45 (2001) 199–270.
[4] E.C. Pesci, J.B.J. Milbank, J.P. Pearson, S. McKnight, A.S. Kende, E.P. Greenberg, B.H. Iglewski, Quinolone signaling in the cell-to-cell communication system of *Pseudomonas aeruginosa*, Proceedings of the National Academy of Sciences of the United States of America 96 (1999) 11229–11234.
[5] H. Cao, G. Krishnan, B. Goumnerov, J. Tsongalis, R. Tompkins, L.G. Rahme, A quorum sensing-associated virulence gene of *Pseudomonas aeruginosa* encodes a LysR-like transcription regulator with a unique self-regulatory mechanism, Proceedings of the National Academy of Sciences of the United States of America 98 (2001) 14613–14618.
[6] G. Xiao, E. Deziel, J. He, F. Lepine, B. Lesic, M.H. Castonguay, S. Milot, A.P. Tampakaki, S.E. Stachel, L.G. Rahme, MvfR, a key *Pseudomonas aeruginosa* pathogenicity LTTR-class regulatory protein, has dual ligands, Molecular Microbiology 62 (2006) 1689–1699.
[7] E. Deziel, S. Gopalan, A.P. Tampakaki, F. Lepine, K.E. Padfield, M. Saucier, G. Xiao, L.G. Rahme, The contribution of MvfR to *Pseudomonas aeruginosa* pathogenesis and *quorum sensing* circuitry regulation: multiple *quorum sensing*-regulated genes are modulated without affecting lasRI, rhlRI or the production of N-acyl-L-homoserine lactones, Molecular Microbiology 55 (2005) 998–1014.
[8] L.A. Gallagher, S.L. McKnight, M.S. Kuznetsova, E.C. Pesci, C. Manoil, Functions required for extracellular quinolone signaling by *Pseudomonas aeruginosa*, Journal of Bacteriology 184 (2002) 6472–6480.
[9] E. Deziel, F. Lepine, S. Milot, J.X. He, M.N. Mindrinos, R.G. Tompkins, L.G. Rahme, Analysis of *Pseudomonas aeruginosa* 4-hydroxy-2-alkylquinolines (HAQs) reveals a role for 4-hydroxy-2-heptylquinoline in cell-to-cell communication, Proceedings of the National Academy of Sciences of the United States of America 101 (2004) 1339–1344.
[10] J.W. Schertzer, S.A. Brown, M. Whiteley, Oxygen levels rapidly modulate *Pseudomonas aeruginosa* social behaviours via substrate limitation of PqsH, Molecular Microbiology 77 (2010) 1527–1538.
[11] S. McGrath, D.S. Wade, E.C. Pesci, Dueling *quorum sensing* systems in *Pseudomonas aeruginosa* control the production of the Pseudomonas quinolone signal (PQS), FEMS Microbiology Letters 230 (2004) 27–34.
[12] T. Bjarnsholt, M. Givskov, *Quorum sensing* blockade as a strategy for enhancing host defences against bacterial pathogens, Philosophical Transactions of the Royal Society B: Biological Sciences 362 (2007) 1213–1222.
[13] L. Cegelski, G.R. Marshall, G.R. Eldridge, S.J. Hultgren, The biology and future prospects of antivirulence therapies, Nature Reviews Microbiology 6 (2008) 17–27.
[14] W.R.J.D. Galloway, J.T. Hodgkinso, S. Bowden, M. Welch, D.R. Spring, Applications of small molecule activators and inhibitors of *quorum sensing* in Gram-negative bacteria, Trends in Microbiology 20 (2012) 449–458.
[15] A. Ilangovan, M. Fletcher, G. Rampioni, C. Pustelny1, K. Rumbaugh, S. Heeb, M. Camara, A. Truman, S.R. Chhabra, J. Emsley, P. Williams, Structural basis for native agonist and synthetic inhibitor recognition by the *Pseudomonas aeruginosa quorum sensing* regulator PqsR (MvfR), PLoS Pathogens 9 (2013) e1003508.
[16] M. Zender, T. Klein, C. Henn, B. Kirsch, C.K. Maurer, D. Kail, C. Ritter, O. Dolezal, A. Steinbach, R.W. Hartmann, Discovery and biophysical characterization of 2-amino-oxadiazoles as novel antagonists of PqsR, an important regulator of *Pseudomonas aeruginosa* virulence, Journal of Medicinal Chemistry 56 (2013) 6761–6774.
[17] C. Lu, B. Kirsch, C. Zimmer, J.C. de Jong, C. Henn, C.K. Maurer, M. Müsken, S. Häussler, A. Steinbach, R.W. Hartmann, Discovery of antagonists of PqsR, a key player in 2-alkyl-4-quinolone-dependent *quorum sensing* in *Pseudomonas aeruginosa*, Chemistry & Biology 19 (2012) 381–390.

[18] A. Cheng, K.M. Merz Jr., Prediction of aqueous solubility of a diverse set of compounds using quantitative structure-property relationships, Journal of Medicinal Chemistry 46 (2003) 3572–3580.
[19] S. Venkatesh, R.A. Lipper, Role of the development scientist in compound lead selection and optimization, Journal of Pharmaceutical Sciences 89 (2000) 145–154.
[20] M. Ishikawa, Y. Hashimoto, Improvement in aqueous solubility in small molecule drug discovery programs by disruption of molecular planarity and symmetry, Journal of Medicinal Chemistry 54 (2011) 1539–1554.
[21] R.M. Cross, A. Monastyrskyi, T.S. Mutka, J.N. Burrows, D.E. Kyle, R. Manetsch, Endochin optimization: structure-activity and structure-property relationship studies of 3-substituted 2-methyl-4(1H)-quinolones with antimalarial activity, Journal of Medicinal Chemistry 53 (2010) 7076–7094.
[22] C. Lu, C.K. Maurer, B. Kirsch, A. Steinbach, R.W. Hartmann, Overcoming unexpected functional inversion of PqsR antagonist in *Pseudomonas aeruginosa* led to the first in vivo potent anti-virulence agent targeting pqs quorum sensing, Angewandte Chemie International Edition 126 (2014) 1127–1130.
[23] R.T. Ellison 3rd, T.J. Giehl, F.M. LaForce, Damage of the outer membrane of enteric Gram-negative bacteria by lactoferrin and transferring, Infection and Immunity 56 (1988) 2774–2781.
[24] H. Nikaido, Molecular basis of bacterial outer membrane permeability revisited, Microbiology and Molecular Biology Reviews 67 (2003) 593–656.
[25] J.J. Marx, Iron and infection: competition between host and microbes for a precious element, Best Practice & Research Clinical Haematology 15 (2002) 411–426.
[26] S.P. Diggle, S. Matthijs, V.J. Wright, M.P. Fletcher, S.R. Chhabra, I.L. Lamont, X. Kong, R.C. Hider, P. Cornelis, M. Camara, P. Williams, The *Pseudomonas aeruginosa* 4-quinolone signal molecules HHQ and PQS play multifunctional roles in *quorum sensing* and iron entrapment, Chemistry & Biology 14 (2007) 87–96.
[27] J.M. Harris, S.F. Neelamkavil, B.R. Neustadt, C.D. Boyle, H. Liu, J. Hao, A. Stamford, S. Chackalamannil, W.J. Greenlee, Preparation of aminoquinazolinone derivatives and analogs for use as GPR119 modulators, PCT Int. Appl., 2009143049.
[28] I. Purcell, Bacterial Autoinducer Derived 4-quinolones as Novel Immune Modulators (PhD thesis University of Nottingham), 2006.
[29] R.M. Cross, R. Manetsch, Divergent route to access structurally diverse 4-quinolones via mono or sequential cross-couplings, Journal of Organic Chemistry 75 (2010) 8654–8657.
[30] M. Li, L. Li, H. Ge, Direct C3-Alkenylation of quinolones via palladium-catalyzed C-H functionalization with low catalyst loading, Advanced Synthesis & Catalysis 352 (2010) 2445–2449.
[31] A.L. Ruchelman, J.E. Kerrigan, T.K. Li, N. Zhou, A. Liu, L.F. Liu, E.J. LaVoie, Nitro and amino substitution within the A-ring of 5*H*-8,9-dimethoxy-5-(2-*N*,*N*-dimethylaminoethyl)dibenzo[c,h][1,6]naphthyridin-6-ones: influence on topoisomerase I-targeting activity and cytotoxicity, Bioorganic & Medicinal Chemistry 12 (2004) 3731–3742.
[32] J.P. Moerdyk, A.L. Speelman, K.E. Kuper III, B.R. Heiberger, R.P. Ter Louw, D.J. Zeller, A.J. Radler, J.G. Gillmore, Synthesis and photochemistry of two quinoline analogs of the perimidinespirohexadienone family of photochromes, Journal of Photochemistry and Photobiology A: Chemistry 205 (2009) 84–92.
[33] J. Escribano, C. Rivero-Hernández, H. Rivera, D. Barros, J. Castro-Pichel, E. Pérez-Herrán, A. Mendoza-Losana, I. Angulo-Barturen, S. Ferrer-Bazaga, E. Jiménez-Navarro, L. Ballell, 4-Substituted thioquinolines and thiazoloquinolines: potent, selective, and Tween-80 in vitro dependent families of antitubercular agents with moderate in vivo activity, ChemMedChem 6 (2011) 2252–2263.
[34] C. Pidathala, R. Amewu, B. Pacorel, G.L. Nixon, P. Gibbons, W.D. Hong, S.C. Leung, N.G. Berry, R. Sharma, P.A. Stocks, A. Srivastava, A.E. Shone, S. Charoensutthivarakul, L. Taylor, O. Berger, A. Mbekeani, A. Hill, N.E. Fisher, A.J. Warman, G.A. Biagini, S.A. Ward, P.M. O'Neill, Identification, design and biological evaluation of bisaryl quinolones targeting Plasmodium falciparum type II NADH:quinone oxidoreductase (PfNDH2), Journal of Medicinal Chemistry 55 (2012) 1831–1843.
[35] Y. Zhang, W.A. Guiguemde, M. Sigal, F. Zhu, M.C. Connelly, S. Nwaka, R.K. Guy, Synthesis and structure-activity relationships of antimalarial 4-oxo-3-carboxyl quinolones, Bioorganic & Medicinal Chemistry 18 (2010) 2756–2766.
[36] G. Giacomelli, A. Porcheddu, M. Salaris, Simple one-flask method for the preparation of hydroxamic acids, Organic Letters 5 (2003) 2715–2717.
[37] H. Schmidt, Cyclisierungsreaktionen von Ethoxymethylenmalononitril mit 4-substituierten Acetessigestern, Monatshefte fuer Chemie 120 (1989) 891–897.
[38] P.H. Lambert, M. Vaultier, R. Carrie, Application of the intramolecular aza-Wittig reaction to the synthesis of vinylogous urethanes and amides, Journal of Organic Chemistry 50 (1985) 5352–5356.
[39] M. Takakiyo, M. Hiroshi, Y. Tomoyuki, J. Masahiro, Process for the Production of an Optically Active Alcohol and a Novel Optically Active Alcohol, US6103517.
[40] C.K. Maurer, A. Steinbach, R.W. Hartmann, Development and validation of a UHPLC-MS/MS procedure for quantification of the *Pseudomonas* quinolone signal in bacterial culture after acetylation for characterization of new *quorum sensing* inhibitors, Journal of Pharmaceutical and Biomedical Analysis 86C (2013) 127–134.
[41] D.W. Essar, L. Eberly, A. Hadero, I.P. Crawford, Identification and characterization of genes for a second anthranilate synthase in *Pseudomonas aeruginosa*: interchangeability of the two anthranilate synthases and evolutionary implications, Journal of Bacteriology 172 (1990) 884–890.
[42] T. Klein, C. Henn, J.C. de Jong, C. Zimmer, B. Kirsch, C.K. Maurer, D. Pistorius, R. Müller, A. Steinbach, R.W. Hartmann, Identification of small-molecule antagonists of the *Pseudomonas aeruginosa* transcriptional regulator PqsR: biophysically guided hit discovery and optimization, ACS Chemical Biology 7 (2012) 1496–1501.

# Chapter 3: Publication B: "Overcoming the unexpected functional inversion of a PqsR antagonist in Pseudomonas aeruginosa: an in vivo potent antivirulence agent targeting pqs quorum sensing" (DOI: 10.1002/anie.201307547)

Angewandte International Edition Chemie

Drug Discovery

DOI: 10.1002/anie.201307547

## Overcoming the Unexpected Functional Inversion of a PqsR Antagonist in *Pseudomonas aeruginosa*: An In Vivo Potent Antivirulence Agent Targeting *pqs* Quorum Sensing**

*Cenbin Lu, Christine K. Maurer, Benjamin Kirsch, Anke Steinbach,* and Rolf W. Hartmann**

***Abstract:*** *The virulence regulator PqsR of Pseudomonas aeruginosa is considered as an attractive target for attenuating the bacterial pathogenicity without eliciting resistance. However, despite efforts and desires, no promising PqsR antagonist has been discovered thus far. Now, a surprising functionality change of a highly affine PqsR antagonist in P. aeruginosa is revealed, which is mediated by a bacterial signal molecule synthase and responsible for low cellular potency. Blockade of the susceptible position led to the discovery of the first antivirulence compound that is potent in vivo and targets PqsR, thus providing a proof of concept for this novel antivirulence therapy.*

Nowadays, human beings are confronted with an alarming situation in view of the lack of effective therapies against antibiotic-resistant bacterial infections.[1] The predicament is attributed to the mode of action of marketed antibiotics, which is based on interference with bacterial growth, which results in an inevitable selection of resistant strains.[2] Consequently, the discovery of novel anti-infectives that are less prone to resistance is challenging. However, the interest of the pharmaceutical industry to develop new antibiotics is decreasing.[3] Furthermore, progress is hampered by a high attrition rate of compounds that are active in cell-free assays, but inefficient in bacteria.[4] A promising strategy to overcome the growing and challenging resistance problem is to selectively target non-vital functions that are associated with the pathogenicity of a bug, such as the production of virulence factors.[5–8] The human opportunistic pathogen *P. aeruginosa* causes severe and fatal infections in cystic fibrosis patients. Aside from an extensive inflammatory response that is dominated by polymorphonuclear neutrophils,[9] virulence factors play a critical role in progressive lung deterioration during infection. Their production is controlled by a cell-density-dependent extraordinary cell-to-cell communication system, which is known as quorum sensing (QS) and uses signal molecules.[10,11] With a focus on developing anti-infectives with novel modes of action, recent contributions from academia[12–14] highlight quorum sensing inhibitors (QSIs) as potential powerful agents for antivirulence therapy. The quorum sensing of the *Pseudomonas* quinolone signal (*pqs*) is a potential target in *P. aeruginosa*. A first attempt to interfere with this system resulted in compounds with low efficiency in an animal model.[15] Herein, we describe an unexpected functional inversion of a QS receptor antagonist (a QSI) into an agonist by *P. aeruginosa* and report the first in vivo potent antivirulence agent targeting *pqs* QS.

PqsR is a key DNA-binding receptor of this *pqs* QS system that is specific to *P. aeruginosa* and a critical regulator that fine-tunes a large set of genes that encode for virulence factors, such as pyocyanin, elastase B, and hydrogen cyanide.[16,17] PQS and 2-heptyl-4-hydroxyquinoline (HHQ) are the natural ligands and agonists of the receptor (Figure 1a), and function as the signal molecules of *pqs* QS.[18,19] The biosynthesis of HHQ is conducted by the enzymes PqsABCD, which are encoded by genes located in the *pqs* operon. The transcription of this operon is in turn positively regulated by PqsR. The synthase PqsH finally hydroxylates HHQ to form PQS (Figure 1a).[20–22] A *pqsR* knock-out mutant of *P. aeruginosa* that is deficient in *pqs* QS does not produce any pyocyanin, and displays reduced pathogenicity.[19,21] Thus, we considered PqsR as an attractive target for the development of QSIs. Based on the scaffold of HHQ, we recently reported compound **1** (Figure 1a), which is, to the best of our knowledge, the only PqsR antagonist described to date. It showed an $IC_{50}$ of 51 nM in an *E. coli* reporter gene assay.[23] Considering its high activity towards PqsR, **1** only moderately reduced the production of pyocyanin (Table 1). Therefore, we decided to further characterize the behavior of the antagonist in *P. aeruginosa*. Most interestingly, **1**, which showed a purely antagonistic activity in *E. coli* reporter gene assays (Figure 1b and c), displayed a dose-dependent agonistic activity in *P. aeruginosa* (Figure 1c), which could be the reason for the marked loss of antagonistic activity of **1** ($IC_{50}$ = 51 nM in *E. coli*, 60% inhibition at 10 μM in *P. aeruginosa*; Table 1). The opposite nature of the functional properties in the two bacterial species suggests that a biotransformation of the compound may have occurred in *P. aeruginosa*. We turned our attention to the enzymes that are involved in the *pqs* QS signaling pathway and speculated that a biochemical modification of **1** into **2** by PqsH occurs (Figure 1a) for the following reasons: 1) Compound **1** is structurally very similar

[*] C. Lu,[+] C. K. Maurer,[+] B. Kirsch, Dr. A. Steinbach, Prof. Dr. R. W. Hartmann
Helmholtz-Institute for Pharmaceutical Research Saarland & Pharmaceutical and Medicinal Chemistry, Saarland University Campus C2.3, 66123 Saarbrücken (Germany)
E-mail: anke.steinbach@helmholtz-hzi.de
rolf.hartmann@helmholtz-hzi.de

[+] These authors contributed equally to this work.

[**] We thank Drs. Daniele Bano and Kostoula Troullinaki (German Center for Neurodegenerative Diseases, Bonn, Germany) for providing *C. elegans*, Dr. Matthew Wand (Health Protection Agency, Salisbury, UK) for valuable advice regarding the *G. mellonella* infection model, and Dr. Andrea Braunshausen for helpful discussions. *pqs* = *Pseudomonas* quinolone signal.

Supporting information for this article is available on the WWW under http://dx.doi.org/10.1002/anie.201307547.

  

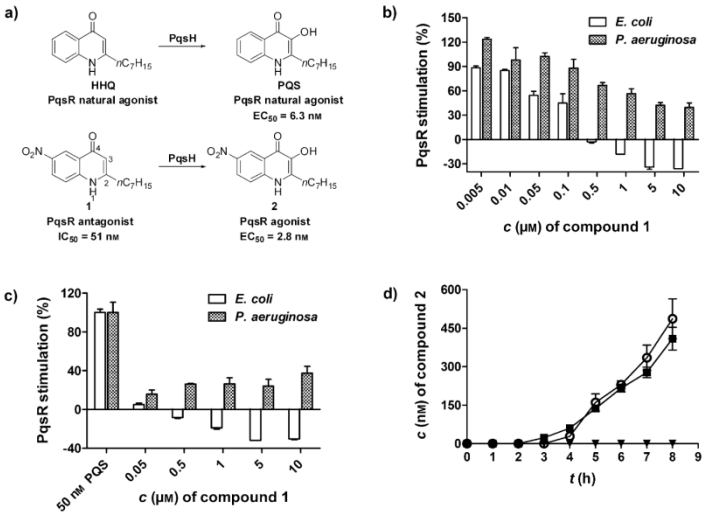


***Figure 1.*** Characterization of the PqsR antagonist **1** in *E. coli* and *P. aeruginosa* and time-dependent formation of **2**. a) Chemical structures of HHQ, PQS, **1**, and **2**. b) Antagonist test of **1** in β-galactosidase reporter gene assays based on *E. coli* or *P. aeruginosa*. The assays were performed in the presence of PQS (50 nM). For the *y* axis, 0% is defined as the basal PqsR stimulation without ligands, and 100% is defined as the PqsR stimulation by PQS (50 nM). Mean values of two independent experiments with $n=4$ are given, error bars represent standard deviation. c) Agonist test of **1** in β-galactosidase reporter gene assays based on *E. coli* or *P. aeruginosa*. For the *y* axis, 0% and 100% stimulation are defined as above. Mean values of two independent experiments with $n=4$ are given, error bars represent standard deviation. Significance of agonistic activity for **1** in *P. aeruginosa* compared to basal level: $p<0.05$. d) Time-course studies of the production of **2** in PA14 (○), *pqsH* (▼), and *pqsA* (■) mutants. Strains were incubated with **1** (5 μM). Mean values of one experiment with $n=3$ are given, error bars represent standard deviation.

***Table 1:*** Determination of antagonistic activity and effects on PQS, HHQ, and the virulence factor pyocyanin.

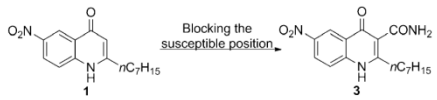


| Parameter | **1** | **3** |
|---|---|---|
| $IC_{50}$ in *E. coli* [nM] | 51 | 35 |
| $IC_{50}$ in *P. aeruginosa* [nM] | 60% inhibition[a] | 404 |
| Reduction of PQS levels[b] | 14%* | 37%* |
| Reduction of HHQ levels[b] | 1% | 54%* |
| Reduction of pyocyanin levels[b] | 44%* | 81%* ($IC_{50}$: 2 μM) |

PQS, HHQ, and pyocyanin assays were performed in PA14. Mean values of at least two independent experiments with $n=3$ are given, standard deviation less than 25%. Significance: * $p<0.05$. [a] Tested at 10 μM. [b] Tested at 15 μM.

to the natural ligand HHQ, which is converted into PQS by PqsH; 2) Many PQS analogues show agonistic activity towards PqsR;[23,24] 3) **1** revealed an agonistic activity in *P. aeruginosa* as mentioned above. To prove this hypothesis, ultrahigh-performance liquid chromatography (UHPLC) tandem mass spectrometry was applied to observe the supposed product of biotransformation **2** in *P. aeruginosa* (wild type; PA14). Interestingly, after incubation of PA14 with **1**, the chromatogram of selected reaction monitoring (SRM) transition $m/z$ $303>218$ revealed a signal peak with identical retention times for the proposed product and the chemically synthesized compound **2** (Supporting Information, Figure S1). To further validate bacterial-cell-mediated conversion of **1** into **2**, and to examine the involvement of PqsH in this process, a time-course study was conducted. The production of **2** in PA14 and in the native-ligand-free mutant *pqsA*[21] with functional PqsH was time-dependent, whereas the *pqsH* mutant failed to synthesize **2** (Figure 1d; for the results after 16 h, see Figure S2). This result clearly identifies PqsH as the enzyme responsible for the biotransformation. Subsequently, we examined the activity of product **2**. In a competition experiment performed in *E. coli*, **2** efficiently restored the PqsR stimulation that was repressed by antagonist **1** (in the antagonist test, **2** restored almost 50% of the PqsR stimulation, even in competition with **1** at ten times higher concentrations; Figure S3). Compound **2** ($EC_{50}=2.8$ nM; $EC_{50}$: ligand concentration to achieve a half-maximal degree of PqsR receptor stimulation) is even more active than the strongest natural PqsR agonist PQS ($EC_{50}=6.3$ nM). Taken together, these findings explain that the unexpected agonistic activity that was observed for **1** in *P. aeruginosa* is due to PqsH-mediated functional inversion (Figure 1a).

For a rational development of potent and stable PqsR antagonists, the susceptible 3-position had to be blocked by substitution of the hydrogen atom with an appropriate functional group. A small library of 3-substituted compounds ($CONH_2$, COOH, COOEt, and CONHOH) were synthesized (data not shown). In terms of their agonistic/antagonistic profiles, the carboxamide **3** (for its synthesis, see Figure S4) turned out to be the most promising derivative. Accordingly, **3** was used for further biological evaluation. Most interestingly, **3** showed high potency in the *E. coli* reporter gene assay, but retained its antagonistic activity in *P. aeruginosa* without displaying any agonistic activity up to 15 μM (Table 1).

Next, the effects of the antagonists on the production of the signal molecules were examined in PA14.[25] Compared with **1**, the improved antagonist **3** was able to strongly reduce the HHQ and PQS levels by over 50% and 30%, respectively, at a concentration of 15 μM (Table 1). We then investigated the production of pyocyanin, an important virulence factor

  

and a major contributor to the pathogenicity of *P. aeruginosa*.[26] Strikingly, **3** efficiently decreased the pyocyanin levels with an $IC_{50}$ of 2 μM, whereas **1** revealed a strongly reduced potency (44% at 15 μM). A growth-inhibition effect could be excluded based on growth curves of PA14 that were measured in the presence of antagonist (15 μM) in minimal medium (Figure S5). Overall, optimization of the antagonist led to enhanced effects on the reduction of signal-molecule and pyocyanin levels, which is in agreement with the improved antagonistic activity that was observed in the *P. aeruginosa* reporter gene assay. To the best of our knowledge, **3** is the compound that most effectively interferes with the *pqs* QS system in *P. aeruginosa*.

Encouraged by these results, we validated the PqsR antagonistic properties of **3** in appropriate animal experiments.[27] As *Caenorhabditis elegans* is sensitive towards a *P. aeruginosa* infection and its virulence factor pyocyanin,[28] **3** was evaluated in a *C. elegans* fast killing assay. The survival rate of *C. elegans* that were incubated on agar plates containing PA14 and **3** (15 μM) remained at 94%; in the absence of the antagonist, however, the survival rate continuously decreased to 47% (control) within six hours (Figure 2a). These results highlight a protective effect of **3** against *P. aeruginosa* infection in the nematode assay.

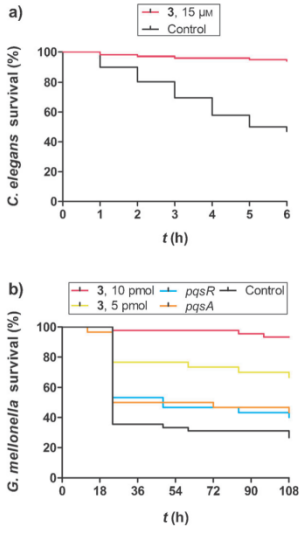


***Figure 2.*** Evaluation of the PqsR antagonist **3** in animal infection models. a) Kaplan–Meier survival curves of *C. elegans* incubated on agar plates containing PA14 and DMSO (control) or **3** (15 μM). Results represent cumulative data from three independent experiments. The survival rate was significantly larger for treated nematodes than for those in the control experiment ($p < 0.0001$; log-rank test). b) Survival curves of *G. mellonella* larvae infected with PA14 receiving no treatment (control) or receiving treatment with compound **3** (5 pmol or 10 pmol), and of larvae infected with the PA14 *pqsR* or *pqsA* mutants. Results represent combined data from at least two independent experiments. The survival rate was significantly larger for treated larvae than for larvae in the control experiment (5 pmol of **3**: $p < 0.001$, 10 pmol of **3**: $p < 0.0001$; log-rank test).

We further challenged a more complex animal infection model with *Galleria mellonella*. This insect model displays a significant positive correlation with a mouse model and is therefore considered as a powerful tool to investigate pathogenicity causing mammalian infections. The larvae of the greater wax moth are susceptible to PA14, with a 50% lethal dose of one bacterium.[29] *G. mellonella* larvae were infected with PA14 in the absence and presence of antagonist **3**. Most interestingly, the treatment of the PA14-infected larvae with antagonist **3** (10 pmol) led to a survival rate of 93% (Figure 2b), whereas only 36% of the infected larvae survived the first 24 h in the absence of **3** (control). Treatment with only 5 pmol of antagonist provided partial protection with a survival rate of 67%. It should be noted that **3** is intensively diluted by the hemolymph after injection. Given an average weight of 450 mg and assuming a total hemolymph volume of 450 μL for each larva, the antagonist exerted its therapeutic effect at a final concentration of 22 nM (corresponding to 7.3 $ng\,g^{-1}$ body weight) in the larva. Most interestingly, PA14-infected larvae receiving treatment with antagonist **3** showed much higher survival rates than those infected with the mutants *pqsA* and *pqsR*, which are deficient in *pqs* QS (Figure 2b). This implies that disruption of QS with small molecules, rather than genetic deletion, can be advantageous. Overall, the results from the two animal studies clearly show that **3** is a strong antivirulence agent.

In summary, we have revealed that the synthase PqsH converts the potent PqsR antagonist into a strong agonist; this process is responsible for the low efficacy of compound **1**. Surprisingly, such a slight structural modification (hydroxylation) leads to complete loss of the antagonistic activity of compound **1** and dramatically imparts the opposite functionality (agonism) to the ligand. A high percentage of anti-infectives suffer from ineffectiveness in cell-based assays or under in vivo conditions, which is generally considered to be due to penetration problems or efflux-pump-mediated excretion. As an optimization addressing these drawbacks is regarded as highly challenging, these compounds are usually discarded. Herein, we suggested that a rational consideration of other potential factors that impair the activity is rewarding. As shown in this case study, ineffective compounds can be rescued by medicinal-chemistry strategies, which decreases the attrition rate during the drug development process. Moreover, our research identified the PqsR antagonist **3** as an antivirulence agent that is highly potent in vivo, which provides the first proof of concept that PqsR antagonists reduce the mortality caused by *P. aeruginosa* in two animal models. This finding provides a promising starting point for further in vivo investigations using mammalian organisms and may open new avenues for the development of anti-infectives that are less prone to resistance. Furthermore, species-selective targeting of specific regulatory pathways might help to minimize adverse effects that are observed with broad-spectrum antibiotics.

Received: August 27, 2013
Revised: October 10, 2013
Published online: December 11, 2013

  

**Keywords:** antivirulence · drug discovery · inhibitors · medicinal chemistry · resistance

[1] C. A. Arias, B. E. Murray, *N. Engl. J. Med.* **2010**, *362-363*, 439 – 443.
[2] S. B. Levy, B. Marshall, *Nat. Med.* **2004**, *10*, 122 – 129.
[3] K. Lewis, *Nature* **2012**, *485*, 439 – 440.
[4] A. R. M. Coates, G. Halls, Y. Hu, *Br. J. Pharmacol.* **2011**, *163*, 184 – 194.
[5] L. Cegelski, G. R. Marshall, G. R. Eldridge, S. J. Hultgren, *Nat. Rev. Microbiol.* **2008**, *6*, 17 – 27.
[6] D. A. Rasko, V. Sperandio, *Nat. Rev. Drug Discovery* **2010**, *9*, 117 – 128.
[7] W. R. Galloway, J. T. Hodgkinson, S. Bowden, M. Welch, D. R. Spring, *Trends Microbiol.* **2012**, *20*, 449 – 458.
[8] K. M. O'Connell, J. T. Hodgkinson, H. F. Sore, M. Welch, G. P. Salmond, D. R. Spring, *Angew. Chem.* **2013**, *125*, 10904 – 10932; *Angew. Chem. Int. Ed.* **2013**, *52*, 10706 – 10733.
[9] D. G. Downey, S. C. Bell, J. S. Elborn, *Thorax* **2009**, *64*, 81 – 88.
[10] S. Swift, J. A. Downie, N. A. Whitehead, A. M. L. Barnard, G. P. C. Salmond, P. Williams, *Adv. Microb. Physiol.* **2001**, *45*, 199 – 270.
[11] S. T. Rutherford, B. L. Bassler, *Cold Spring Harbor Perspect. Med.* **2012**, *2*, a012427.
[12] R. Frei, A. S. Breitbach, H. E. Blackwell, *Angew. Chem.* **2012**, *124*, 5316 – 5319; *Angew. Chem. Int. Ed.* **2012**, *51*, 5226 – 5229.
[13] G. Brackman, S. Celen, K. Baruah, P. Bossier, S. V. Calenbergh, H. J. Nelis, T. Coenye, *Microbiology* **2009**, *155*, 4114 – 4122.
[14] M. P. Storz, C. K. Maurer, C. Zimmer, N. Wagner, C. Brengel, J. C. de Jong, S. Lucas, M. Müsken, S. Häussler, A. Steinbach, R. W. Hartmann, *J. Am. Chem. Soc.* **2012**, *134*, 16143 – 16146.
[15] B. Lesic, F. Lepine, E. Deziel, J. Zhang, Q. Zhang, K. Padfield, M. Castonguay, S. Milot, S. Stachel, A. A. Tzika, R. G. Tompkins, L. G. Rahme, *PLoS Pathog.* **2007**, *3*, 1229 – 1239.
[16] H. Cao, G. Krishnan, B. Goumnerov, J. Tsongalis, R. Tompkins, L. G. Rahme, *Proc. Natl. Acad. Sci. USA* **2001**, *98*, 14613 – 14618.
[17] E. Déziel, S. Gopalan, A. P. Tampakaki, F. Lépine, K. E. Padfield, M. Saucier, G. Xiao, L. G. Rahme, *Mol. Microbiol.* **2005**, *55*, 998 – 1014.
[18] E. C. Pesci, J. B. J. Milbank, J. P. Pearson, S. McKnight, A. S. Kende, E. P. Greenberg, B. H. Iglewski, *Proc. Natl. Acad. Sci. USA* **1999**, *96*, 11229 – 11234.
[19] G. Xiao, E. Deziel, J. He, F. Lepine, B. Lesic, M. Castonguay, S. Milot, A. P. Tampakaki, S. E. Stachel, L. G. Rahme, *Mol. Microbiol.* **2006**, *62*, 1689 – 1699.
[20] L. A. Gallagher, S. L. McKnight, M. S. Kuznetsova, E. C. Pesci, C. Manoil, *J. Bacteriol.* **2002**, *184*, 6472 – 6480.
[21] E. Deziel, F. Lepine, S. Milot, J. X. He, M. N. Mindrinos, R. G. Tompkins, L. G. Rahme, *Proc. Natl. Acad. Sci. USA* **2004**, *101*, 1339 – 1344.
[22] J. W. Schertzer, S. A. Brown, M. Whiteley, *Mol. Microbiol.* **2010**, *77*, 1527 – 1538.
[23] C. Lu, B. Kirsch, C. Zimmer, J. C. de Jong, C. Henn, C. K. Maurer, M. Müsken, S. Häussler, A. Steinbach, R. W. Hartmann, *Chem. Biol.* **2012**, *19*, 381 – 390.
[24] J. Hodgkinson, S. D. Bowden, W. R. J. D. Galloway, D. R. Spring, M. Welch, *J. Bacteriol.* **2010**, *192*, 3833 – 3837.
[25] C. K. Maurer, A. Steinbach, R. W. Hartmann, *J. Pharm. Biomed. Anal.* **2013**, *86C*, 127 – 134.
[26] J. M. Courtney, J. Bradley, J. Mccaughan, T. M. O'Connor, C. Shortt, C. P. Bredin, I. Bradbury, J. S. Elborn, *Pediatr. Pulmonol.* **2007**, *42*, 525 – 532.
[27] E. Papaioannou, P. D. Utari, W. J. Quax, *Int. J. Mol. Sci.* **2013**, *14*, 19309 – 19340.
[28] S. Mahajan-Miklos, M. Tan, L. G. Rahme, F. M. Ausubel, *Cell* **1999**, *96*, 47 – 56.
[29] G. Jander, L. G. Rahme, F. M. Ausubel, *J. Bacteriol.* **2000**, *182*, 3843 – 3845.

  

# Discussion

The present thesis describes several studies to explore the nature and functionality of compounds interfering with PqsR. Efforts were undertaken to investigate the different activities between an *E. coli* and PA test system. However, even with potent pathogenicity blockers in hand, the underlying molecular mechanism still needs to be explored in detail.

## Molecular mechanism of inverse agonists

As mentioned in the introduction of this thesis, PqsR requires the autoinducer molecules HHQ and PQS for boosting its transcription-promoting activity. While, in general, many compounds act as PqsR blockers by competing with the natural agonist, the presented work addresses such that, in addition, possess the functional properties of inverse agonists (Figure 6).

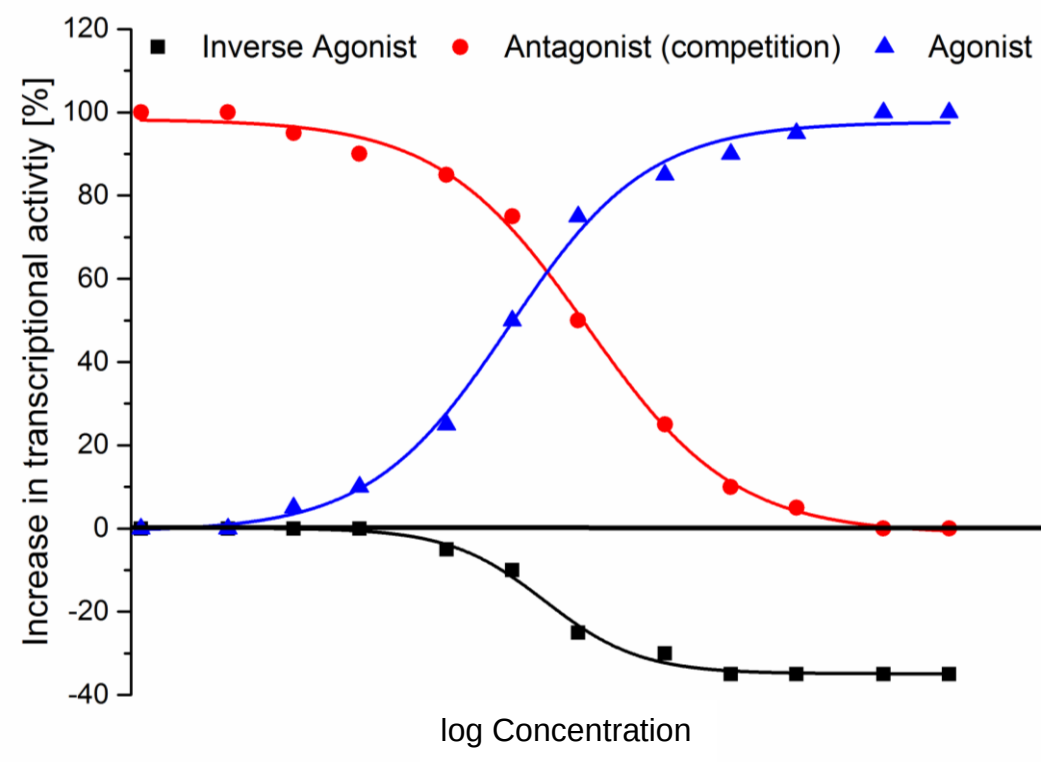


**Figure 6:** Examples of agonistic, antagonistic, and inverse agonistic dose-response curves. The basal transcription rate is expressed by an increase of 0%. Here, the agonist leads to a concentration-dependent increase in transcriptional activity (blue curve), while the antagonist is able to compete with the agonist to reduce the activity back to the basal expression level (red curve). In contrast, the

inverse agonist lowers the basal expression level (black line) in a concentration-dependent manner (black curve).

The functional behavior of basal inverse agonism shown in Figure 6 corresponds to that of compound **1** described in chapter 1. As can be seen in chapter 1, as well as in publications **A** & **B**, almost every antagonistic compound tested for PqsR activity additionally possessed an inverse agonistic functionality. Therefore, not only preventing the virulence-boosting abilities of HHQ and PQS but also suppressing the natural, positive gene-regulating effects of unliganded PqsR. Chapter 1 tried to explore the mechanism behind the inverse agonistic functionality that render the transcriptional machinery (promotor DNA / (RNAP) / PqsR) inactive. In general, LTTRs are proposed to interact with the RNAP in a direct manner causing an increase in polymerase activity, which corresponds to gene upregulation (Tropel and van der Meer, J.R., 2004). This interaction requires a close position of both RNAP and LTTR. The surprising fact that several inverse agonistic ligands increased the affinity to the promotor DNA let us hypothesize that PqsR might be locked on the promotor DNA in a position that hinders productive PqsR-RNAP interactions. As can be seen in Figure 9 of chapter 1, the inverse agonists force PqsR to a binding sequence that is located more upstream in relation to the agonist-liganded DNA binding site. This switch in binding position might impair the interactions of RNAP and regulator due to increased distance.

## *In vitro* versus *in cellulo*

The finding that inverse agonists of PqsR favor the binding to a defined binding pattern that differs from the one observed for the apo and the agonist- liganded form allows a possible functional characterization of the ligands *in vitro*. So far, we used cell- based assay systems for the functional characterization of compounds targeting PqsR. However, these reporter gene-based test systems suffer from some weaknesses. The usage of whole cell systems always includes additional PK barriers such as the bacterial cell envelope (Silver, 2011). This actually might prevent compounds with potent target activity from reaching their intracellular target. Even

when entering the cell, compounds might be susceptible to metabolic alteration as demonstrated in publication **B**. As a result, potentially promising inhibitors are often discarded, without looking for a way to rescue the activity by e.g. turning them less prone to metabolization. Furthermore, the results of the β- galactosidase- based systems can be misguiding when testing compounds that influence the galactosidase enzyme itself. In contrast, the *in vitro* based approach using purified protein allows a verification of on-target activity. In this setup, no PK issues like the disturbing cell wall barrier, efflux pumps, or metabolizing enzymes are present. However, the fact that it only allows a qualitative statement regarding the functionality depicts a disadvantage of this method. Compounds that alter the binding affinity to different DNA fragments depending on their functionality (as shown in Figure 6 of chapter 1) could be characterized as antagonists or agonists. In case of diverse PqsR ligands, the titration of defined mutated DNA fragments would yield altered DNA affinities depending on the ligand functionality (agonist or inverse agonist). Additionally, the identification of novel DNA promotor sequences that are addressed by the regulator under addition of different ligands is also an option. However, a quantitative assessment of a compound's functional activity (e.g., determination of its $IC_{50}$) requires distinct methods like the former mentioned reporter gene tests. For this purpose, the use of cell- based assays represents a powerful tool, not only for PqsR agonists and antagonists. This highlights the general necessity for a combination of both, cell- based and cell- free test systems. The usage of only one setup does not guarantee an exclusion of false positive or false negative results.

## Novel anti- virulence compounds

In publications **A** and **B,** we reported on potent PqsR antagonists derived from natural quinolone-based coinducers. This compound class presented the first potent PqsR antagonists (Lu et al., 2012). The HHQ derivative harboring a nitro substituent in 6-position of the quinolone core (6-$NO_2$-HHQ or compound **1** from publication **B**) served as starting point for the development of PqsR antagonists with improved potency. While the above-mentioned compound possessed a nanomolar $IC_{50}$ in the *E. coli* based reporter gene system, we unexpectedly observed a dramatic decrease in activity in the *P. aeruginosa* background by more than 200- fold. This lack of

activity also correlated with poor effects on virulence factor production (Lu et al., 2014b). Besides the possibility of an altered PK profile due to the different organisms, we also thought of pharmacodynamic effects caused by *P. aeruginosa*. The usage of Liquid Chromatography Mass Spectrometry (LCMS-MS) based methods revealed that the monooxygenase PqsH converted compound **1** into the hydroxylated metabolite **2**. In addition to the depletion of the antagonistic compound, the formed metabolite exhibited a strong agonistic functional profile ($EC_{50}$ = 2.8 nM), being around 2- fold more potent than the natural ligand PQS. In that way, the bacteria were able to synthesize a "superagonist" (Galloway, Warren R J D et al., 2012) that enhanced the activity of the PQS QS. This finding forced us to improve the metabolic stability of compound **1** against a PqsH- mediated hydroxylation. Therefore, a carboxamide substituent was introduced in the susceptible 3- position of the quinolone core. The yielded compound **3** not only possessed good activity in *E. coli* but also showed high potency in *Pseudomonas* with simultaneously enhanced reduction of virulence factor formation. This strategy rehabilitated the quinolone compound class as potent anti- virulence agents and highlights the importance for the combination of different assay systems.

However, all of the identified antagonists with increased potency (Lu et al., 2012; Lu et al., 2014b) suffered from poor physicochemical properties, especially regarding water solubility. Publication **A** addressed this problem by trying several strategies to improve this parameter. *E. coli*-based reporter gene experiments monitoring the functional properties of the derivatives in combination with High Performance Liquid Chromatography (HPLC)-based solubility tests guided the structural optimization process. For the majority of the synthesized derivatives, we observed only weak to moderate antagonistic activity at simultaneously increased water solubility. This phenomenon might be caused by permeation issues regarding the possibility that hydrophilic compounds cannot easily pass the cell layer. Another possible explanation might be given when looking at a reported crystal structure with the HHQ derivative NHQ (Ilangovan et al., 2013). Here, a hydrophobic pocket that harbors the lipophilic alkyl chain part of NHQ forms an important space for the ligand- receptor interaction. In case of more hydrophilic derivatives this hydrophobic pocket would be less favorable for interactions in contrast to the lipophilic NHQ sidechain. Nevertheless, the optimization process yielded compound **16** that possessed increased water solubility as well as an $IC_{50}$ on PqsR in the nanomolar range.

Therefore, in combination with the described structure activity relationship (SAR) (Lu et al., 2014a) studies, this compound can be regarded as a good starting point for future optimization strategies. In parallel, the described SAR allows a better understanding and deeper insight into the functional nature of different PqsR ligands. However, the exact structural properties that render compounds agonists or antagonists still have to be elucidated. In addition to the findings described in the present thesis, discussions regarding synthesis and solubility properties as well as biological activities of the different compounds from publications **A** and **B** were described by my colleagues Dr. Cenbin Lu (Lu, 2014) and Dr. Christine K. Maurer (Maurer, 2015) in their dissertations.

# Outlook

These studies contributed to a better understanding of the complex regulatory transcriptional machinery. However, to date, the lack of a crystal structure for the full length PqsR only allows artificial studies regarding the molecular behavior of the receptor. For future investigations, the crystallization of a full length PqsR in complex with target promotor DNA and different ligands would be of great interest to the community. Finally, the compounds identified and characterized in the present thesis are in particular possible candidates for more detailed *in vivo* studies and should therefore be tested in more complex animal models like a mouse model.

# Summary

The present thesis was directed at establishing assay systems for the characterization of PqsR and its ligands. The conducted reporter gene experiments identified various agonistic and antagonistic compounds with, high potency in *Pseudomonas aeruginosa*. As presented in publication **B**, an unexpected change in the functional activity could be explained by cell- mediated hydroxylation. This fact demonstrates how bacteria can inactivate an anti-virulence agent and turn it into a compound even favoring the virulence. The quinolone-based antagonists turned out to suffer from poor physicochemical properties, especially regarding water solubility. Publication **A** intended to address this issue and as a result, several compounds with improved solubility/antagonistic activity profile were obtained. Chapter 1 pointed towards exploring the origin of the inverse agonistic effects. Using a fluorescence polarization-based *in vitro* assay, it could be shown that these inverse agonistic characteristics are presumably caused by locking the regulator PqsR at a formerly unknown binding sequence on the promotor DNA. Furthermore, it was shown that the apo- and the agonist- liganded forms of PqsR occupy the same binding sequence, while the antagonist- liganded form binds to a more narrow region.

# Zusammenfassung

Die vorliegende Arbeit beschäftigt sich mit der Entwicklung von Testsystemen zur Identifizierung und Charakterisierung von PqsR Liganden. Die durchgeführten Reportergenassay Experimente führten zur Identifikation verschiedener, agonistischer und antagonistischer Verbindungen mit teilweise nanomolaren Aktivitäten in *Pseudomonas aeruginosa*. Wie in Publikation **B** beschrieben, konnte der Verlust an Aktivität in *Pseudomonas aeruginosa* auf bakteriellen Metabolismus zurückgeführt werden. Eine gezielte Modifikation der Verbindung stellte die Aktivität wieder her. Publikation **A** verfolgte das Ziel, Verbindungen mit besserer Wasserlöslichkeit bei gleichzeitigem Erhalt der antagonistischen Aktivität herzustellen. Kapitel 1 beschäftigte sich mit dem Phänomen des inversen Agonismus, eine Wirkweise, die mehrere der hier beschriebenen PqsR Antagonisten besitzen. Mit Hilfe eines *in vitro* Fluoreszenzpolarisationsassays, konnte gezeigt werden, dass diese invers agonistischen Aktivitäten möglicherweise durch Einfrieren einer bestimmten Konformation des Regulators PqsR zustande kommen. Der Regulator bindet in Anwesenheit dieser inversen Agonisten an eine bisher unbekannte Bindestelle auf der Promotor DNA, wodurch eventuell produktive Interaktionen mit der RNA Polymerase verhindert werden.

# List of Abbreviations

| | |
|---|---|
| AHL | N-acyl L-homoserine lactone |
| BS3 | bis[sulfosuccinimidyl]suberate |
| CF | Cystic Fibrosis |
| Cpd. | Compound |
| DMSO | Dimethyl sulfoxide |
| FP | Fluorescence Polarization |
| HHQ | 2-heptyl-4(1H)-quinolone |
| HHQ-d4 | 5,6,7,8-tetradeutero-2-heptyl-4(1H)-quinolone |
| HPLC | High Performance Liquid Chromatography |
| HTH | Helix-Turn-Helix |
| IC50 | Half maximal inhibitory concentration |
| ITC | Isothermal Titration Calorimetry |
| Kd | Dissociation constant |
| kDa | Protein mass in Kilo-Dalton |
| LCMS-MS | Liquid Chromatography Mass Spectrometry |
| LTTR | LysR-Type Transcriptional Regulator |
| MBP | Maltose-Binding Protein |
| MvfR | Multiple Virulence factor Regulator |
| ONP | Ortho- Nitrophenol |
| ONPG | Ortho- Nitrophenol β-D-Galactospyranoside |
| PA | Pseudomonas aeruginosa |
| PAGE | Polyacrylamide gel electrophoresis |
| PQS | 3-hydroxy-2-heptyl-4(1H)-quinolone |

| | |
|---|---|
| PqsR | Pseudomonas Quinolone Signal Receptor |
| QS | Quorum Sensing |
| QSI | Quorum Sensing Inhibitor |
| RNAP | RNA Polymerase |
| SDS | Sodium dodecyl sulfate |
| SPR | Surface Plasmon Resonance |
| TSS | Transcriptional Start Site |

# References


Abdel-Mawgoud AM, Lépine F, and Déziel E (2010) Rhamnolipids: diversity of structures, microbial origins and roles. *Applied microbiology and biotechnology* **86:** 1323–1336.

Allegretta G, Weidel E, Empting M, and Hartmann RW (2015) Catechol-based substrates of chalcone synthase as a scaffold for novel inhibitors of PqsD. *European journal of medicinal chemistry* **90:** 351–359.

Anderson BJ, Larkin C, Guja K & Schildbach JF Chapter 12 Using Fluorophore-Labeled Oligonucleotides to Measure Affinities of Protein–DNA Interactions. *Methods in Enzymology* **450,** 253–272.

Bendig JW, Kyle PW, Giangrande PL, Samson DM, and Azadian BS (1987) Two neutropenic patients with multiple resistant Pseudomonas aeruginosa septicaemia treated with ciprofloxacin. *Journal of the Royal Society of Medicine* **80:** 316–317.

Bennett PM (2008) Plasmid encoded antibiotic resistance: acquisition and transfer of antibiotic resistance genes in bacteria. *British journal of pharmacology* **153 Suppl 1:** S347-57.

Blackwood LL, Stone RM, Iglewski BH, and Pennington JE (1983) Evaluation of Pseudomonas aeruginosa exotoxin A and elastase as virulence factors in acute lung infection. *Infection and immunity* **39:** 198–201.

Bodey GP, Bolivar R, Fainstein V, and Jadeja L (1983) Infections caused by Pseudomonas aeruginosa. *Reviews of infectious diseases* **5:** 279–313.

Bonomo RA, and Szabo D (2006) Mechanisms of multidrug resistance in Acinetobacter species and Pseudomonas aeruginosa. *Clinical infectious diseases* **43 Suppl 2:** 49–56.

Bradley DE (1980) A function of Pseudomonas aeruginosa PAO polar pili: twitching motility. *Canadian journal of microbiology* **26:** 146–154.

Bronstein I, Fortin J, Stanley PE, Stewart GS, and Kricka LJ (1994) Chemiluminescent and bioluminescent reporter gene assays. *Analytical biochemistry* **219:** 169–181.

Calfee MW, Coleman JP, and Pesci EC (2001) Interference with Pseudomonas quinolone signal synthesis inhibits virulence factor expression by Pseudomonas aeruginosa. *Proceedings of the National Academy of Sciences of the United States of America* **98:** 11633–11637.

Cao H, Krishnan G, Goumnerov B, Tsongalis J, Tompkins R, and Rahme LG (2001) A quorum sensing-associated virulence gene of Pseudomonas aeruginosa encodes a LysR-like transcription regulator with a unique self-regulatory mechanism. *Proceedings of the National Academy of Sciences of the United States of America* **98:** 14613–14618.

Checovich WJ, Bolger RE, and Burke T (1995) Fluorescence polarization--a new tool for cell and molecular biology. *Nature* **375:** 254–256.

Chitkara YK, and Feierabend TC (1981) Endogenous and exogenous infection with Pseudomonas aeruginosa in a burns unit. *International surgery* **66:** 237–240.

Coleman JP, Hudson LL, McKnight SL, Farrow JM, Calfee MW, Lindsey CA, and Pesci EC (2008) Pseudomonas aeruginosa PqsA is an anthranilate-coenzyme A ligase. *Journal of Bacteriology* **190:** 1247–1255.

Cugini C, Calfee MW, Farrow JM, Morales DK, Pesci EC, and Hogan DA (2007) Farnesol, a common sesquiterpene, inhibits PQS production in Pseudomonas aeruginosa. *Molecular microbiology* **65:** 896–906.

Davies D (2003) Understanding biofilm resistance to antibacterial agents. *Nature reviews. Drug discovery* **2:** 114–122.

Davies J, and Davies D (2010) Origins and Evolution of Antibiotic Resistance. *Microbiology and Molecular Biology Reviews* **74:** 417–433.

Davies JC (2002) Pseudomonas aeruginosa in cystic fibrosis: pathogenesis and persistence. *Paediatric Respiratory Reviews* **3:** 128–134.

Déziel E, Gopalan S, Tampakaki AP, Lépine F, Padfield KE, Saucier M, Xiao G, and Rahme LG (2005) The contribution of MvfR to Pseudomonas aeruginosa pathogenesis and quorum sensing circuitry regulation: multiple quorum sensing-regulated genes are modulated without affecting lasRI, rhlRI or the production of N-acyl-L-homoserine lactones. *Molecular microbiology* **55:** 998–1014.

Déziel E, Lépine F, Milot S, He J, Mindrinos MN, Tompkins RG, and Rahme LG (2004) Analysis of Pseudomonas aeruginosa 4-hydroxy-2-alkylquinolines (HAQs) reveals a role for 4-hydroxy-2-heptylquinoline in cell-to-cell communication. *Proceedings of the National Academy of Sciences of the United States of America* **101:** 1339–1344.

Diggle SP, Matthijs S, Wright VJ, Fletcher MP, Chhabra SR, Lamont IL, Kong X, Hider RC, Cornelis P, Cámara M, and Williams P (2007) The Pseudomonas aeruginosa 4-quinolone signal molecules HHQ and PQS play multifunctional roles in quorum sensing and iron entrapment. *Chemistry & biology* **14:** 87–96.

Diggle SP, Winzer K, Chhabra SR, Worrall KE, Cámara M, and Williams P (2003) The Pseudomonas aeruginosa quinolone signal molecule overcomes the cell density-dependency of the quorum sensing hierarchy, regulates rhl-dependent genes at the onset of stationary phase and can be produced in the absence of LasR. *Molecular microbiology* **50:** 29–43.

Drees SL, and Fetzner S (2015) PqsE of Pseudomonas aeruginosa Acts as Pathway-Specific Thioesterase in the Biosynthesis of Alkylquinolone Signaling Molecules. *Chemistry & biology* **22:** 611–618.

Dubbs P, Dubbs JM, and Tabita FR (2004) Effector-mediated interaction of CbbRI and CbbRII regulators with target sequences in Rhodobacter capsulatus. *Journal of Bacteriology* **186:** 8026–8035.

Dulcey CE, Dekimpe V, Fauvelle D, Milot S, Groleau M, Doucet N, Rahme LG, Lépine F, and Déziel E (2013) The end of an old hypothesis: the pseudomonas signaling molecules 4-hydroxy-2-alkylquinolines derive from fatty acids, not 3-ketofatty acids. *Chemistry & biology* **20:** 1481–1491.

Flemming H, and Wingender J (2010) The biofilm matrix. *Nature reviews. Microbiology* **8:** 623–633.

Franzetti F, Cernuschi M, Esposito R, and Moroni M (1992) Pseudomonas infections in patients with AIDS and AIDS-related complex. *Journal of internal medicine* **231:** 437–443.

Gallagher LA, and Manoil C (2001) Pseudomonas aeruginosa PAO1 kills Caenorhabditis elegans by cyanide poisoning. *Journal of Bacteriology* **183:** 6207–6214.

Gallagher LA, McKnight SL, Kuznetsova MS, Pesci EC, and Manoil C (2002) Functions Required for Extracellular Quinolone Signaling by Pseudomonas aeruginosa. *Journal of Bacteriology* **184:** 6472–6480.

Galloway DR (1991) Pseudomonas aeruginosa elastase and elastolysis revisited: recent developments. *Molecular microbiology* **5:** 2315–2321.

Galloway, Warren R J D, Hodgkinson JT, Bowden S, Welch M, and Spring DR (2012) Applications of small molecule activators and inhibitors of quorum sensing in Gram-negative bacteria. *Trends in microbiology* **20:** 449–458.

Gerdt JP, and Blackwell HE (2014) Competition studies confirm two major barriers that can preclude the spread of resistance to quorum-sensing inhibitors in bacteria. *ACS chemical biology* **9:** 2291–2299.

Giannoni E, Sawa T, Allen L, Wiener-Kronish J, and Hawgood S (2006) Surfactant proteins A and D enhance pulmonary clearance of Pseudomonas aeruginosa. *American journal of respiratory cell and molecular biology* **34:** 704–710.

Goethals K, van Motagu M, and Holsters M (1992) Conserved motifs in a divergent nod box of Azorhizobium caulinodans ORS571 reveal a common structure in promoters regulated by LysR-type proteins. *Proceedings of the National Academy of Sciences of the United States of America* **89:** 1646–1650.

Gong W, Xiong G, and Maser E (2012) Oligomerization and negative autoregulation of the LysR-type transcriptional regulator HsdR from Comamonas testosteroni. *The Journal of steroid biochemistry and molecular biology* **132:** 203–211.

Green SK, Schroth MN, Cho JJ, Kominos SK, and Vitanza-jack VB (1974) Agricultural plants and soil as a reservoir for Pseudomonas aeruginosa. *Applied microbiology* **28:** 987–991.

Hart CA (1998) Antibiotic resistance: an increasing problem? It always has been, but there are things we can do. *BMJ (Clinical research ed.)* **316:** 1255–1256.

Hill JJ, and Royer CA (1997) Fluorescence approaches to study of protein-nucleic acid complexation. *Methods in enzymology* **278:** 390–416.

Hodgkinson J, Bowden SD, Galloway, Warren R J D, Spring DR, and Welch M (2010) Structure-activity analysis of the Pseudomonas quinolone signal molecule. *Journal of Bacteriology* **192:** 3833–3837.

Høiby N, Ciofu O, and Bjarnsholt T (2010) Pseudomonas aeruginosa biofilms in cystic fibrosis. *Future microbiology* **5:** 1663–1674.

Hryniewicz MM, and Kredich NM (1994) Stoichiometry of Binding of CysB to the cysJIH, cysK, and cysP Promoter Regions of Salmonella typhimurium. *Journal of Bacteriology* **176:** 3673–3682.

Huang X (2003) Fluorescence polarization competition assay: the range of resolvable inhibitor potency is limited by the affinity of the fluorescent ligand. *Journal of biomolecular screening* **8:** 34–38.

Ilangovan A, Fletcher M, Rampioni G, Pustelny C, Rumbaugh K, Heeb S, Cámara M, Truman A, Chhabra SR, Emsley J, and Williams P (2013) Structural basis for native agonist and synthetic inhibitor

recognition by the Pseudomonas aeruginosa quorum sensing regulator PqsR (MvfR). *PLoS pathogens* **9:** e1003508.

Invitrogen Corporation (2006) Fluorescence Polarization. *Technical Resource Guide Fourth Edition*.

Jaffar-Bandjee MC, Lazdunski A, Bally M, Carrère J, Chazalette JP, and Galabert C (1995) Production of elastase, exotoxin A, and alkaline protease in sputa during pulmonary exacerbation of cystic fibrosis in patients chronically infected by Pseudomonas aeruginosa. *Journal of clinical microbiology* **33:** 924–929.

Jameson DM, and Sawyer WH (1995) Fluorescence anisotropy applied to biomolecular interactions. *Methods in enzymology* **246:** 283–300.

Jarvis WR, and Martone WJ (1992) Predominant pathogens in hospital infections. *The Journal of antimicrobial chemotherapy* **29 Suppl A:** 19–24.

Kefala K, Kotsifaki D, Providaki M, Kapetaniou EG, Rahme L, and Kokkinidis M (2012) Purification, crystallization and preliminary X-ray diffraction analysis of the C-terminal fragment of the MvfR protein from Pseudomonas aeruginosa. *Acta crystallographica. Section F, Structural biology and crystallization communications* **68:** 695–697.

Klein T, Henn C, de Jong, Johannes C, Zimmer C, Kirsch B, Maurer CK, Pistorius D, Müller R, Steinbach A, and Hartmann RW (2012) Identification of small-molecule antagonists of the Pseudomonas aeruginosa transcriptional regulator PqsR: biophysically guided hit discovery and optimization. *ACS chemical biology* **7:** 1496–1501.

Kownatzki R, Tümmler B, and Döring G (1987) Rhamnolipid of Pseudomonas aeruginosa in sputum of cystic fibrosis patients. *Lancet (London, England)* **1:** 1026–1027.

Lea WA & Simeonov A (2011) Fluorescence polarization assays in small molecule screening. *Expert Opinion on Drug Discovery* **6,** 17–32.

Lee J, Wu J, Deng Y, Wang J, Wang C, Wang J, Chang C, Dong Y, Williams P, and Zhang L (2013) A cell-cell communication signal integrates quorum sensing and stress response. *Nature chemical biology* **9:** 339–343.

Lee J, and Zhang L (2015) The hierarchy quorum sensing network in Pseudomonas aeruginosa. *Protein & cell* **6:** 26–41.

Lépine F, Déziel E, Milot S, and Rahme LG (2003) A stable isotope dilution assay for the quantification of the Pseudomonas quinolone signal in Pseudomonas aeruginosa cultures. *Biochimica et Biophysica Acta (BBA) - General Subjects* **1622:** 36–41.

Lépine F, Milot S, Déziel E, He J, and Rahme LG (2004) Electrospray/mass spectrometric identification and analysis of 4-hydroxy-2-alkylquinolines (HAQs) produced by Pseudomonas aeruginosa. *Journal of the American Society for Mass Spectrometry* **15:** 862–869.

Lesic B, Lépine F, Déziel E, Zhang J, Zhang Q, Padfield K, Castonguay M, Milot S, Stachel S, Tzika AA, Tompkins RG, and Rahme LG (2007) Inhibitors of pathogen intercellular signals as selective anti-infective compounds. *PLoS pathogens* **3:** 1229–1239.

Lewis K (2008) Multidrug tolerance of biofilms and persister cells. *Current topics in microbiology and immunology* **322:** 107–131.

Li X, and Nikaido H (2009) Efflux-mediated drug resistance in bacteria: an update. *Drugs* **69:** 1555–1623.

Lipp EK, Huq A, and Colwell RR (2002) Effects of global climate on infectious disease: the cholera model. *Clinical microbiology reviews* **15:** 757–770.

Lochowska A, Iwanicka-Nowicka R, Plochocka D, and Hryniewicz MM (2001) Functional dissection of the LysR-type CysB transcriptional regulator. Regions important for DNA binding, inducer response, oligomerization, and positive control. *The Journal of biological chemistry* **276:** 2098–2107.

Lu C (2014) Discovery and Optimization of the First PqsR Antagonists as Anti-virulence Agents Combating Pseudomonas aeruginosa Infections. *Dissertation, Faculty 8, Saarland University, Saarbrücken*.

Lu C, Kirsch B, Maurer CK, de Jong, Johannes C, Braunshausen A, Steinbach A, and Hartmann RW (2014a) Optimization of anti-virulence PqsR antagonists regarding aqueous solubility and biological properties resulting in new insights in structure-activity relationships. *European journal of medicinal chemistry* **79:** 173–183.

Lu C, Kirsch B, Zimmer C, de Jong, Johannes C, Henn C, Maurer CK, Müsken M, Häussler S, Steinbach A, and Hartmann RW (2012) Discovery of antagonists of PqsR, a key player in 2-alkyl-4-quinolone-dependent quorum sensing in Pseudomonas aeruginosa. *Chemistry & biology* **19:** 381–390.

Lu C, Maurer CK, Kirsch B, Steinbach A, and Hartmann RW (2014b) Overcoming the unexpected functional inversion of a PqsR antagonist in Pseudomonas aeruginosa: an in vivo potent antivirulence agent targeting pqs quorum sensing. *Angewandte Chemie (International ed. in English)* **53:** 1109–1112.

Lyczak JB, Cannon CL, and Pier GB (2000) Establishment of Pseudomonas aeruginosa infection: lessons from a versatile opportunist. *Microbes and infection / Institut Pasteur* **2:** 1051–1060.

Maddocks SE, and Oyston P (2008) Structure and function of the LysR-type transcriptional regulator (LTTR) family proteins. *Microbiology (Reading, England)* **154:** 3609–3623.

Maurer CK (2015) From in vitro to in vivo: Establishment of a Test System for the Biological Evaluation of Novel Quorum Sensing Inhibitors as Anti-infectives Against Pseudomonas aeruginosa. *Dissertation, Faculty 8, Saarland University, Saarbrücken*.

Maurer CK, Lu C, Empting M, and Hartmann RW (2015) Synthetic quorum sensing inhibitors (QSIs) blocking receptor signaling or signal molecule biosynthesis in P. aeruginosa. *In: Kalia, V. C. Quorum sensing vs quorum quenching: a battle with no end in sight. Springer India, New Delhi,*303–317.

Mavrodi DV, Bonsall RF, Delaney SM, Soule MJ, Phillips G, and Thomashow LS (2001) Functional analysis of genes for biosynthesis of pyocyanin and phenazine-1-carboxamide from Pseudomonas aeruginosa PAO1. *Journal of Bacteriology* **183:** 6454–6465.

Miller BE, and Kredich NM (1987) Purification of the cysB Protein from Salmonella typhimurium. *J. Biol. Chem.* **13:** 6006–6009.

Muraoka S, Okumura R, Ogawa N, Nonaka T, Miyashita K, and Senda T (2003) Crystal Structure of a Full-length LysR-type Transcriptional Regulator, CbnR: Unusual Combination of Two Subunit Forms and Molecular Bases for Causing and Changing DNA Bend. *Journal of molecular biology* **328:** 555–566.

Naylor LH (1999) Reporter gene technology: the future looks bright. *Biochemical pharmacology* **58:** 749–757.

Neu HC (1992) The crisis in antibiotic resistance. *Science (New York, N.Y.)* **257:** 1064–1073.

New DC, Miller-Martini DM, and Wong YH (2003) Reporter gene assays and their applications to bioassays of natural products. *Phytotherapy research : PTR* **17:** 439–448.

Nikolovska-Coleska Z, Wang R, Fang X, Pan H, Tomita Y, Li P, Roller PP, Krajewski K, Saito NG, Stuckey JA, and Wang S (2004) Development and optimization of a binding assay for the XIAP BIR3 domain using fluorescence polarization. *Analytical biochemistry* **332:** 261–273.

Ortiz-Castro R, Pelagio-Flores R, Méndez-Bravo A, Ruiz-Herrera LF, Campos-García J, and López-Bucio J (2014) Pyocyanin, a virulence factor produced by Pseudomonas aeruginosa, alters root development through reactive oxygen species and ethylene signaling in Arabidopsis. *Molecular plant-microbe interactions : MPMI* **27:** 364–378.

O'Toole GA, and Kolter R (1998) Flagellar and twitching motility are necessary for Pseudomonas aeruginosa biofilm development. *Molecular microbiology* **30:** 295–304.

Persat A, Inclan YF, Engel JN, Stone HA, and Gitai Z (2015) Type IV pili mechanochemically regulate virulence factors in Pseudomonas aeruginosa. *Proceedings of the National Academy of Sciences of the United States of America* **112:** 7563–7568.

Pustelny C, Albers A, Büldt-Karentzopoulos K, Parschat K, Chhabra SR, Cámara M, Williams P, and Fetzner S (2009) Dioxygenase-mediated quenching of quinolone-dependent quorum sensing in Pseudomonas aeruginosa. *Chemistry & biology* **16:** 1259–1267.

Ran H, Hassett DJ, and Lau GW (2003) Human targets of Pseudomonas aeruginosa pyocyanin. *Proceedings of the National Academy of Sciences of the United States of America* **100:** 14315–14320.

Ryall B, Davies JC, Wilson R, Shoemark A, and Williams HD (2008) Pseudomonas aeruginosa, cyanide accumulation and lung function in CF and non-CF bronchiectasis patients. *The European respiratory journal* **32:** 740–747.

Sauer K, Camper AK, Ehrlich GD, Costerton JW, and Davies DG (2002) Pseudomonas aeruginosa Displays Multiple Phenotypes during Development as a Biofilm. *Journal of Bacteriology* **184:** 1140–1154.

Seong-Cheol P, Yoonkyung P and Kyung-Soo H (2011) The Role of Antimicrobial Peptides in Preventing Multidrug-Resistant Bacterial Infections and Biofilm Formation. *International Journal of Molecular Science* **12:** 5971-5992.

Sevenich FW, Langowski J, Weiss V & Rippe K (1998) DNA binding and oligomerization of NtrC studied by fluorescence anisotropy and fluorescence correlation spectroscopy. *Nucleic Acids Research* **26,** 1373–1381.

Schell MA (1993) Molecular Biology of the LysR Family of Transcriptional Regulators. *Annual review of microbiology* **47:** 597–626.

Schell MA, Brown PH, and Raju S (1990) Use of Saturation Mutagenesis to Localize Probable Functional Domains in the NahR Protein, a LysR-type Transcription Activator*. *Journal of biological chemistry* **265:** 3844–3850.

Silver LL (2011) Challenges of antibacterial discovery. *Clinical microbiology reviews* **24:** 71–109.

Smirnov, V.V. and Kiprianova E.A. (1990) Bacteria of Pseudomonas genus100–111.

Soberón-Chávez G, Lépine F, and Déziel E (2005) Production of rhamnolipids by Pseudomonas aeruginosa. *Applied microbiology and biotechnology* **68:** 718–725.

Sordé R, Pahissa A, and Rello J (2011) Management of refractory Pseudomonas aeruginosa infection in cystic fibrosis. *Infection and drug resistance* **4:** 31–41.

Starkey M, Lepine F, Maura D, Bandyopadhaya A, Lesic B, He J, Kitao T, Righi V, Milot S, Tzika A, and Rahme L (2014) Identification of anti-virulence compounds that disrupt quorum-sensing regulated acute and persistent pathogenicity. *PLoS pathogens* **10:** e1004321.

Storz MP, Allegretta G, Kirsch B, Empting M, and Hartmann RW (2014) From in vitro to in cellulo: structure-activity relationship of (2-nitrophenyl)methanol derivatives as inhibitors of PqsD in Pseudomonas aeruginosa. *Organic & biomolecular chemistry* **12:** 6094–6104.

Storz MP, Maurer CK, Zimmer C, Wagner N, Brengel C, de Jong, Johannes C, Lucas S, Müsken M, Häussler S, Steinbach A, and Hartmann RW (2012) Validation of PqsD as an anti-biofilm target in Pseudomonas aeruginosa by development of small-molecule inhibitors. *Journal of the American Chemical Society* **134:** 16143–16146.

Strateva T, and Mitov I (2011) Contribution of an arsenal of virulence factors to pathogenesis of Pseudomonas aeruginosa infections. *Ann Microbiol* **61:** 717–732.

Thomann A, de Mello Martins, Antonio G G, Brengel C, Empting M, and Hartmann RW (2016) Application of Dual Inhibition Concept within Looped Autoregulatory Systems toward Antivirulence Agents against Pseudomonas aeruginosa Infections. *ACS chemical biology*.

Tropel D, and van der Meer, J.R. (2004) Bacterial transcriptional regulators for degradation pathways of aromatic compounds. *Microbiology and molecular biology reviews : MMBR* **68:** 474-500, table of contents.

Vadlamani G, Thomas MD, Patel TR, Donald LJ, Reeve TM, Stetefeld J, Standing KG, Vocadlo DJ, and Mark BL (2015) The β-lactamase gene regulator AmpR is a tetramer that recognizes and binds the D-Ala-D-Ala motif of its repressor UDP-N-acetylmuramic acid (MurNAc)-pentapeptide. *The Journal of biological chemistry* **290:** 2630–2643.

van Delden C, and Iglewski BH (1998) Cell-to-cell signaling and Pseudomonas aeruginosa infections. *Emerging infectious diseases* **4:** 551–560.

Wade DS, Calfee MW, Rocha ER, Ling EA, Engstrom E, Coleman JP, and Pesci EC (2005) Regulation of Pseudomonas Quinolone Signal Synthesis in Pseudomonas aeruginosa. *Journal of Bacteriology* **187:** 4372–4380.

Wagner S, Sommer R, Hinsberger S, Lu C, Hartmann RW, Empting M, and Titz A (2016) Novel Strategies for the treatment of Pseudomonas aeruginosa infections. *Journal of medicinal chemistry*.

Wilson R, Sykes DA, Watson D, Rutman A, Taylor GW, and Cole PJ (1988) Measurement of Pseudomonas aeruginosa phenazine pigments in sputum and assessment of their contribution to sputum sol toxicity for respiratory epithelium. *Infection and immunity* **56:** 2515–2517.

Wolter DJ, and Lister PD (2013) Mechanisms of β-lactam resistance among Pseudomonas aeruginosa. *Current pharmaceutical design* **19:** 209–222.

Woods DE, Cryz SJ, Friedman RL, and Iglewski BH (1982) Contribution of toxin A and elastase to virulence of Pseudomonas aeruginosa in chronic lung infections of rats. *Infection and immunity* **36:** 1223–1228.

Wretlind B, and Pavlovskis OR (1983) Pseudomonas aeruginosa elastase and its role in pseudomonas infections. *Reviews of infectious diseases* **5 Suppl 5:** S998-1004.

Wright JR (2005) Immunoregulatory functions of surfactant proteins. *Nature reviews. Immunology* **5:** 58–68.

Xiao G, Déziel E, He J, Lépine F, Lesic B, Castonguay M, Milot S, Tampakaki AP, Stachel SE, and Rahme LG (2006) MvfR, a key Pseudomonas aeruginosa pathogenicity LTTR-class regulatory protein, has dual ligands. *Molecular microbiology* **62:** 1689–1699.

Xiao G, He J, and Rahme LG (2006a) Mutation analysis of the Pseudomonas aeruginosa mvfR and pqsABCDE gene promoters demonstrates complex quorum-sensing circuitry. *Microbiology (Reading, England)* **152:** 1679–1686.

Xu N, Yu S, Moniot S, Weyand M, and Blankenfeldt W (2012) Crystallization and preliminary crystal structure analysis of the ligand-binding domain of PqsR (MvfR), the Pseudomonas quinolone signal (PQS) responsive quorum-sensing transcription factor of Pseudomonas aeruginosa. *Acta crystallographica. Section F, Structural biology and crystallization communications* **68:** 1034–1039.

Zaim J (2003) The structure of full-length LysR-type transcriptional regulators. Modeling of the full-length OxyR transcription factor dimer. *Nucleic acids research* **31:** 1444–1454.

Zender M, Klein T, Henn C, Kirsch B, Maurer CK, Kail D, Ritter C, Dolezal O, Steinbach A, and Hartmann RW (2013) Discovery and biophysical characterization of 2-amino-oxadiazoles as novel antagonists of PqsR, an important regulator of Pseudomonas aeruginosa virulence. *Journal of medicinal chemistry* **56:** 6761–6774.

Zhou X, Lou Z, Fu S, Yang A, Shen H, Li Z, Feng Y, Bartlam M, Wang H, and Rao Z (2010) Crystal structure of ArgP from Mycobacterium tuberculosis confirms two distinct conformations of full-length LysR transcriptional regulators and reveals its function in DNA binding and transcriptional regulation. *Journal of molecular biology* **396:** 1012–1024.

# Acknowledgments

Mein Dank gilt meinem Doktorvater Professor Dr. Rolf W. Hartmann, der mich über die Jahre in meinem Projekt begleitete und mich stets anspornte und mit Rat zur Seite stand.

Professor Dr. Dr. h.c. H.H. Maurer danke ich für die Übernahme des Zweitgutachtens dieser Arbeit.

Herrn Dr. Matthias Engel danke ich für seine Rolle als akademischer Beisitzer.

Ganz besonders danken möchte ich meinen beiden Betreuern, Dr. Anke Steinbach und Dr. Martin Empting, die mich immer unterstützt und auch schwierigen Situationen sehr gut beraten haben.

Ich möchte allen ehemaligen und aktuellen Mitgliedern des PQS Projektes für die gute Zusammenarbeit und angenehme Arbeitsatmosphäre danken!

Ich danke meinem ehemaligen Büro für die gute Zeit! Danke an: Lilli, Kristina, Martina, Christine, Michael S., Roman, Ines, Ghamdan und Marica.

Danke, an das ehemalige, sowie aktuelle Carré d´amour: Coach, Ändy, Mize Henning und „2 Meter Kany“

Den Mitgliedern der Arbeitsgruppe CBCH für ihre große Hilfsbereitschaft!

Für wunderbare Geschichten und lustige Momente: Alberto („Herrö Herrö“), Guiseppe, Ahmed, Stefan H., Juliette und dem HG.

Unseren technischen Assistenten Jeannine, Dirk und besonders meinem Sonnenschein Simone!

Für die technische Unterstützung in allem LCMS Fragen: Besonderer Dank an Dr. Christine Maurer und Dr. Stefan Böttcher.

Meinen Freunden, die mich nie haben vergessen lassen, dass es auch ein Leben außerhalb des Labors gibt. Besonderer Dank an Leif, Maddin, Spätzje Andreas und Jonas.

Meinen Eltern danke ich für all den Beistand über die Jahre und dafür, dass sie immer für mich da waren und sind!

Meiner Verlobten Jessica, die mich unzählige Male aufgemuntert und wieder aufgebaut hat und dafür, dass sie Teil meines Lebens ist.

# Appendix

## Supporting information for Publication A

**Fig. S1: $^{1}$H NMR spectra (500 MHz, $CDCl_3$) of *2-heptyl-4-methoxyquinoline* (compound 3)**

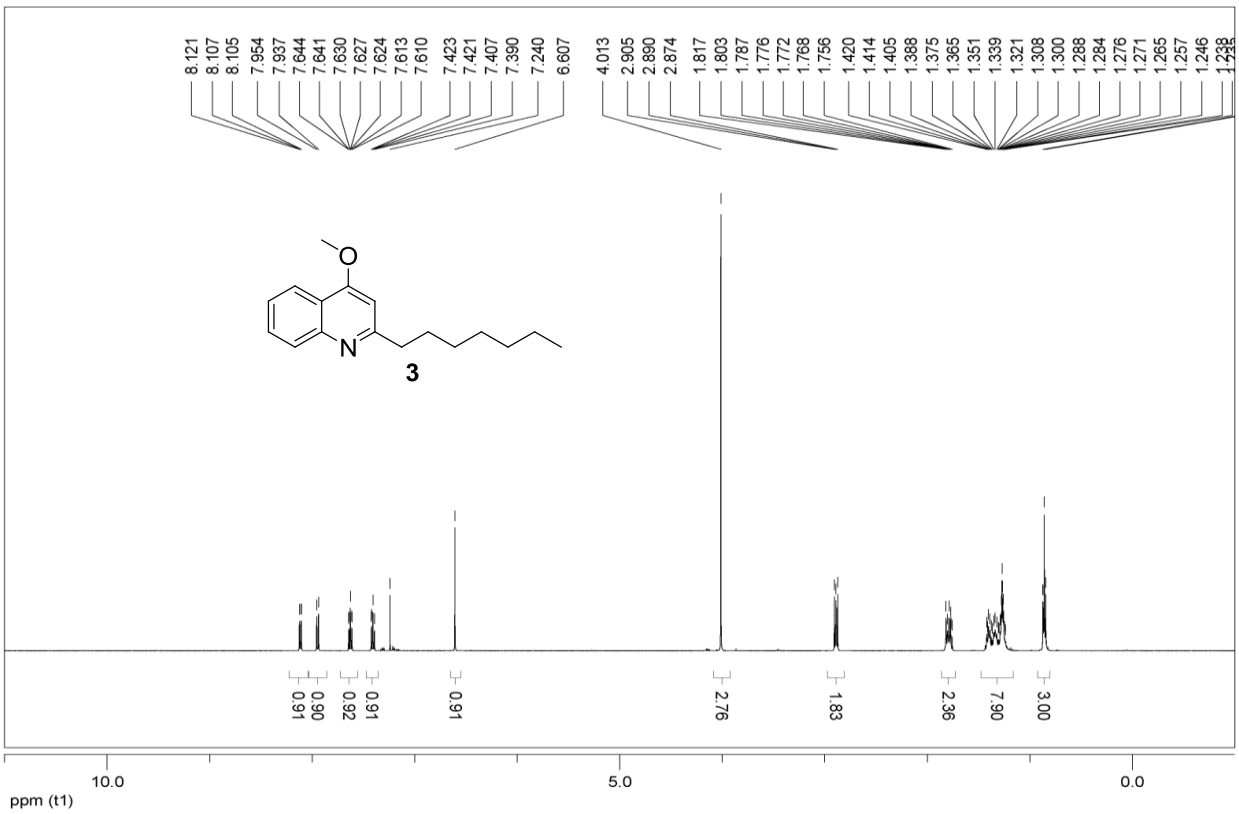

**Fig. S2: $^{13}$C NMR spectra (125 MHz, $CDCl_3$) of *2-heptyl-4-methoxyquinoline* (compound 3)**

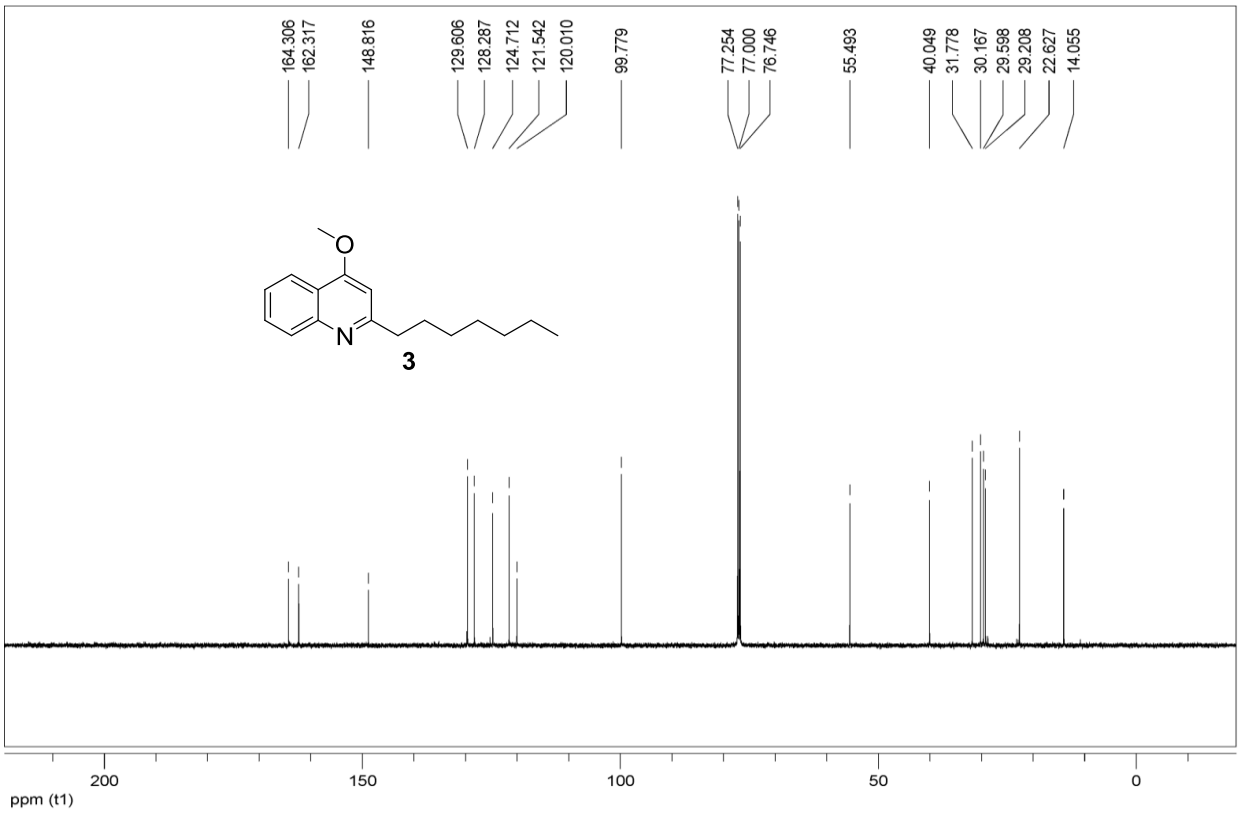


**Fig. S3: $^{1}$H NMR spectra (500 MHz, MeOH-$d_4$) of *2-heptyl-1-methyl-6-(trifluoromethyl)quinolin-4(1H)-one* (compound 4)**

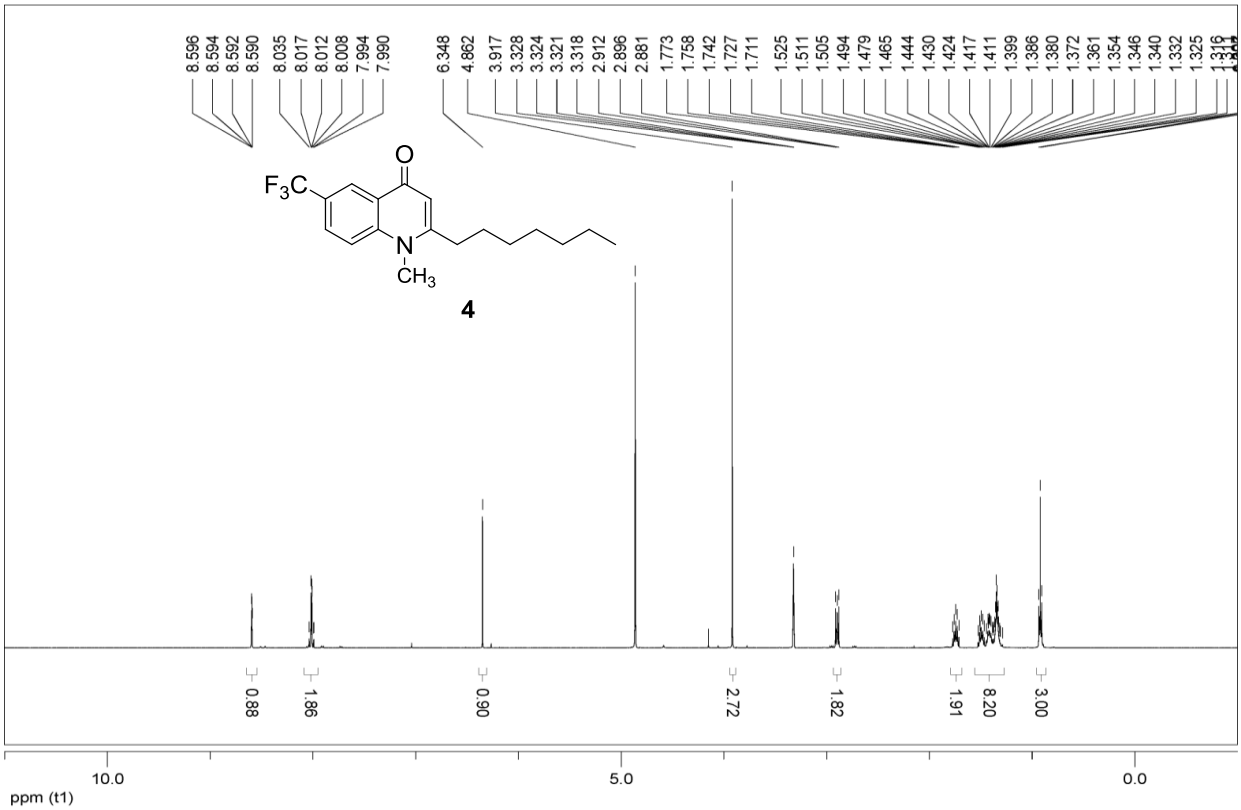

**Fig. S4: $^{13}$C NMR spectra (125 MHz, MeOH-$d_4$) of *2-heptyl-1-methyl-6-(trifluoromethyl)quinolin-4(1H)-one* (compound 4)**

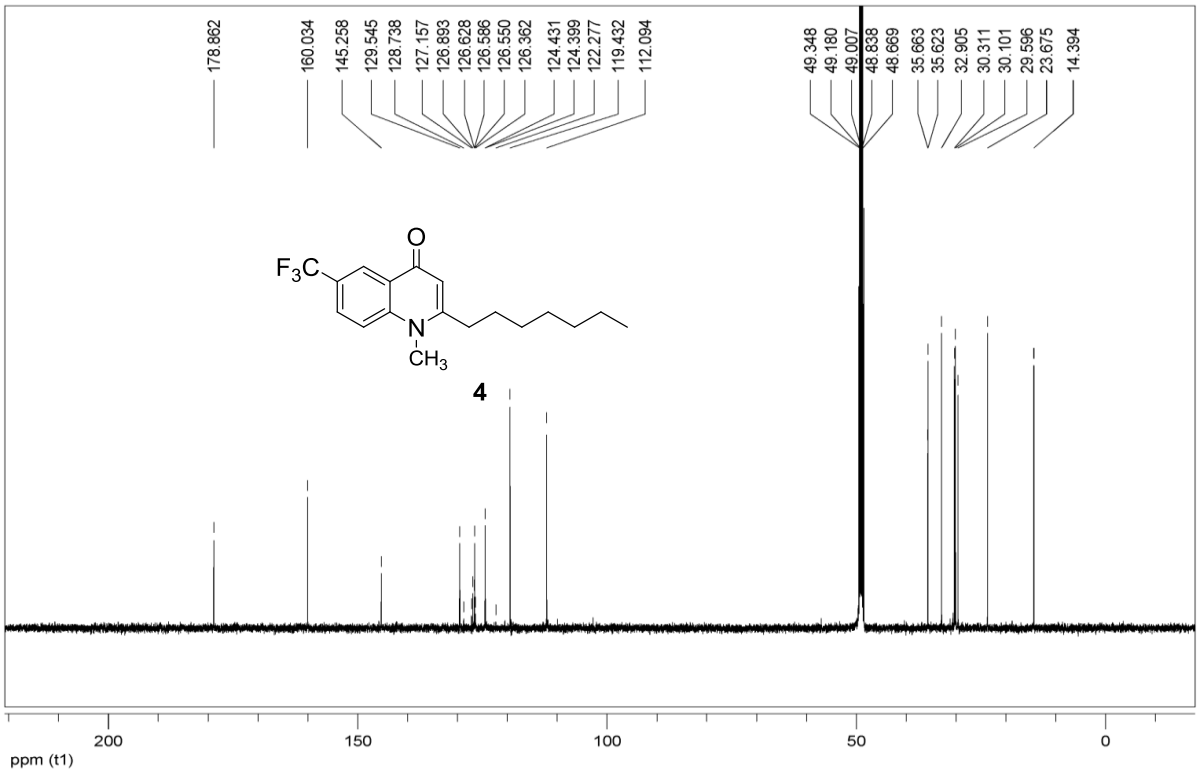


**Fig. S5: $^{1}$H NMR spectra (500 MHz, MeOH-$d_4$) of *6-nitro-2-(pentyloxymethyl)quinolin-4(1H)-one* (compound 8)**

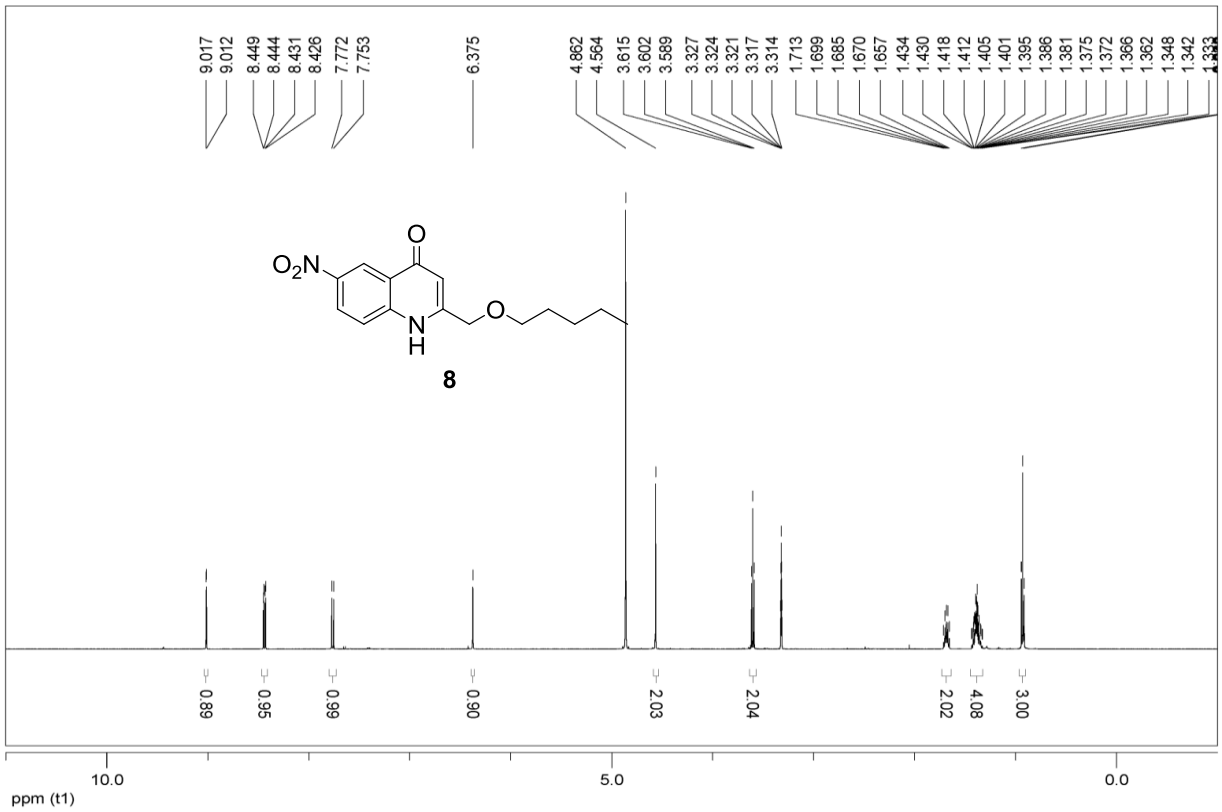

**Fig. S6: $^{13}$C NMR spectra (125 MHz, MeOH-$d_4$) of *6-nitro-2-(pentyloxymethyl)quinolin-4(1H)-one* (compound 8)**

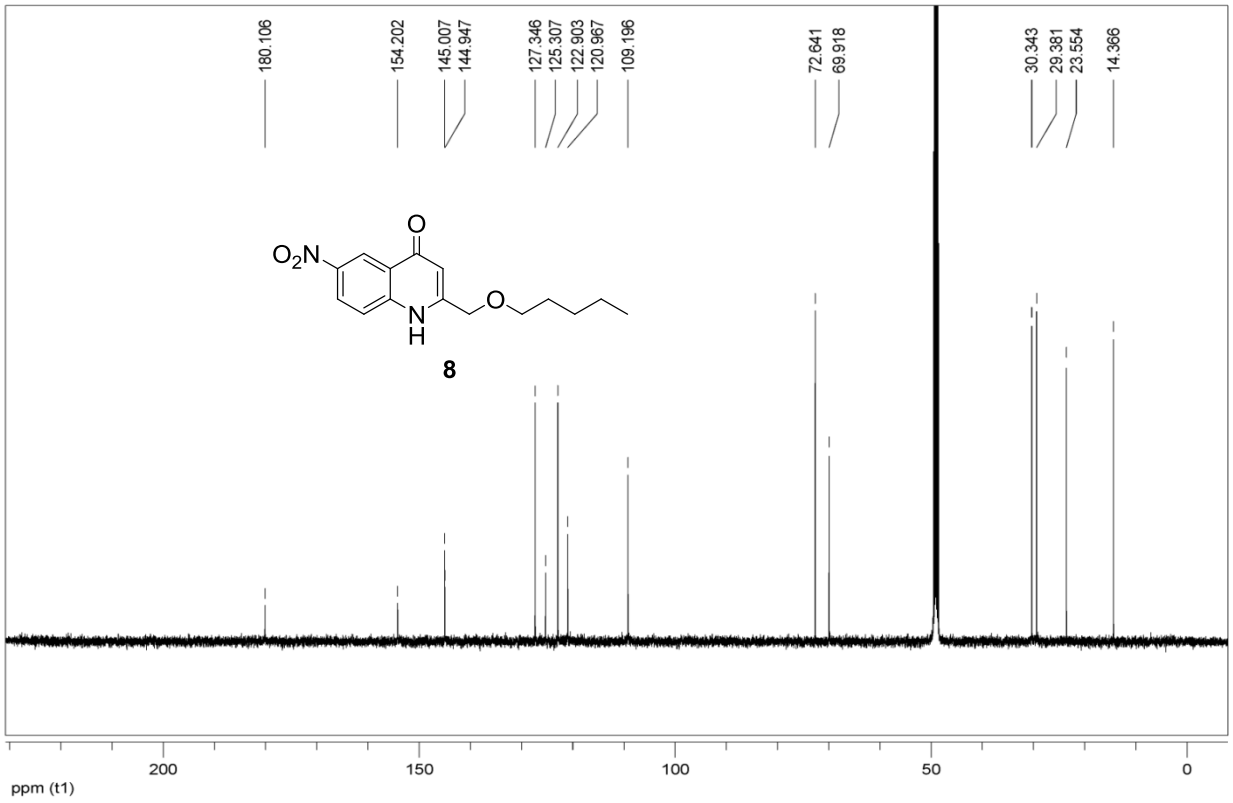


**Fig. S7: $^{1}$H NMR spectra (500 MHz, MeOH-$d_4$) of *2-(4-ethoxybutyl)-6-nitroquinolin-4(1H)-one* (compound 11)**

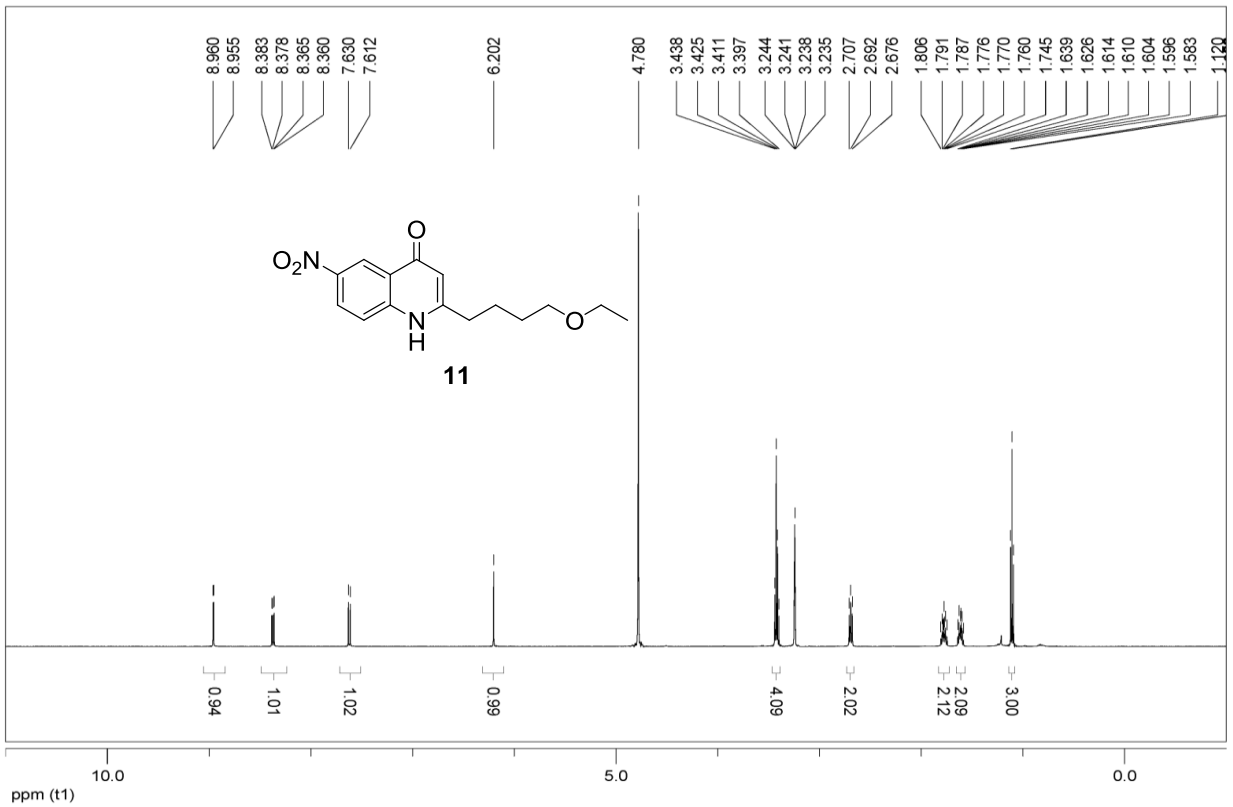

**Fig. S8: $^{13}$C NMR spectra (125 MHz, MeOH-$d_4$) of *2-(4-ethoxybutyl)-6-nitroquinolin-4(1H)-one* (compound 11)**

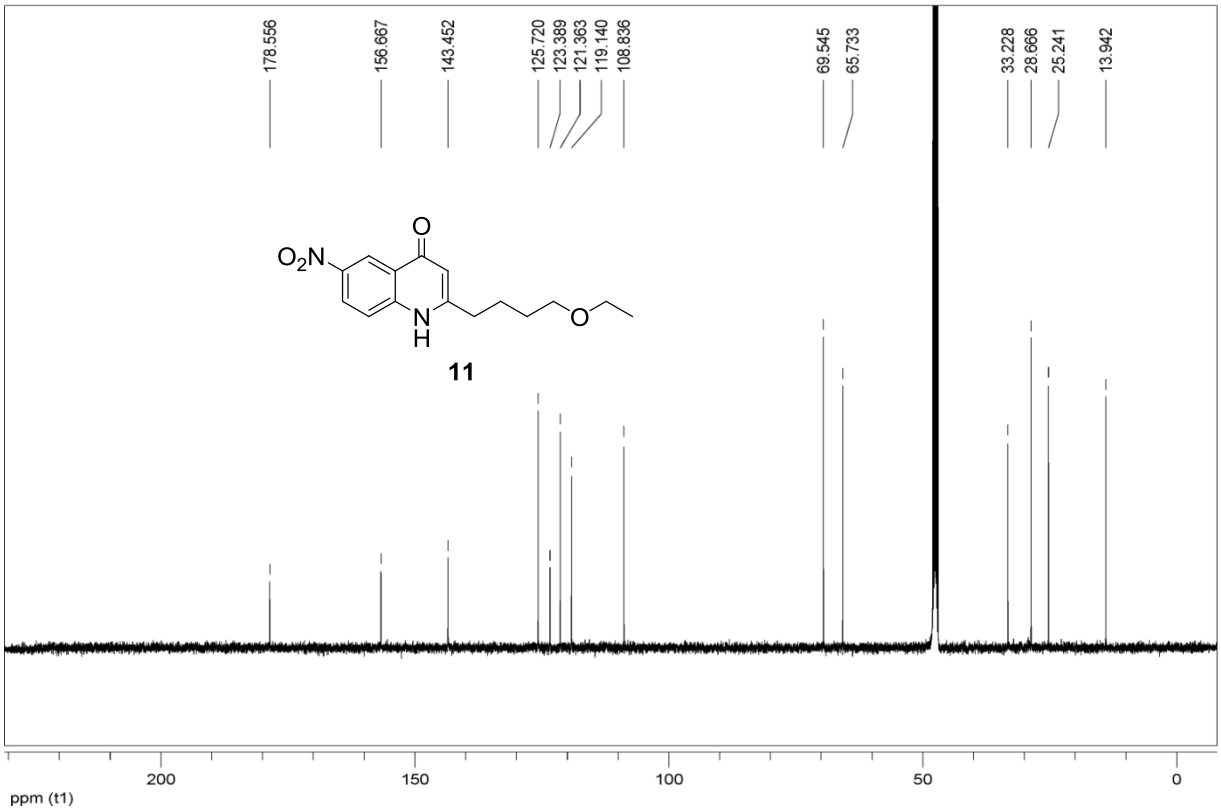


**Fig. S9: $^{1}$H NMR spectra (500 MHz, DMSO-$d_6$) of *2-heptyl-3-hydroxy-6-nitroquinolin-4(1H)-one* (compound 14)**

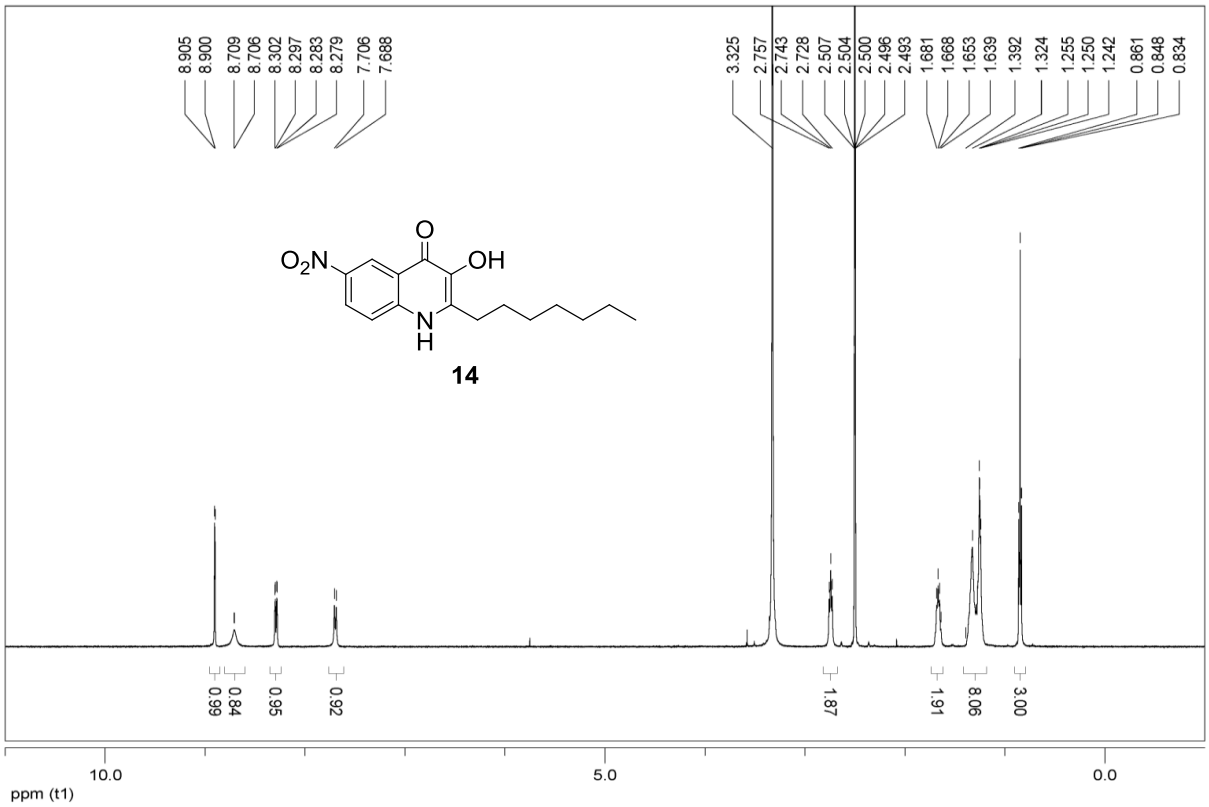

**Fig. S10: $^{13}$C NMR spectra (125 MHz, DMSO-$d_6$) of *2-heptyl-3-hydroxy-6-nitroquinolin-4(1H)-one* (compound 14)**

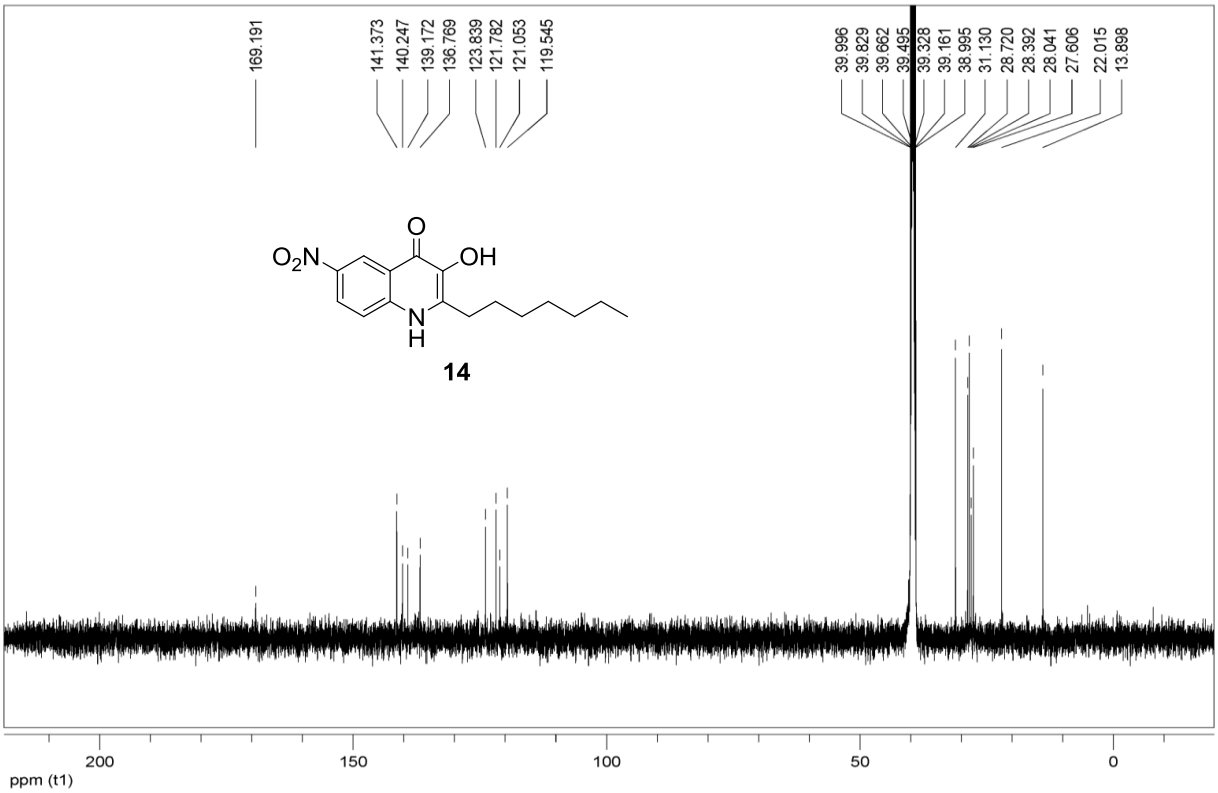


**Fig. S11: $^{1}$H NMR spectra (500 MHz, DMSO-$d_6$) of *2-heptyl-3-(hydroxymethyl)-6-nitroquinolin-4(1H)-one* (compound 16)**

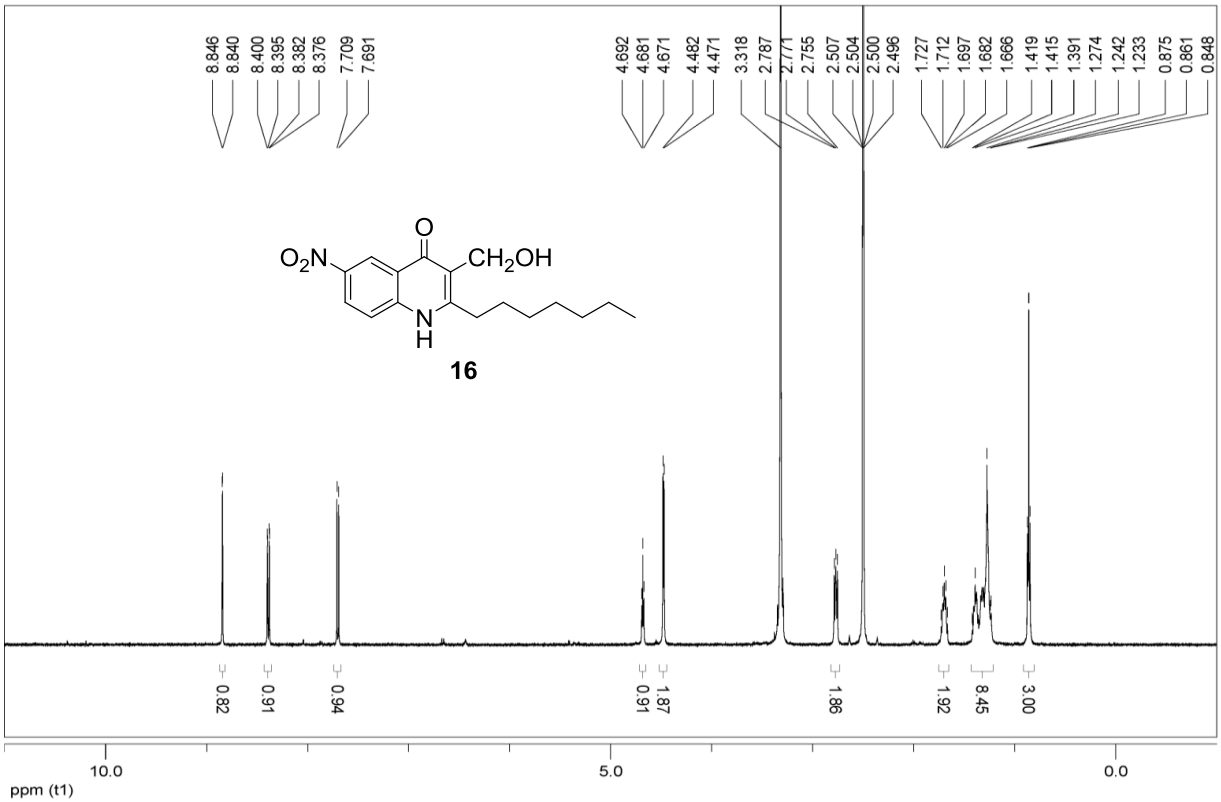

**Fig. S12: $^{13}$C NMR spectra (125 MHz, DMSO-$d_6$) of *2-heptyl-3-(hydroxymethyl)-6-nitroquinolin-4(1H)-one* (compound 16)**

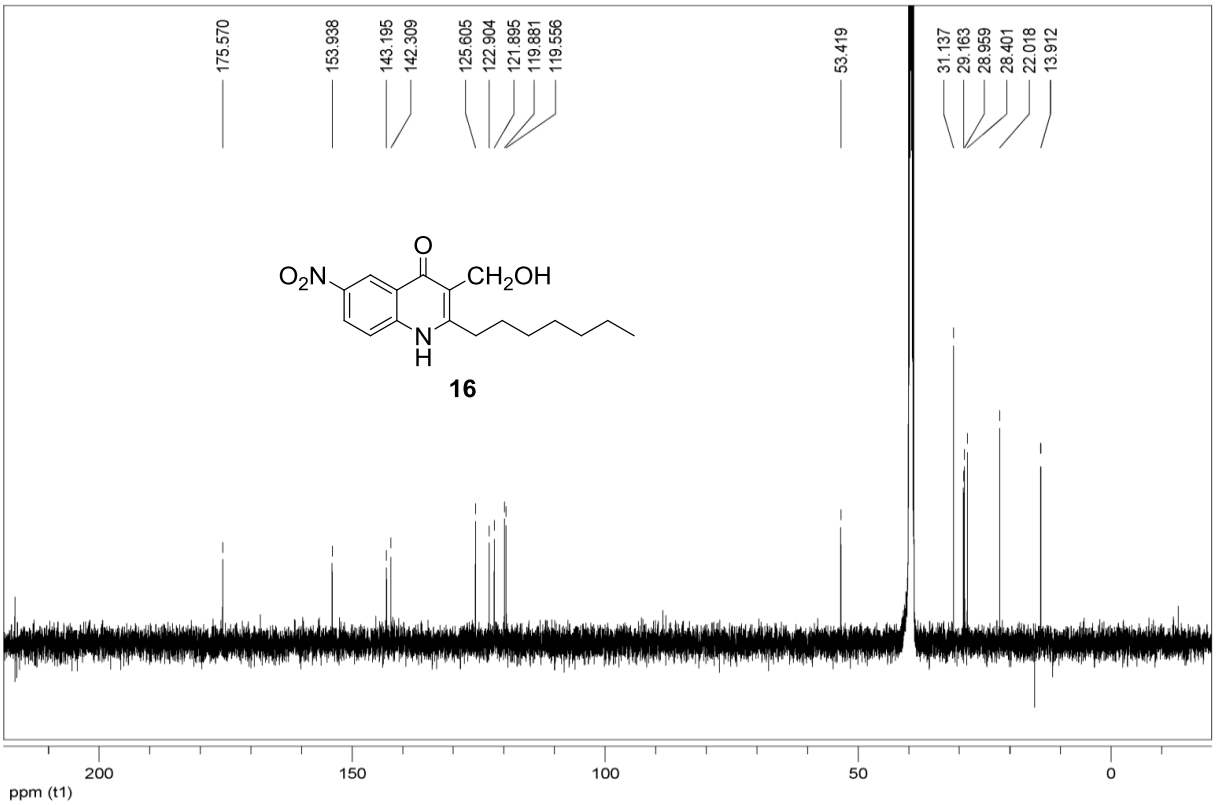


**Fig. S13: $^{1}$H NMR spectra (500 MHz, MeOH-$d_4$) of *ethyl 2-heptyl-6-nitro-4-oxo-1,4-dihydroquinoline-3-carboxylate* (compound 18)**

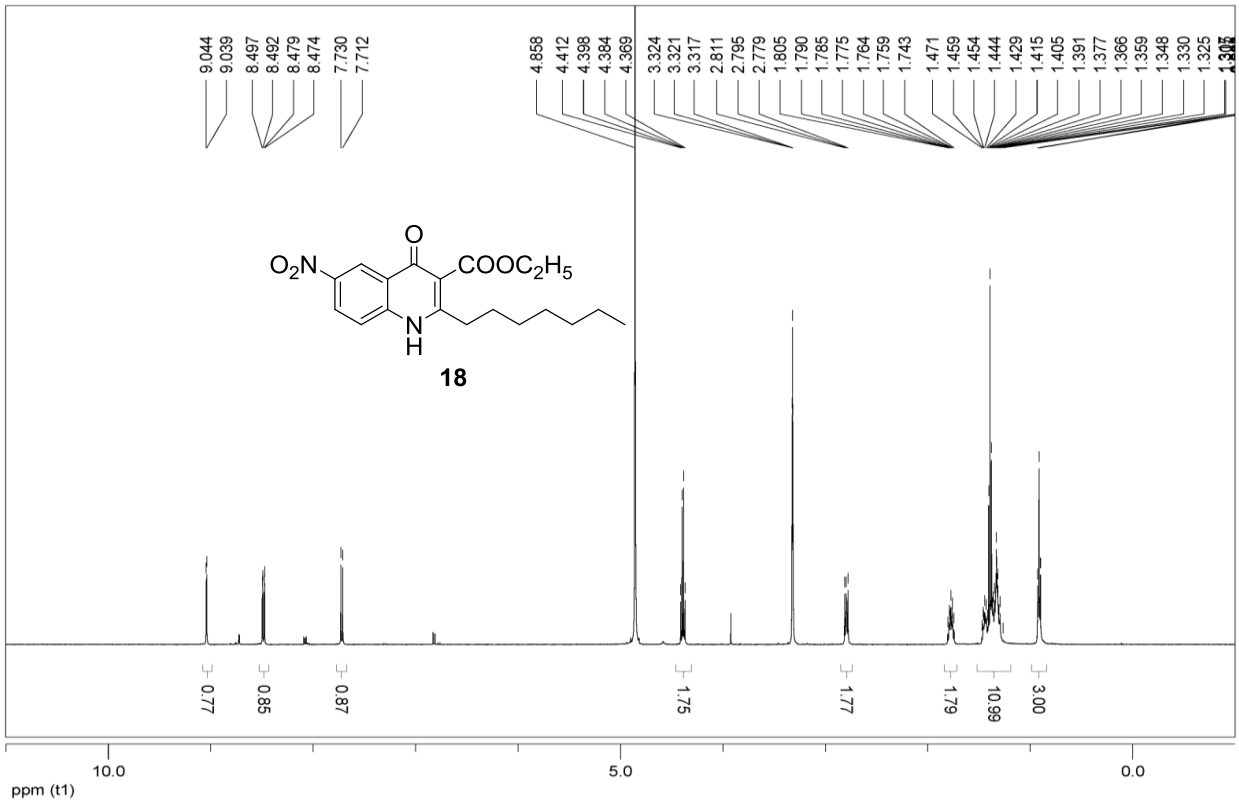

**Fig. S14: $^{13}$C NMR spectra (125 MHz, MeOH-$d_4$) of *ethyl 2-heptyl-6-nitro-4-oxo-1,4-dihydroquinoline-3-carboxylate* (compound 18)**

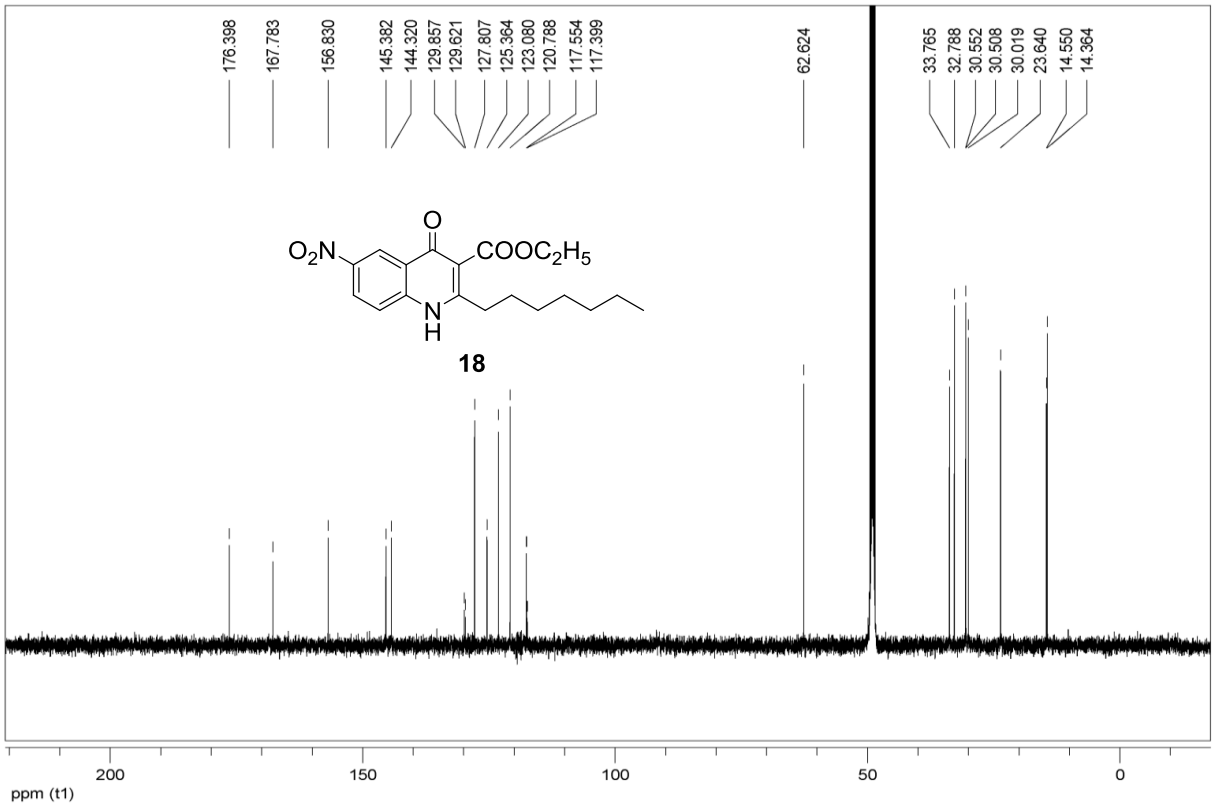


**Fig. S15: $^{1}$H NMR spectra (500 MHz, DMSO-$d_6$) of *2-heptyl-6-nitro-4-oxo-1,4-dihydroquinoline-3-carboxylic acid* (compound 22)**

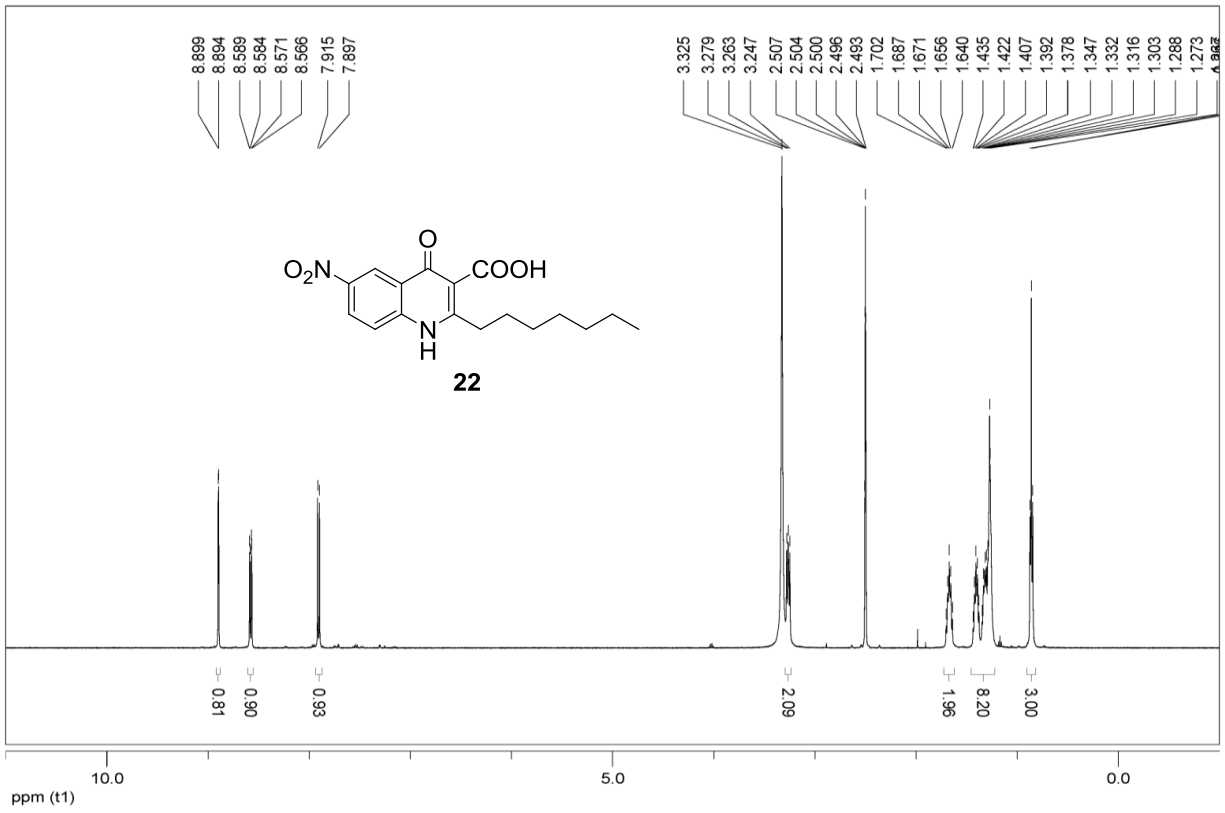

**Fig. S16: $^{13}$C NMR spectra (125 MHz, DMSO-$d_6$) of *2-heptyl-6-nitro-4-oxo-1,4-dihydroquinoline-3-carboxylic acid* (compound 22)**

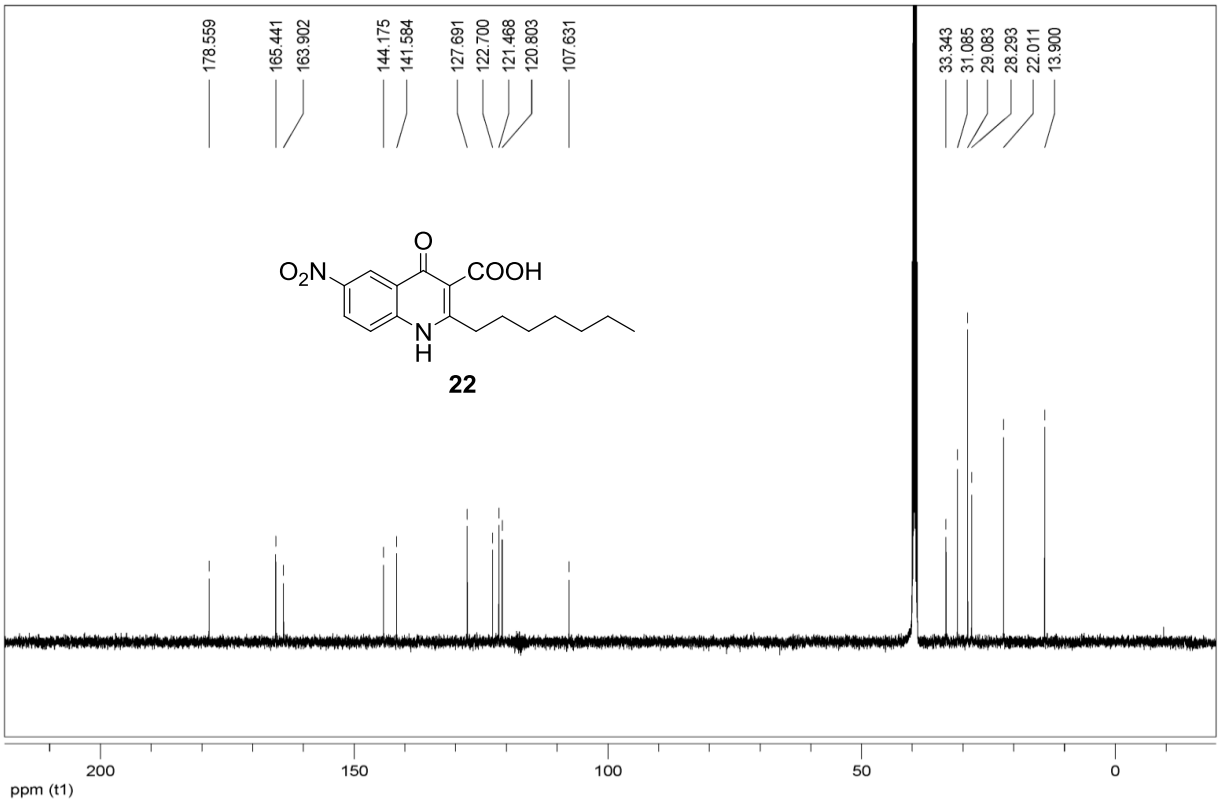


**Fig. S17: $^{1}$H NMR spectra (500 MHz, DMSO-$d_6$) of *2-heptyl-6-nitro-4-oxo-1,4-dihydroquinoline-3-carboxamide* (compound 26)**

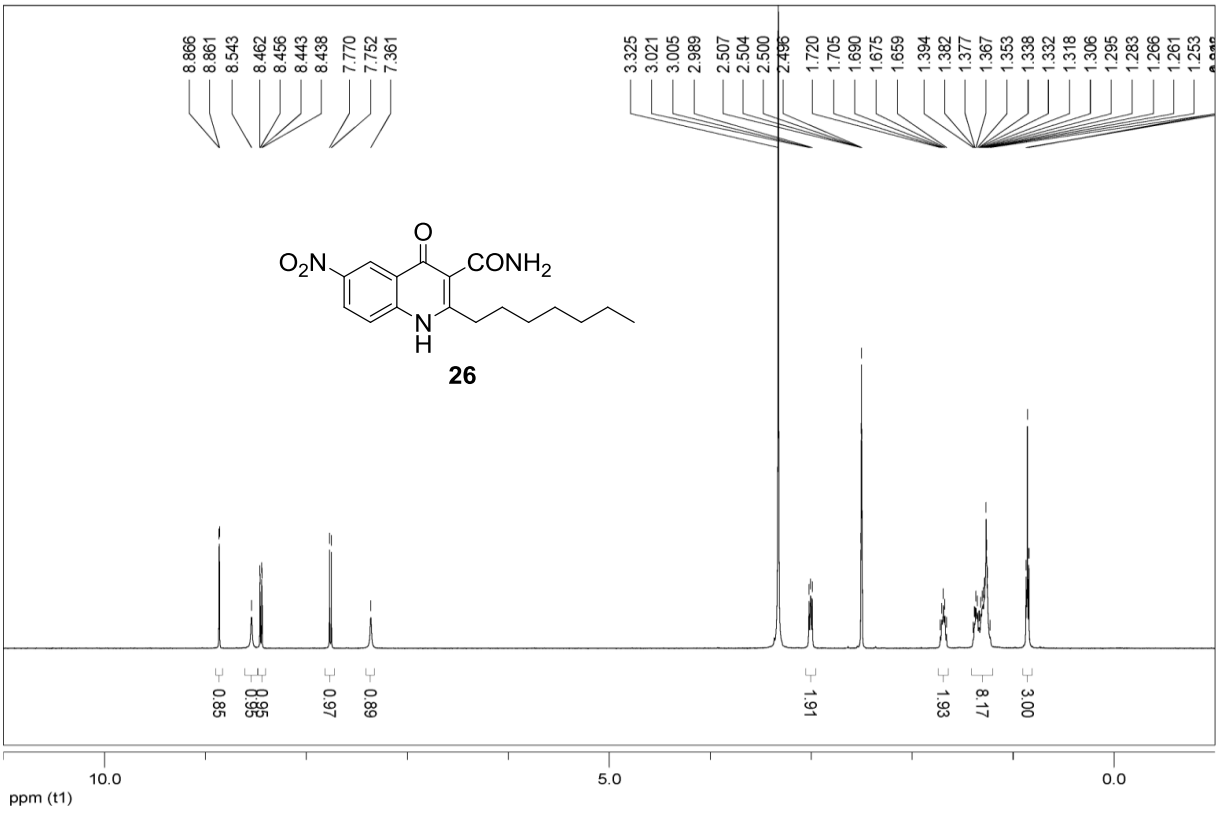

**Fig. S18: $^{13}$C NMR spectra (125 MHz, DMSO-$d_6$) of *2-heptyl-6-nitro-4-oxo-1,4-dihydroquinoline-3-carboxamide* (compound 26)**

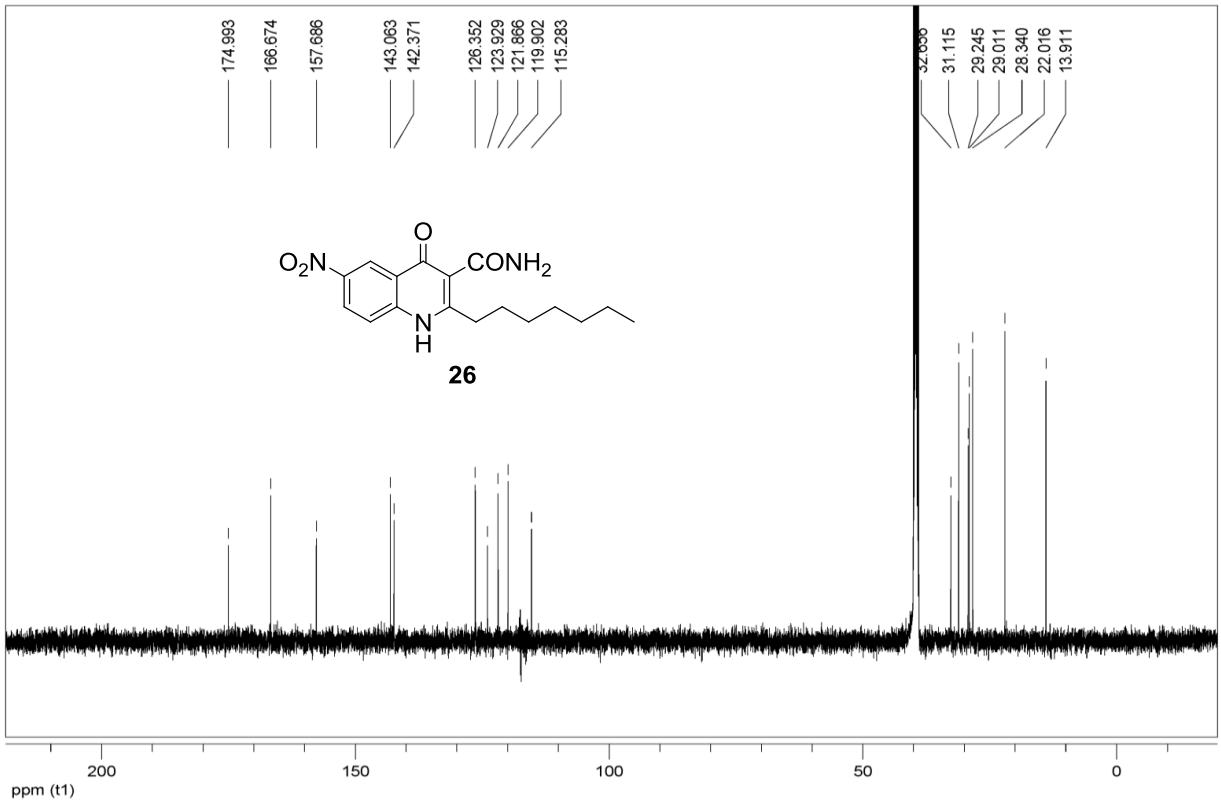


**Fig. S19: $^{1}$H NMR spectra (500 MHz, DMSO-$d_6$) of *2-heptyl-N-hydroxy-6-nitro-4-oxo-1,4-dihydroquinoline-3-carboxamide* (compound 28)**

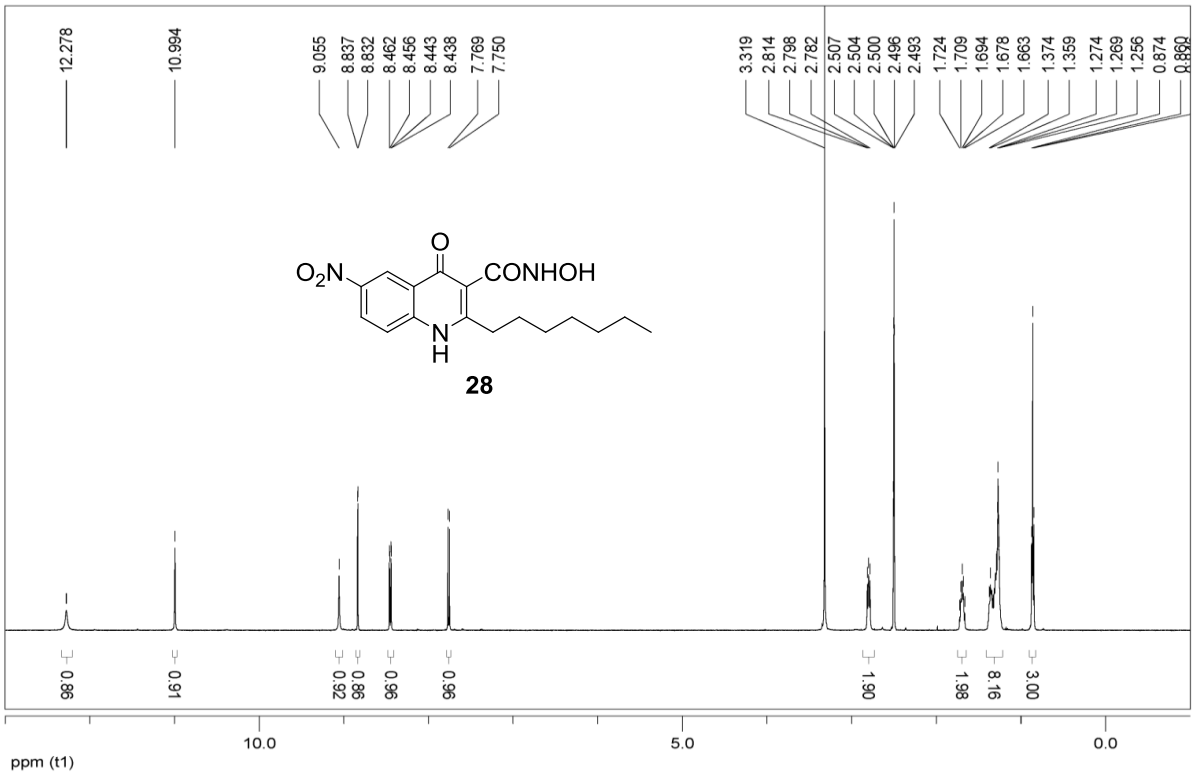

**Fig. S20: $^{13}$C NMR spectra (125 MHz, DMSO-$d_6$) of *2-heptyl-N-hydroxy-6-nitro-4-oxo-1,4-dihydroquinoline-3-carboxamide* (compound 28)**

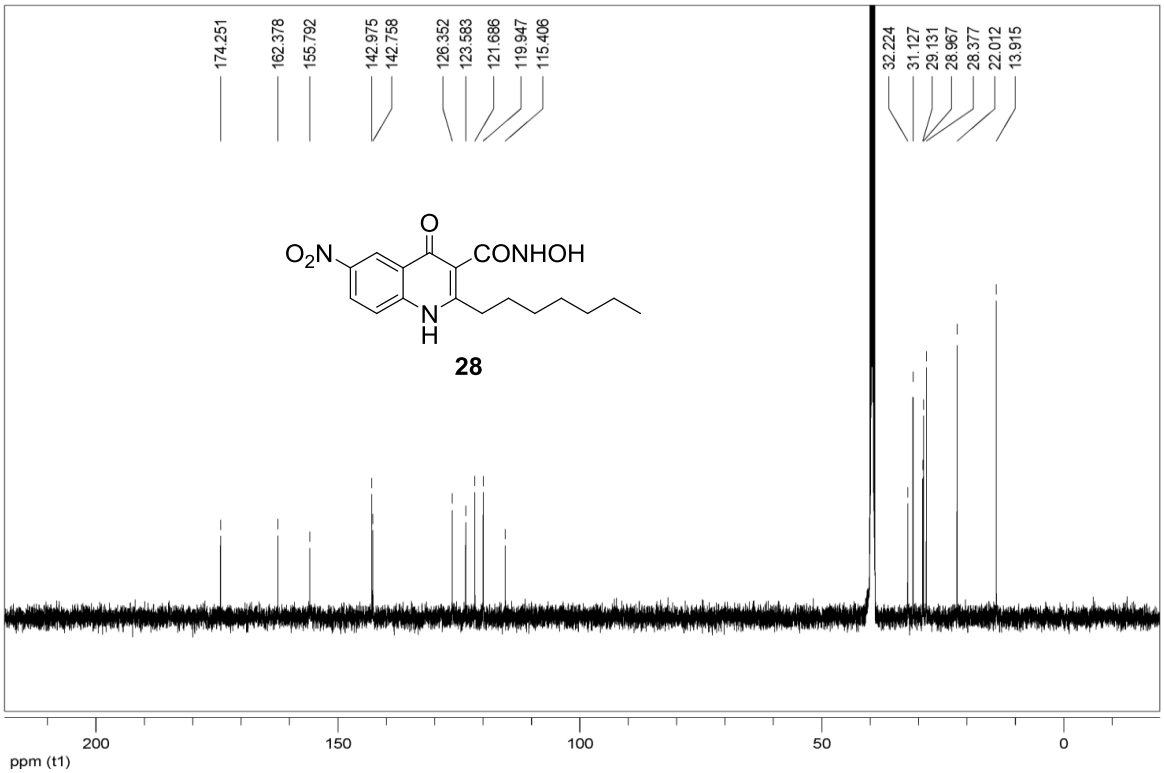


**Fig. S21: $^{1}$H NMR spectra (500 MHz, DMSO-$d_6$) of *2-heptyl-1,6-naphthyridin-4(1H)-one* (compound 31)**

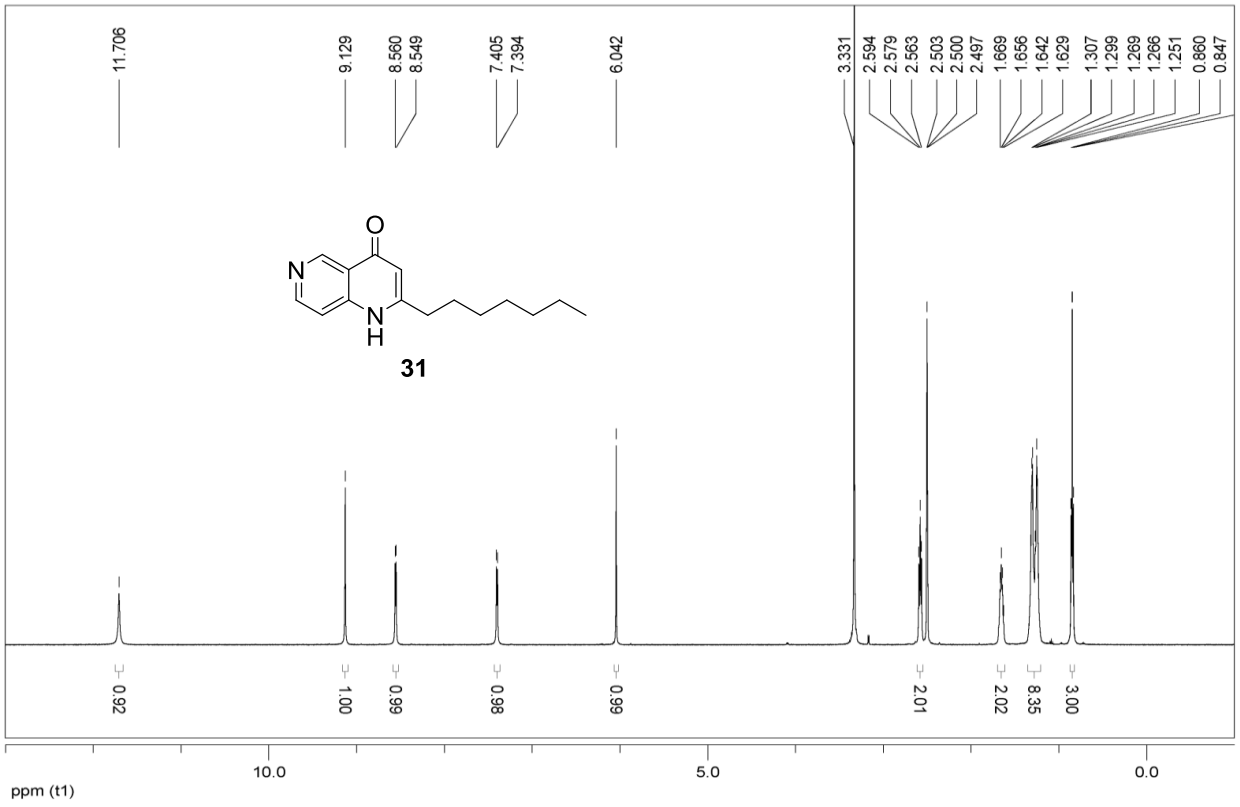

**Fig. S22: $^{13}$C NMR spectra (125 MHz, DMSO-$d_6$) of *2-heptyl-1,6-naphthyridin-4(1H)-one* (compound 31)**

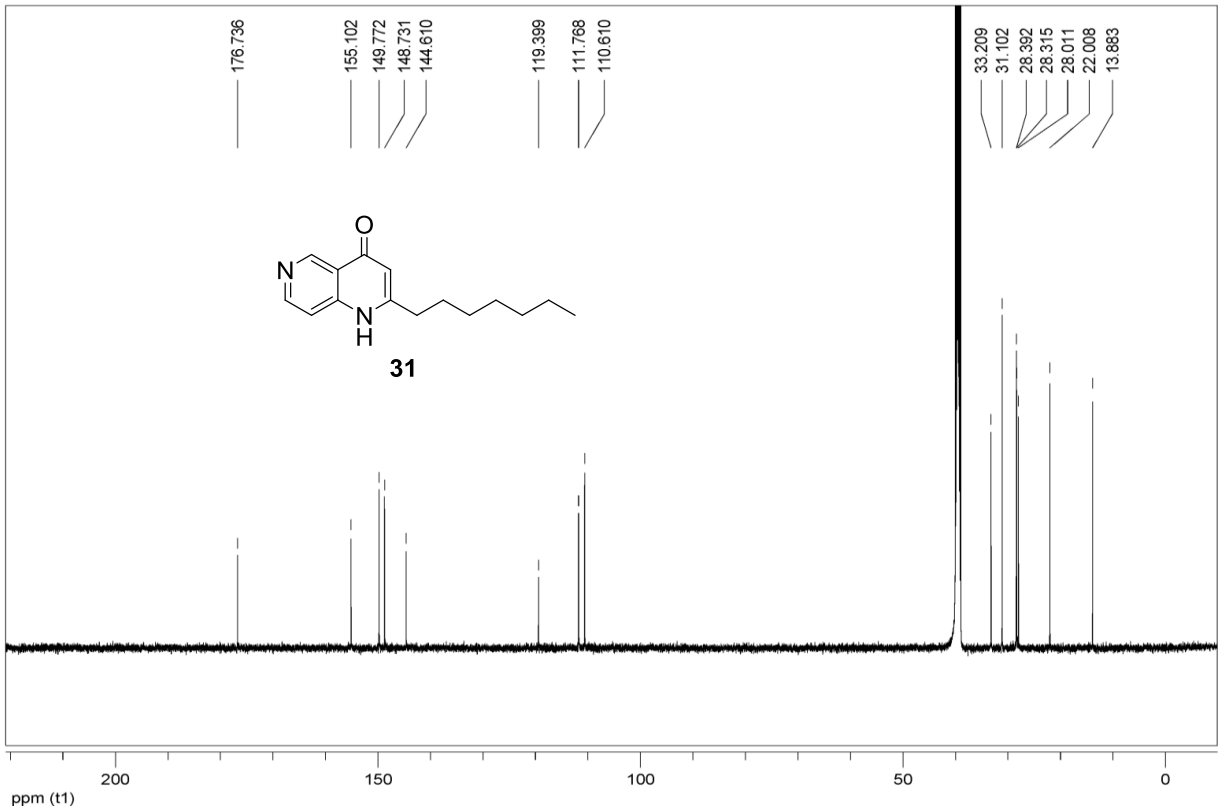

# Supporting information for Publication B

**Contents**



## 1. General experimental information-Chemistry

### 1.1 Chemicals and analytical methods

$^{1}H$ and $^{13}C$ NMR spectra were recorded on a Bruker DRX-500 instrument. Chemical shifts are given in parts per million (ppm) with the solvent resonance as internal standard for spectra obtained in $CDCl_3$,

MeOH-$d_4$ and DMSO-$d_6$. All coupling constants ($J$) are given in hertz. Mass spectrometry (LC/MS) was performed on a MSQ® electro spray mass spectrometer (Thermo Fisher). The system was operated by the standard software Xcalibur®. A RP C18 NUCLEODUR® 100-5 (125 × 3 mm) column (Macherey-Nagel GmbH) was used as stationary phase with water/acetonitrile mixtures as eluent. All solvents were HPLC grade. Reagents were used as obtained from commercial suppliers without further purification. Flash chromatography was performed on silica gel 60, 70-230 mesh (Fluka) and the reaction progress was determined by thin-layer chromatography (TLC) analyses on silica gel 60, $F_{254}$ (Merck). Visualization was accomplished with UV light and staining with basic potassium permanganate ($KMnO_4$). The melting points were measured using melting point apparatus SMP3 (Stuart Scientific). The apparatus is uncorrected.

The following compounds were prepared according to previously described procedures: HHQ, PQS, **1** and **7**.[1]

**1.2 Synthesis of title compounds**

**2-Heptyl-3-hydroxy-6-nitroquinolin-4(1*H*)-one (compound 2).**

A solution of **4** (200 mg, 0.63 mmol, 1.0 equiv) in dry THF (50 mL) was added dropwise to pure activated $MnO_2$ (540 mg, 6.21 mmol, 9.9 equiv) at room temperature. The mixture was then stirred overnight. After filtration through Celite the solvent was removed under reduced pressure and the residue was purified by column chromatography on silica gel (dichloromethane:methanol, 80:1 v/v) to give 2-heptyl-6-nitro-4-oxo-1,4-dihydroquinoline-3-carbaldehyde as a yellow solid (80 mg, 0.25 mmol), which was unstable and used immediately in the next step. Boric acid (80 mg, 1.30 mmol, 5.0 equiv) was suspended in THF (20 mL), followed by the addition of 30% $H_2O_2$ (90 µL, 3.0 equiv) and conc. $H_2SO_4$ (0.5 mL). After stirring for 30 min a solution of the aldehyde (80 mg, 0.25 mmol) in THF (10 mL) was added dropwise over 10 min. After additional stirring for 5 h, the mixture was filtered. The filtrate was neutralized by addition of a sat. $NaHCO_3$ solution (120 mL) and the aqueous layer was extracted with ethyl acetate (3 x 30 mL). After drying of the combined organic layers over $MgSO_4$ the solvent was removed under reduced pressure. The residue was purified by preparative thin layer chromatography on

silica gel (dichloromethane:methanol, 30:1 v/v) to give **2** as a yellow solid (60 mg, 0.20 mmol, 32% for 2 steps). mp: 217.1-219.7 °C; $^{1}$H-NMR (500 MHz, DMSO-$d_6$): δ 0.85 (t, $J$ = 7.0 Hz, 3H), 1.24-1.39 (m, 8H), 1.67 (quint, $J$ = 7.5 Hz, 2H), 2.74 (t, $J$ = 7.5 Hz, 2H), 7.70 (d, $J$ = 9.0 Hz, 1H), 8.29 (dd, $J$ = 2.5, 9.0 Hz, 1H), 8.71 (br, 1H), 8.90 (d, $J$ = 2.5 Hz, 1H), 11.99 (br, 1H); $^{13}$C-NMR (125 MHz, DMSO-$d_6$): δ 13.9, 22.0, 27.6, 28.0, 28.4, 28.7, 31.1, 119.5, 121.1, 121.8, 123.8, 136.8, 139.2, 140.2, 141.4, 169.2; LC/MS: *m/z* 305.03 $[M + H]^+$, 99.9%.[1]

**2-Heptyl-6-nitro-4-oxo-1, 4-dihydroquinoline-3-carboxamide (compound 3).**

*N,N'*-Carbonyldiimidazole (62 mg, 0.38 mmol, 2.0 equiv) was added to **5** (62 mg, 0.19 mmol, 1.0 equiv) in dry DMF (1 mL). After stirring at 65 °C for 5 h, the mixture was cooled to 0 °C and iced conc. $NH_3$•$H_2O$ (5 mL) was added. After stirring overnight at room temperature the solvent was evaporated under reduced pressure. To the residue was added iced water (5 mL) and the pricipitate was isolated by filtration. After purification by column chromatography on silica gel (dichloromethane:methanol, 70:1 v/v) **3** was isolated as a white solid (43 mg, 0.13 mmol, 68%), mp: 237.6-239.1 °C; $^{1}$H-NMR (500 MHz, DMSO-$d_6$): δ 0.86 (t, $J$ = 7.0 Hz, 3H), 1.23-1.39 (m, 8H), 1.69 (quint, $J$ = 7.5 Hz, 2H), 3.00 (t, $J$ = 8.0 Hz, 2H), 7.36 (br, 1H), 7.76 (d, $J$ = 9.0 Hz, 1H), 8.45 (dd, $J$ = 2.5, 9.0 Hz, 1H), 8.54 (br, 1H), 8.86 (d, $J$ = 2.5 Hz, 1H), 12.30 (br, 1H); $^{13}$C-NMR (125 MHz, DMSO-$d_6$): δ 13.9, 22.0, 28.3, 29.0, 29.2, 31.1, 32.7, 115.3, 119.9, 121.9, 123.9, 126.4, 142.4, 143.1, 157.7, 166.7, 175.0; LC/MS: *m/z* 332.92 $[M + H]^+$, 96.8%.[2]

**2-Heptyl-3-(hydroxymethyl)-6-nitroquinolin-4(1*H*)-one (compound 4).**

At 0 °C $LiAlH_4$ (90 mg, 2.37 mmol, 2.0 equiv) was added to a stirred solution of **6** (420 mg, 1.17 mmol, 1.0 equiv) in dry THF (20 mL). After stirring at room temperature for 2 h water (8 drops) and NaOH (2 drops, 15%) were added at 0 °C and after filtration the solvent was removed under reduced pressure. The residue was purified by column chromatography (dichloromethane:methanol, 60:1 v/v) and washed with *n*-hexane to give **4** as a yellow solid (35 mg, 0.11 mmol, 9%), mp: >350 °C; $^{1}$H-NMR (500 MHz, DMSO-$d_6$): δ 0.86 (t, $J$ = 7.0 Hz, 3H), 1.23-1.42 (m, 8H), 1.70 (quint, $J$ = 7.5 Hz, 2H), 2.77 (t, $J$ = 7.5 Hz, 2H), 4.48 (d, $J$ = 5.5 Hz, 2H), 4.68 (t, $J$ = 5.5 Hz, 1H), 7.70 (d, $J$ = 9.0 Hz, 1H), 8.39 (dd, $J$ = 2.5, 9.0 Hz, 1H),

8.84 (d, $J$ = 3.0 Hz, 1H), 11.93 (br, 1H); $^{13}$C-NMR (125 MHz, DMSO-$d_6$): δ 13.9, 22.0, 28.4, 29.0, 29.2, 31.1, 53.4, 119.6, 119.9, 121.9, 122.9, 125.6, 142.3, 143.2, 153.9, 175.6; LC/MS: *m/z* 319.06 $[M + H]^+$, 99.9%.[3]

**2-Heptyl-6-nitro-4-oxo-1, 4-dihydroquinoline-3-carboxylic acid (compound 5).**

**6** (250 mg, 0.69 mmol) was suspended in 10% NaOH (50 mL) solution and heated at reflux for 4 h. After cooling to 0 °C on an ice water bath and extraction with ethyl acetate, the water phase was acidified with conc. HCl to reach a pH of 4.0-6.0. **5** was isolated by filtration, washed with water and dried under vacuum as a gray solid (32 mg, 0.10 mmol, 14%). mp: 192.7-194.9 °C; $^1$H-NMR (500 MHz, DMSO-$d_6$): δ 0.86 (t, $J$ = 7.0 Hz, 3H), 1.27-1.44 (m, 8H), 1.67 (quint, $J$ = 7.5 Hz, 2H), 3.26 (t, $J$ = 7.5 Hz, 2H), 7.91 (d, $J$ = 9.0 Hz, 1H), 8.58 (dd, $J$ = 2.5, 9.0 Hz, 1H), 8.90 (d, $J$ = 2.5 Hz, 1H), 13.22 (br, 1H), 15.64 (br, 1H); $^{13}$C-NMR (125 MHz, DMSO-$d_6$): δ 13.9, 22.0, 28.3, 29.1, 31.1, 33.3, 107.6, 120.8, 121.5, 122.7, 127.7, 141.6, 144.2, 163.9, 165.4, 178.6; LC/MS: *m/z* 332.90 $[M + H]^+$, 98.8%.

**Ethyl 2-heptyl-6-nitro-4-oxo-1, 4-dihydroquinoline-3-carboxylate (compound 6).**

Under nitrogen atmosphere **7** (3.40 g, 15 mmol, 1.0 equiv) was added to a suspension of sodium hydride (50-65% w/w, 0.75 g, 15 mmol, 1.0 equiv) in dry DMF (50 mL), causing the liberation of hydrogen gas. A solution of 6-nitro-1*H*-benzo[*d*][1,3]oxazine-2,4-dione (3.0 g, 14 mmol, 0.9 equiv) in dry DMF (30 mL) was added dropwise and stirred overnight. Most of the solvent was removed under reduced pressure and the remaining solvent treated with 1M HCl, yielding the crude product as a yellow solid. After recrystallization from ethyl acetate/methanol **6** was isolated as a yellow solid (1.8 g, 5.71 mmol, 41%). mp: 239.6-241.8 °C; $^1$H-NMR (500 MHz, MeOH-$d_4$): δ 0.91 (t, $J$ = 7.0 Hz, 3H), 1.29-1.47 (m, 11H), 1.78 (quint, $J$ = 7.5 Hz, 2H), 2.80 (t, $J$ = 8.0 Hz, 2H), 4.39 (q, $J$ = 8.0 Hz, 2H), 7.72 (d, $J$ = 9.0 Hz, 1H), 8.49 (dd, $J$ = 2.5, 9.0 Hz, 1H), 9.04 (d, $J$ = 2.5 Hz, 1H); $^{13}$C-NMR (125 MHz, MeOH-$d_4$): δ 14.4, 14.6, 23.3, 30.3, 30.5, 30.6, 32.8, 33.8, 62.6, 117.6, 120.8, 123.1, 125.4, 127.8, 144.3, 145.4, 156.8, 167.8, 176.4. LC/MS; *m/z* 360.77 $[M + H]^+$, 96.3%.[4]

**2. General experimental information-Biology**

**2.1 Chemicals, bacterial strains, and media**

Yeast extract was purchased from Fluka (Neu-Ulm, Germany), peptone from casein from Merck (Darmstadt, Germany), Bacto™ Tryptone from BD Biosciences (Heidelberg, Germany), and Gibco® phosphate-buffered saline (PBS) from Life Technologies (Darmstadt, Germany). Salts and organic solvents of analytical grade were obtained from VWR (Darmstadt, Germany).

*P. aeruginosa* strain PA14 (PA14), the isogenic *pqsH* and *pqsA* transposon mutants, and the isogenic *pqsR* knockout mutant were stored in glycerol stocks at - 80 °C.

The following media were used: Luria Bertani broth (LB), PPGAS medium,[5] and modified M9 minimal medium (20 mM $NH_4Cl$; 12 mM $Na_2HPO_4$; 22 mM $KH_2PO_4$; 8.6 mM NaCl; 1 mM, $MgSO_4$; 1 mM $CaCl_2$; 11 mM glucose).[6]

**2.2 Reporter gene assay in *E. coli***

The ability of the compounds to either stimulate or antagonize the PqsR-dependent transcription was analysed as previously described[1] using a β-galactosidase reporter gene assay in *E. coli* expressing PqsR. Briefly, a culture of *E. coli* DH5α cells containing the plasmid pEAL08-2, which encodes PqsR under the control of the *tac* promoter and the β-galactosidase reporter gene *lacZ* controlled by the *pqsA* promoter, were co incubated with test compound. Antagonistic effects of compounds were assayed in the presence of 50 nM PQS. After incubation, β- galactosidase activity was measured spectralphotometrically at $OD_{420nm}$ using POLARstar Omega (BMG Labtech, Ortenberg, Germany) and expressed as percent stimulation of controls. For the determination of $IC_{50}$ values, compounds were tested at least at eight different concentrations. The given data represent mean values of two experiments with n = 4.

**2.3 Reporter gene assay in *P. aeruginosa***

In order to study the antagonistic and agonistic properties of compounds **1**, **2** and **3** in *P. aeruginosa*, the PqsR-dependent transcription was evaluated using a β-galactosidase reporter gene assay system. A PA14 strain carrying a non-functional *pqsA* gene to eliminate intracellular HHQ and PQS production was transformed with the plasmid pEAL08-2 and incubated with test compound in the presence or absence of 50 nM PQS and proceeded analogously to reporter gene assay in *E. coli*.

**2.4 Measurement of compound 2 levels**

In order to strengthen the theory of a possible biotransformation of the antagonistic compound **1** levels of compound **2** produced by *P. aeruginosa* were investigated for PA14, *pqsA* and *pqsH* mutants. Cultures were inoculated with a starting $OD_{600}$ = 0.1 in 100 mL Erlenmeyer flasks containing 50 mL LB medium. DMSO as a control or a DMSO solution of **1** (5 µM) was added to the cultures to a final DMSO concentration of 0.5%. The flasks were incubated at 37 °C, 200 rpm for 16 h. Every 60 min, samples of 995 µL of each culture were taken and supplemented with 15 µL of methanol containing 50 µM of the internal standard (HHQ-$d_4$). The cells were lysed via sonification (amplitude 80%, 1 min) and compound **2** was extracted with 995 µL of ethyl acetate for 1 min. After centrifugation (42,000 *g*, 2 min) 800 µL of the organic phase were transferred to a glass vial for vacuum evaporation. The residues were redissolved in 200 µL of methanol and subjected to UHPLC-MS/MS analysis. For each sample, cultivation and extraction were performed in triplicates.

**2.5 UHPLC-MS/MS analysis of extracted compound 2 levels**

UHPLC-MS/MS analysis was carried out on a TSQ Quantum Access Max mass spectrometer equipped with an HESI-II source and a triple quadrupole mass detector (Thermo Scientific, Dreieich, Germany). For analysis of compound **2**, the following chromatographic conditions were used: 0.00-1.20 min, solvent gradient from 60% A up to 99% A, 1.21-1.80 min, isocratic 99% A, 1.81-2.00 min 60% A. Monitored ions were (mother ion [m/z], product ion [m/z], scan time [s], scan width [m/z], collision energy [V], tube lens offset [V], polarity): compound **2**: 303.088, 217.959, 0.2, 0.010, 32, 114, negative; internal standard (HHQ-$d_4$): 248.340, 163.360, 0.2, 0.010, 32, 113, positive. Samples were injected with a volume of 25 µL. The mobile phase consisted of acetonitrile containing 1‰ TFA (*v/v*; A) and 10 mM ammonium acetate buffer containing 1‰ TFA (*v/v*; B) and a flow rate of 0.8 mL/min. Xcalibur software was used for data acquisition and quantification using a calibration curve relative to the area of the IS.

**2.6 Determination of extracellular HHQ and PQS levels**

For determination of extracellular levels of HHQ and PQS produced by PA14, cultivation was performed in the following way: cultures (initial $OD_{600}$ = 0.02) were incubated with or without inhibitor (final

DMSO concentration 1%, *v/v*) at 37 °C, 200 rpm and a humidity of 75% for 16 h in 24-well Greiner Bio-One (Frickenhausen, Germany) Cellstar plates containing 1.5 mL of LB medium per well. For HHQ analysis, according to the method of Lepine *et al*.,[7] 500 µL of the cultures supplemented with 50 µL of a 10 µM methanolic solution of the internal standard (IS) 5,6,7,8-tetradeutero-2-heptyl-4(1*H*)-quinolone (HHQ-$d_4$) were extracted with 1 mL of ethyl acetate. After centrifugation (18,620 *g*, 12 min), 400 µL of the organic phase were evaporated to dryness and redissolved in methanol. UHPLC-MS/MS analysis was carried out as described in detail by Storz *et al*..[8] The monitored ions were (mother ion [m/z], product ion [m/z], scan time [s], scan width [m/z], collision energy [V], tube lens offset [V]): HHQ: 244, 159, 0.5, 0.01, 30, 106; HHQ-*d4* (IS): 248, 163, 0.1, 0.01, 32, 113. Quantification of PQS produced by PA14 was performed according to the method of Maurer *et al.*[9] For each sample, cultivation and sample work-up were performed in triplicates. Inhibition values of HHQ and PQS formation were normalized to $OD_{600}$.

**2.7 Pyocyanin assay**

For analysis of pyocyanin formation, cultivation procedure was the same as for HHQ determination with the exception of using PPGAS medium. Pyocyanin produced by PA14 was quantified using the method of Essar *et al*.[10] with some modifications, as described in detail by Klein *et al*..[11] Briefly, 900 µL of each culture were extracted with 900 µL of chloroform and 800 µL of the organic phase re-extracted with 250 µL of 0.2 M HCl. $OD_{520}$ was measured in the aqueous phase using FLUOstar Omega (BMG Labtech, Ortenberg, Germany). For each sample, cultivation and sample work-up were performed in triplicates. Inhibition values of HHQ and PQS formation were normalized to $OD_{600}$.

**2.8 Determination of growth curves of PA14 in minimal medium**

Cultures of PA14 adjusted to a starting $OD_{600}$ of 0.05 were grown in triplicates in 100 mL Erlenmeyer flasks containing 10 mL modified M9 minimal medium at 37 °C, 200 rpm and a humidity of 75%. DMSO alone or 15 µM DMSO solutions of compound **3** were added to the cultures to a final DMSO concentration of 1% (*v/v*). Bacterial growth was measured as a function of $OD_{600}$ using Thermo Spectronic Helios Epsilon UV-VIS Spectrophotometer (Thermo Scientific, Dreieich, Germany).

**2.9 *Caenorhabditis elegans* fast killing assay**

*C. elegans* nematodes (Bristol *N2*, wild type, German Center for Neurodegenerative Diseases, Bonn, Germany) were synchronized at fourth larval stage (L4) according to the protocol of *Worm Book* (www.wormbook.org). PA14 was incubated overnight in LB medium in the presence or absence of 15 µM antagonist **3** containing 1% DMSO. After spreading of 10 µL of an overnight bacterial culture, the PGS plates with or without 15 µM antagonist **3** containing 1% DMSO were incubated at 37 °C for 24 h and placed at room temperature for further 16 h. After transfer of 15-20 L4 *C. elegans* onto each plate, the mortality was scored every hour.[12] The nematodes were considered dead or alive based on movements elicited by touching their heads gently with a thin wire or shaking the plates. For each condition, data from three independent experiments were combined.

**2.10 *Galleria mellonella* virulence assay**

*G. mellonella* larvae were purchased from local supplier (Angelsport Becker, Saarbrücken, Germany). For infection of the larvae, bacterial cultures were grown to exponential growth phase, adjusted to an $OD_{600}$ of 1.6 in sterile PBS (pH 7.2), and serially diluted in PBS to obtain a lethal cell density (7 ± 1 CFUs/20 µL). CFUs were determined according to the method of Miles and Misra.[13] Aliquots of 5 µL were injected into the *Galleria mellonella* larvae (average weight 450 ± 50 mg) via the hindmost left proleg using a 10 µL Hamilton syringe. Larvae were incubated in Petri-dishes in the dark at 37 °C. Survival rates were monitored in time intervals of 12 h for 108 h post infection. Larvae were considered dead when no movement was observed in response to touch or when melanization of the cuticle occurred. [14] Groups of 15 larvae each were subjected to the following treatments: injection of a) PA14 suspension diluted as described above, b) 10 pmol of compound **3** dissolved in a), c) 5 pmol of compound **3** dissolved in a), d) PA14 isogenic *pqsA* transposon mutant suspension diluted as mentioned above, and e) PA14 isogenic *pqsR* knockout mutant suspension prepared as described above. For each treatment, data from at least two independent experiments were combined.

**2.11 Statistical analysis**

For the animal experiments, statistical analysis was performed using GraphPad Prism 5.04 software. Survival curves were generated by the Kaplan-Meier method and analyzed by the log-rank (Mantel-Cox) test. $IC_{50}$ values were calculated with Origin 8 software.

**3. Supplementary results**

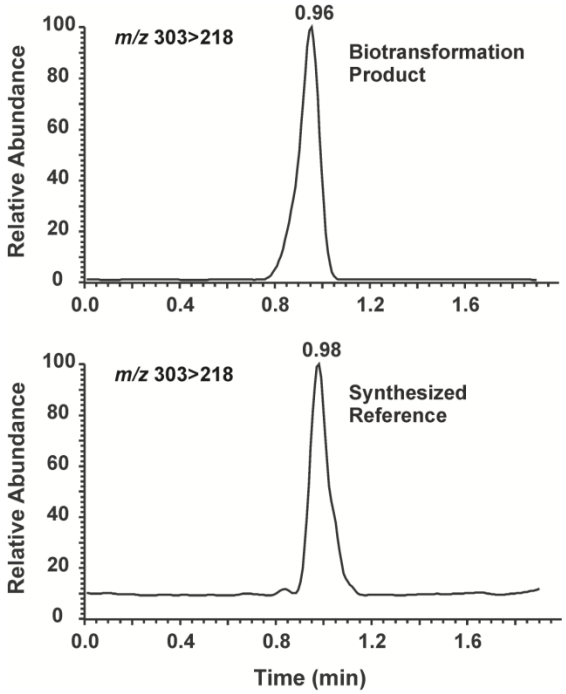


**Figure S1.** Chromatograms of SRM transition *m/z* 303>218 indicating biotransformation product (upper diagram) and chemically synthesized reference **2** (lower diagram).

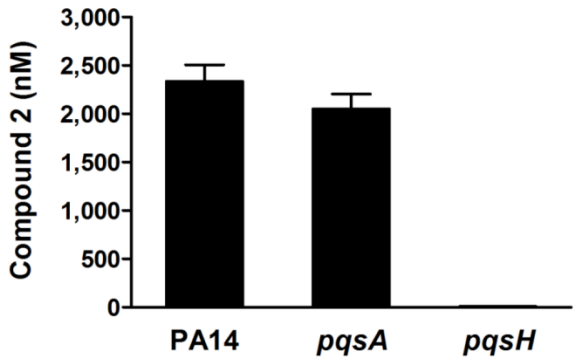


**Figure S2.** Production of compound **2** in PA14, *pqsA* and *pqsH* mutants after 16 hours. Strains were incubated with **1** at 5 µM.

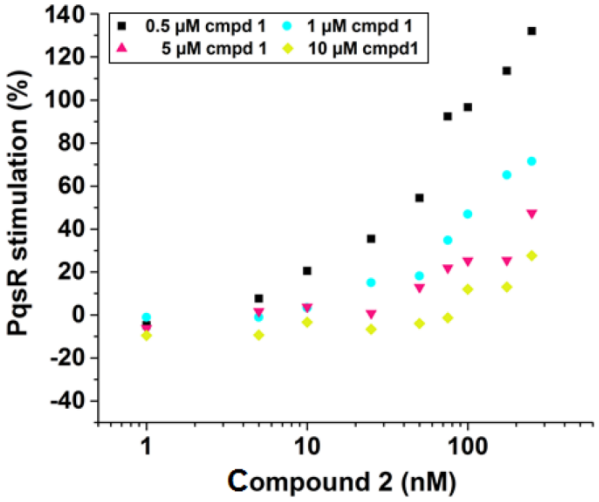


**Figure S3.** Competition experiment with PqsR antagonist **1** and agonist **2** in *E. coli* β-galactosidase reporter gene assay. The assay was performed in the presence of 50 nM PQS. For Y axis, 0% is defined as the basal PqsR stimulation without ligands and 100% is defined as the PqsR stimulation by 50 nM PQS.

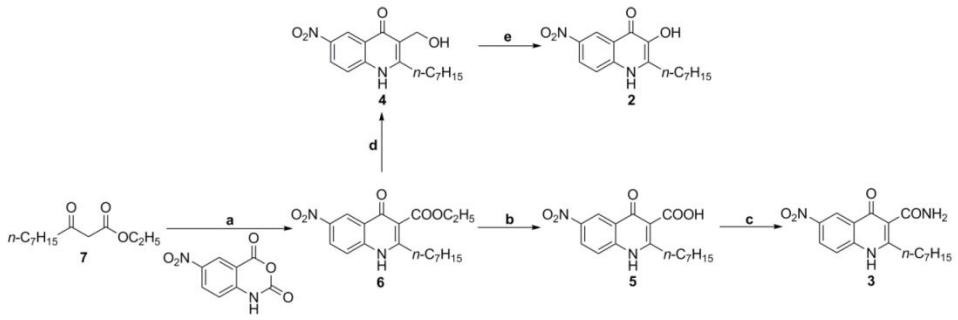

**Figure S4.** Synthetic route of compounds **2** and **3**. Reagents and conditions: a) NaH, dry DMF, r.t. then HCl; b) NaOH, $H_2O$, reflux then HCl; c) *N,N*'-carbonyldiimidazole, $NH_3 \bullet H_2O$, dry DMF, 0 °C – r.t.; d) $LiAlH_4$, dry THF, 0 °C – r.t.; e) $MnO_2$, dry THF, r.t. then $B(OH)_3$, conc. $H_2SO_4$, $H_2O_2$, THF, r.t.

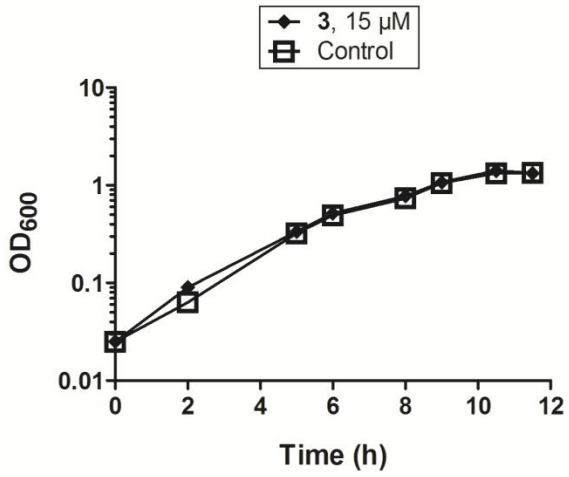


**Figure S5.** Growth curves of PA14 in modified M9 minimal medium in the absence (control) and presence of 15 µM of compound **3**.

**4. References**

[1]. C. Lu, B. Kirsch, C. Zimmer, J. C. de Jong, C. Henn, C. K. Maurer, M. Müsken, S. Häussler, A. Steinbach, R. W. Hartmann, *Chem. Biol.* **2012**, *19*, 381-390

[2]. Y. Zhang, W. A. Guiguemde, M. Sigal, F. Zhu, M. C. Connelly, S. Nwaka, R. K. Guy, *Bioorg. Med. Chem.* **2010**, *18*, 2756-2766.

[3]. C. Pidathala, R. Amewu, B. Pacorel, G. L. Nixon, P. Gibbons, W. D. Hong, S. C. Leung, N. G. Berry, R. Sharma, P. A. Stocks, A. Srivastava, A. E. Shone, S. Charoensutthivarakul, L. Taylor, O. Berger, A. Mbekeani, A. Hill, N. E. Fisher, A. J. Warman, G. A. Biagini, S.A. Ward, P.M. O'Neill. *J. Med. Chem.* **2012**, *55*, 1831-1843.
[4]. Purcell, I.C. thesis, University of Nottingham **2007**.
[5]. Y. Zhang, R. M. Miller, *Appl. Environ. Microbiol.* **1992**, *58*, 3276-3282.
[6]. J. Tremblay, E. Deziel, *J. Basic Microbiol.* **2008**, *48*, 509-515.
[7]. F. Lepine, S. Milot, E. Deziel, J. He, L. G. Rahme, *J. Am. Soc. Mass Spectrom.* **2004**, *15*, 862-869.
[8]. M. P. Storz, C. K. Maurer, C. Zimmer, N. Wagner, C. Brengel, J. C. de Jong, S. Lucas, M. Müsken, S. Häussler, A. Steinbach, R. W. Hartmann, *J. Am. Chem. Soc.* **2012**, *134*, 16143-16146.
[9]. C. K. Maurer, A. Steinbach, R. W. Hartmann, *J. Pharm. Biomed. Anal.* **2013**, http://dx.doi.org/10.1016/j.jpba.2013.07.047.
[10]. D. W. Essar, L. Eberly, A. Hadero, I. P. Crawford, *J. Bacteriol.* **1990**, *172*, 884-890.
[11]. T. Klein, C. Henn, J.C. de Jong, C. Zimmer, B. Kirsch, C. K. Maurer, D. Pistorius, R. Müller, A. Steinbach, R. W. Hartmann, *ACS Chem. Biol.* **2012**, *7*, 1496-1501.
[12]. S. Mahajan-Miklos, M. Tan, L. G. Rahme, F. M. Ausubel, *Cell* **1999**, *96*, 47-56.
[13]. A. A. Miles, S. S. Misra, J. O. Irwin, *J. Hyg. (Lond)* **1938**, *38*, 732-749.
[14]. G. Jander, L. G. Rahme, F. M. Ausubel, *J. Bacteriol.* **2000**, *182*, 3843-3845.